GEOLOGY AND HYDROGEOLOGY OF THE COSTILLA DAM LANDSLIDE, TAOS COUNTY, NEW MEXICO

By

Andrew B. Dunn

Submitted in Partial Fulfillment
of the Requirements for the

Master of Science in Hydrology

New Mexico Institute of Mining and Technology
Department of Earth and Environmental Science

Socorro, New Mexico

May, 2001

ABSTRACT

This study was conducted for a number of reasons. Foremost, the goal was to determine the driving mechanisms for annual groundwater fluctuations observed within and below the Costilla Dam landslide. Possible driving mechanisms for the groundwater fluctuations are fluctuation of the water level within Costilla Reservoir, recharge caused by precipitation events, and recharge caused by snowmelt. Equally important was the process of geologically characterizing the area surrounding the landslide to better understand the geology of the landslide and how it could affect the groundwater hydrology. In addition, a way to manipulate MODFLOW into performing a dipping-layer simulation was formulated, and used herein, in which the model layers dip at the same angle as the ground surface. Finally, information on Costilla Dam and the Costilla Dam landslide was compiled from numerous unpublished documents and reports.

The deep-seated Costilla Dam landslide is a reactivated portion of the Costilla Dam landslide complex that forms the right abutment of Costilla Dam, located in the Sangre de Cristo Mountains, in north central New Mexico. The landslide was reactivated in 1988 or 1989 when construction activities at the dam, specifically the stockpiling of building material on the landslide surface and excavation at the toe of the slope for placement of a new emergency spillway, decreased slope stability. The primary geologic control on movement of the Costilla Dam landslide complex and Costilla Dam landslide is the approximately 10 degree dip of basin-fill deposits (Santa Fe Group) into the valley.

All landslides located in the vicinity are derived from the basin-fill deposits suggesting their susceptibility to slope instability. Interbedded with the basin-fill deposits is a basalt flow with a weathered clay-rich surface. This clay zone provides a plane of low shear strength and is the slip surface for both the Costilla Dam landslide and part of the landslide complex. Landslide deposits overlie a buried channel of alluvium where the landslide projects into the valley.

Groundwater within the landslide is unconfined and flow is dominantly down the axis of the landslide. Groundwater below the slide plane is confined and flow is also dominantly down the axis of the landslide, except near the buried channel of alluvium where a larger component of down-valley flow is present. Nested piezometers indicate that the hydraulic head is always higher within the landslide than below the slide plane. The clay-rich slide plane is a barrier to groundwater flow except near the toe of the landslide where the buried channel of alluvium acts as a drain that captures and discharges all flow within the landslide. Most piezometers, the reservoir, and the stream gauges show one large-amplitude annual fluctuation in groundwater hydraulic head, reservoir level, and stream flow respectively. These fluctuations peak during the summer field season. Groundwater fluctuations within the landslide are likely controlled by snowmelt recharge and occur before, or are synchronous with, the reservoir level fluctuations. Groundwater fluctuations below the slide plane are controlled by reservoir level fluctuations and occur after the reservoir level fluctuates. The time lag of groundwater fluctuations increases and magnitude decreases upslope and away from the reservoir. The buried channel of alluvium provides the main hydrologic connection between the flow domains above and below the slide plane, and the reservoir.

ACKNOWLEDGEMENTS

I would like to thank the following individuals and organizations that assisted me with this study. The members of my committee; William C. Haneberg, Brian J. O. L. McPherson, and John L. Wilson. The Vermejo Park Ranch, Rio Costilla Cooperative Livestock Association, and Carson National Forest (Valle Vidal Unit) for allowing me access to lands that they own and/or manage. The Colorado Scientific Society who provided me with a grant from the Edwin B. Eckel Memorial Fund, which funded my field work. The New Mexico Bureau of Mines and Mineral Resources provided me with a research assistantship. Dan Grundvig of the United States Bureau of Reclamation loaned me his copy of the Final Construction Geology Report completed on the Costilla Dam and Spillway Modification. Finally, I would like to thank my friends and family for their constant support and encouragement.

TABLE OF CONTENTS

LIST OF TABLES

LIST OF FIGURES

LIST OF ABBREVIATIONS

cm	centimeters
DH-	drill hole
ft	feet
I-	inclinometer
km	kilometers
L	lower piezometer completion (below the slide plane)
m	meters
mi	miles
NMISC	New Mexico Interstate Stream Commission
NMOSE	New Mexico Office of the State Engineer
NMSEO	New Mexico State Engineer Office (now called NMOSE)
NMSHD	New Mexico State Highway Department
p.	page number
PZ-	piezometer
sec	seconds
U	upper piezometer completion (within landslide deposit)
USBR	United States Bureau of Reclamation
USGS	United States Geological Survey

1. INTRODUCTION

Costilla Dam and the Costilla Dam landslide are located in north central New Mexico approximately 13 km (8 mi.) south of the Colorado-New Mexico border. They are located in the Costilla Valley upstream from the towns of Costilla and Amalia, New Mexico (Figure 1). The Costilla Dam landslide complex forms the right (northern) abutment of Costilla Dam (Figure 2).

The San Luis Power and Water Company constructed Costilla Dam between 1915 and 1920. Since this time all topographic base maps and scientific measurements at the site have been conducted using English units. In this study both English and metric units are given. However, the measurements recorded in English units are exact while the metric units are a rounded off conversion. In 1915 the access road and outlet works were constructed. In 1916 the dam foundation was prepared, drainage system installed, and placement of earthen material for the embankment began. Construction of the embankment continued from 1917 to 1919 (USBR, 12/1986). After its construction, Costilla Dam remained unchanged from 1920 to 1989. The original embankment was created using homogeneous earth-fill construction. The crest was located at an elevation of 2871.2 meters (9420 feet) with a crest length of 190.5 meters (625 feet) and a height of 37 meters (121.5 feet). The width of the crest was 6.1 meters (20 feet) while the maximum width of the base was 198.1 meters (650 feet) perpendicular to the crest. The

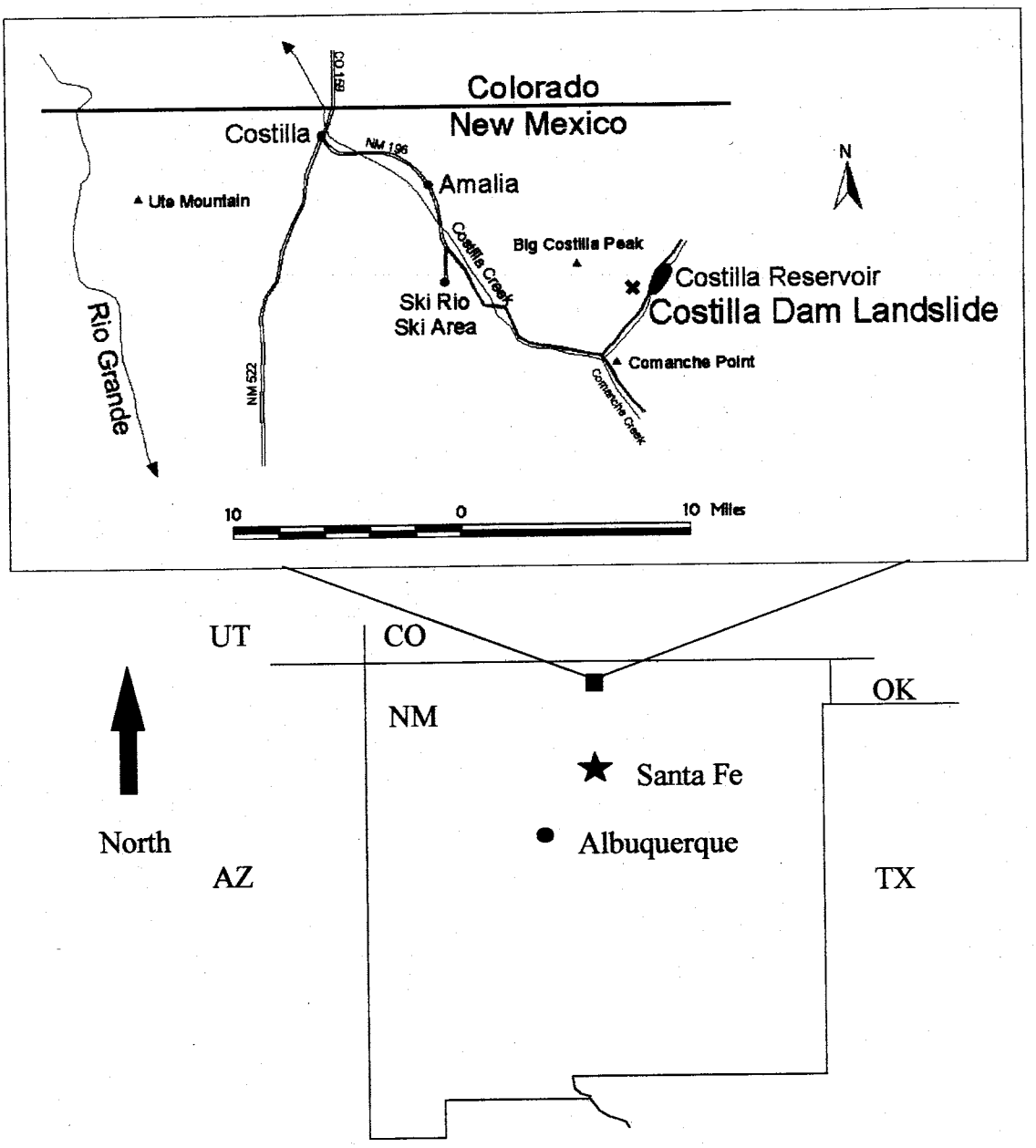

Figure 1 Location of the Costilla Dam landslide. The Costilla Dam landslide is located in Costilla Valley upstream from the towns of Costilla and Amalia, New Mexico. The Costilla Dam landslide complex forms the right (northern) abutment of Costilla Dam.

Figure 2 Oblique aerial photo. This photo, taken by the United States Bureau of Reclamation prior to 1989, shows the Costilla Dam landslide complex protruding into the valley, forming the right abutment of Costilla Dam. The photo is taken roughly facing north.

slope of the upstream embankment face was 3 horizontal to 1 vertical, while the downstream face was 2.5 horizontal to 1 vertical.

The spillway crest elevation for the reservoir was 2867 meters (9406 feet). Before the embankment was emplaced a 9.1 meters (30 foot) deep cutoff trench was excavated parallel to the crest beneath the dam. The emergency spillway consisted of an unlined earthen channel that was cut into the adjacent hillside. (USBR, 12/1986)

The original and continued purpose of Costilla Dam is to "regulate the flows of Costilla Creek to provide an irrigation water supply for lands in the states of New Mexico and Colorado" (NMISC, 3/31/1994). Costilla Creek flows from its headwaters in Colorado to its mouth at the Rio Grande in New Mexico. The water in the creek is regulated and appropriated by an agreement between Colorado and New Mexico. The Costilla Creek Compact of 1944 specifies that 36% of the water in Costilla Reservoir is appropriated to Colorado and 64% is appropriated to New Mexico (NMISC, 3/31/1994). Costilla Dam and Reservoir lie within the property boundary of the privately owned Vermejo Park Ranch. However, the Rio Costilla Cooperative Livestock Association manages discharge from the dam.

1.1 PROBLEMS WITH COSTILLA DAM

Costilla Dam had been operated continuously from 1920 to 1988. During this time the dam was plagued by many problems which eventually led to the rehabilitation construction activities in the 1980s.

During emplacement of the top 12.2 meters (40 feet) of the embankment in 1919, it became difficult to find suitable earthen building material, so sub-grade material was

used during this final phase of construction (USBR, 12/1986). This inferior grade material in the top of the embankment led to problems a few years after the dam became operational. Seepage was first reported through this upper section of the embankment in 1924. The seepage appeared out of the downstream embankment near elevation 2862.1 meters (9390 feet), approximately 9.1 meters (30 feet) below the crest of the dam (USBR, 12/1986). By 1941, seepage had become excessive through this section of the embankment (Bovay Engineers, 8/1978). The seepage problem prompted the New Mexico State Engineer Office (NMSEO; now called the New Mexico Office of the State Engineer, NMOSE) to place restrictions on the maximum elevation of the reservoir level, starting in July 1949. Storage below elevation 2863 meters (9393 feet) was permitted at any time. Special permission was required for reservoir levels to exceed 2863 meters (9393 feet), with a maximum allowable reservoir elevation of 2865.1 meters (9400 feet). Elevated reservoir levels were allowed for only a limited time and required strict monitoring of the dam (Bovay Engineers, 8/1978).

Costilla Dam was classified in the "High-Hazard Potential Category" by the national program of inspection of dams, in May 1975. In the Phase I dam inspection report, serious concerns regarding the insufficiency of the emergency spillway structure are cited (Bovay Engineers, 8/1978). The original design specifications called for a concrete spillway channel with a minimum bottom width of 10.7 meters (35 feet), 1 horizontal to 1 vertical side slopes, and a minimum depth of 3.1 meters (10 feet) (Bovay Engineers, 8/1978). For unknown reasons the spillway was never completed as designed, and instead the spillway was developed as an unlined earthen channel that did not meet any of the original design specifications. The spillway was cut into the adjacent hillside

and followed a 1% slope for a distance of 251.5 meters (825 feet), at which point it turned directly down slope to empty into Costilla Creek.

The performance of the dam and spillway was modeled by Bovay Engineers (1978) to evaluate its response to a Probable Maximum Flood (PMF) with a starting reservoir level of 2866 meters (9403 feet). Results of this analysis indicated that this magnitude of flow would induce the flow of water more than 3.1 meters (10 feet) deep, over the crest of the entire dam. In addition, Bovay Engineers evaluated the dam and spillway's response to a Standard Project Flood (SPF), a flood that is one half the peak and volume of the PMF. Even for this reduced flood, the analysis suggests that the depth of water flowing over the top of the dam would reach 1.5 meters (5 feet). Both of these analyses assumed that the dam would not fail catastrophically even while being overtopped. Because of the unlined spillway channel, Bovay Engineers speculated that even a prolonged spill exclusively through the spillway channel could lead to embankment erosion and dam failure. Based on Bovay Engineers' analysis and the likelihood that the dam could catastrophically fail during a severe flooding event, the construction of an adequate spillway channel was recommended. In addition to the inadequate spillway channel, other problems identified were seepage through the upper 12.2 meters (40 feet) of the dam embankment, and aged outlet works (Bovay Engineers, 8/1978).

From 1920 to 1989 the approximate 141.4 km^2 (54.6 mi^2) drainage basin above Costilla Dam never experienced a major flooding event, and no flow through the dam's spillway was ever recorded. However, reservoir levels approached but did not exceed the

spillway elevation on three separate occasions (2867 meters or 9406 feet) (Bovay Engineers, 8/1978; USBR, 9/1985).

In the 1980s it was determined that Costilla Dam had to be repaired or removed in order to reduce the risk to life and property downstream from the dam. Even though the dam is privately owned, the state of New Mexico, represented by the New Mexico State Engineer Office (NMSEO), and its sister department, the New Mexico Interstate Steam Commission (NMISC) is responsible for its safety. Under the Bureau Technical Assistance to the States program, with cooperation of the state of New Mexico, the United States Bureau of Reclamation (USBR) conducted a feasibility study between 1984 and 1985 to consider methods of rectifying the problems identified in the Bovay Report (D'Appolonia and others, 11/1992).

1.2 NEW MEXICO STATE HIGHWAY DEPARTMENT INVESTIGATION

In 1984, as part of the United States Bureau of Reclamation feasibility study, NMSEO contracted the New Mexico State Highway Department (NMSHD) to perform a limited subsurface investigation of Costilla Dam and the proposed spillway location. In this investigation a total of eleven boreholes were drilled (DH-1, -2, -3, -4, -5, and six in the spillway alignment). Three holes were drilled on the dam crest to examine the properties of the embankment material and 2 holes were drilled near the downstream toe of the dam (Figure 3). Geophysical testing (gamma, neutron, and density) and lab tests (sieve analysis, S.P.T. blow count, moisture %, liquid limit, plastic index, and soil classification) were performed during and after the first five holes were drilled. For the remaining six boreholes drilled along the proposed spillway alignment there was no

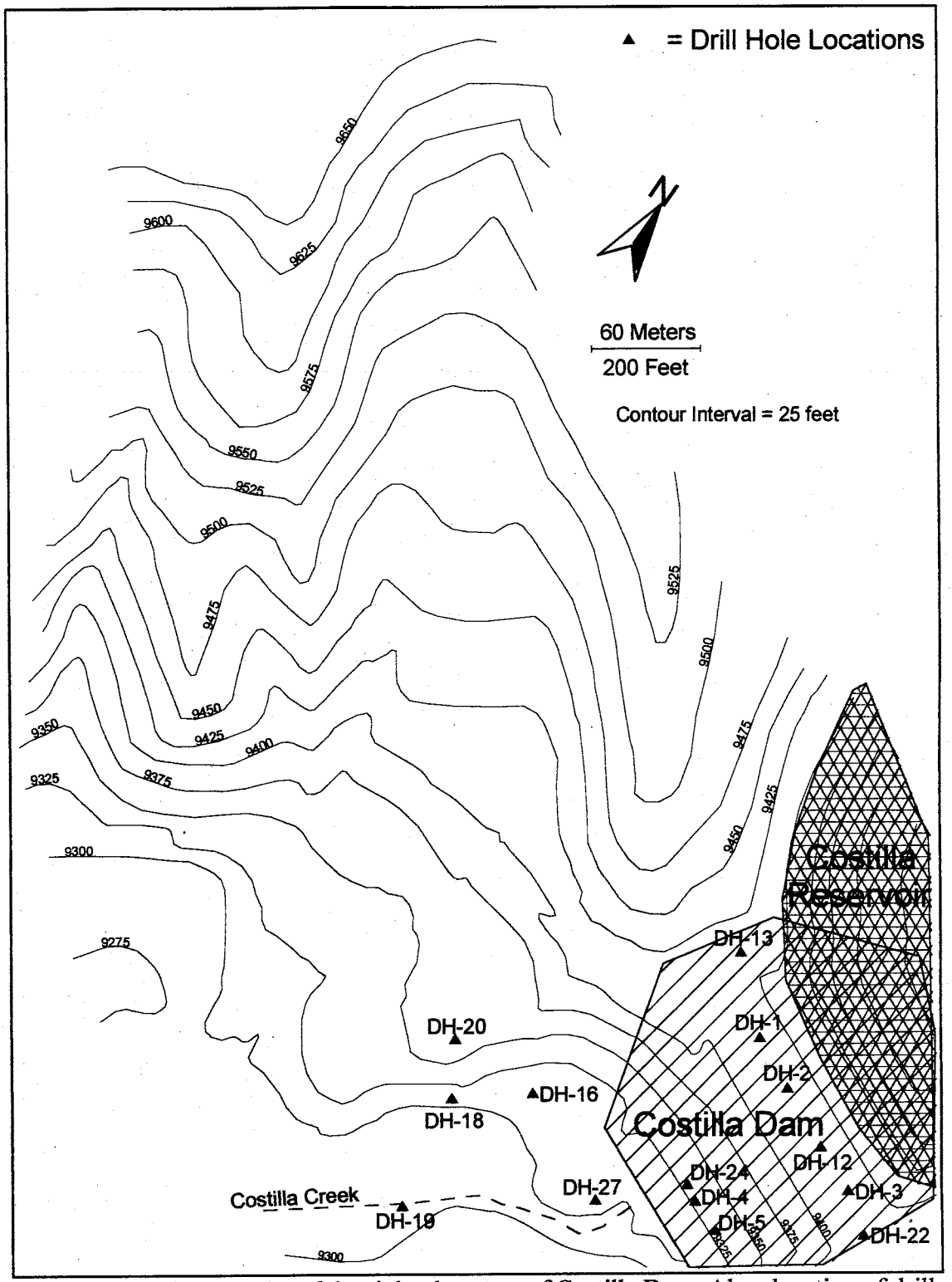

Figure 3 Topography of the right abutment of Costilla Dam. Also, location of drill holes (DH-) drilled during the NMSHD 1984 and the USBR 1986 subsurface investigations. Topography shown on this figure was copied from topographic maps of the landslide area prepared by the USBR.

sample collection or tests run (Haneberg, 9/17/1992). In addition to the boreholes, a seismic refraction survey was run along the downstream toe of the dam (USBR, 12/1986).

1.3 UNITED STATES BUREAU OF RECLAMATION 1986 INVESTIGATION

During 1986, as part of the United States Bureau of Reclamation feasibility study, the United States Bureau of Reclamation drilled 9 boreholes in the vicinity of the dam (DH-12, -13, -16, -18, -19, -20, -22, -24, and -27). Three holes were drilled on the dam crest to accompany the three already drilled by the NMSHD. Four holes were drilled along the centerline of the proposed spillway chute to determine the foundation properties for this structure. Two holes were also drilled along the downstream toe of the embankment (Figure 3) (USBR, 12/1986). Geologic logs for these drill holes are provided in Appendix I.

1.4 APPROPRIATION AND CONSTRUCTION

In 1985, the New Mexico State Legislature voted appropriated $11.589 million, from the New Mexico Irrigation Works Construction Fund, for the rehabilitation of the dam (NMSEO, 1/12/1990). On July 16, 1986, the state of New Mexico contracted the United States Bureau of Reclamation (contract #6-AG-50-5900) to perform design and engineering considerations for the dam, and to manage construction activities (USBR, 7/16/1986; D'Appolonia and others, 11/1992). After design considerations were complete, an additional $2.911 million was appropriated in 1988 by the New Mexico

State Legislature to award a contract for the design. Construction activities began in September 1988 (NMSEO, 1/12/1990; D'Appolonia and others, 11/1992).

Proposed repairs to Costilla Dam included the outlet works, spillway, and upper embankment. The outlet works were to be upgraded and rebuilt due to nearly 70 years of use. The upper 13.7 meters (45 feet) of the dam embankment was going to be excavated and replaced with a compacted, zoned embankment consisting of an impermeable core (zone 1 material) with a permeable shell (zone 3 material) (USBR, 4/1988). The emergency spillway ultimately designed was a straight ogee crest with a spillway chute leading to a stilling basin (USBR, 9/87).

1.5 LANDSLIDE REACTIVATION

Construction began near the end of the 1988 field season. Specific construction activities directly caused the reactivation of a portion of the Costilla Dam landslide complex. The reactivated portion of the complex will be referred to as the Costilla Dam landslide (Figure 4). A timeline of the events surrounding the reactivation of the Costilla Dam landslide follows. Figure 5 is a topographic map that shows the location of important features identified in the timeline below.

Fall 1988	Stockpiling of Zone 1 and 3 building material.
	Began excavation of spillway crest and chute foundations.
	Contractor and United States Bureau of Reclamation personnel remember seeing cracks in the road above the spillway crest but at the time they were thought to be insignificant. (USBR, 11/1989)

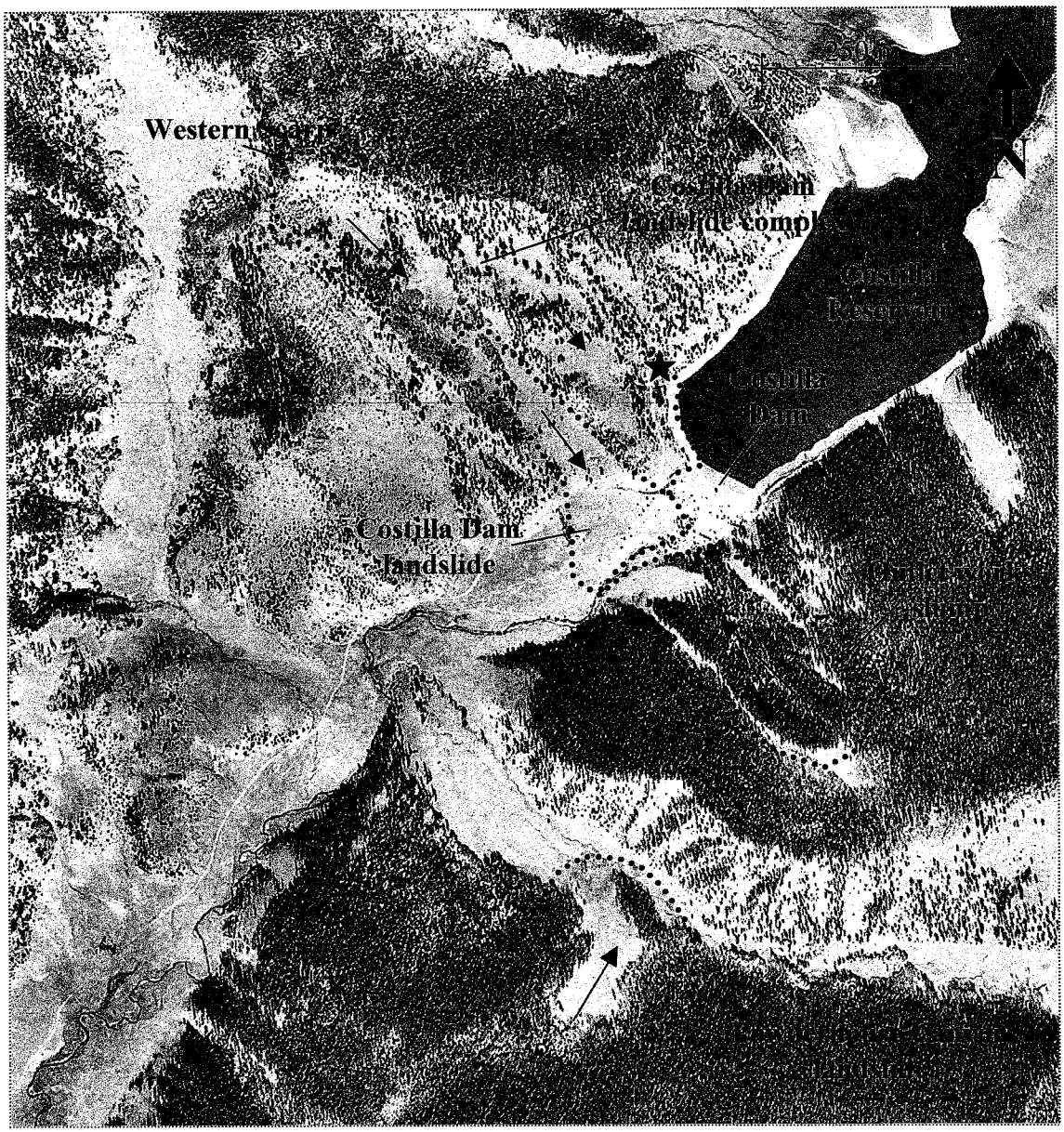

Figure 4 Aerial Photo. This photo was taken in 1962. The Costilla Dam landslide complex has two head scarps, with the eastern scarp being partial. The location of the Costilla Dam landslide activated in 1988 or 1989 is also depicted. Other landslides seen in this photo are the outlet works slump and Powderhouse Canyon landslide. Star indicates the location of the photos taken in figures 12, 16, and 22.

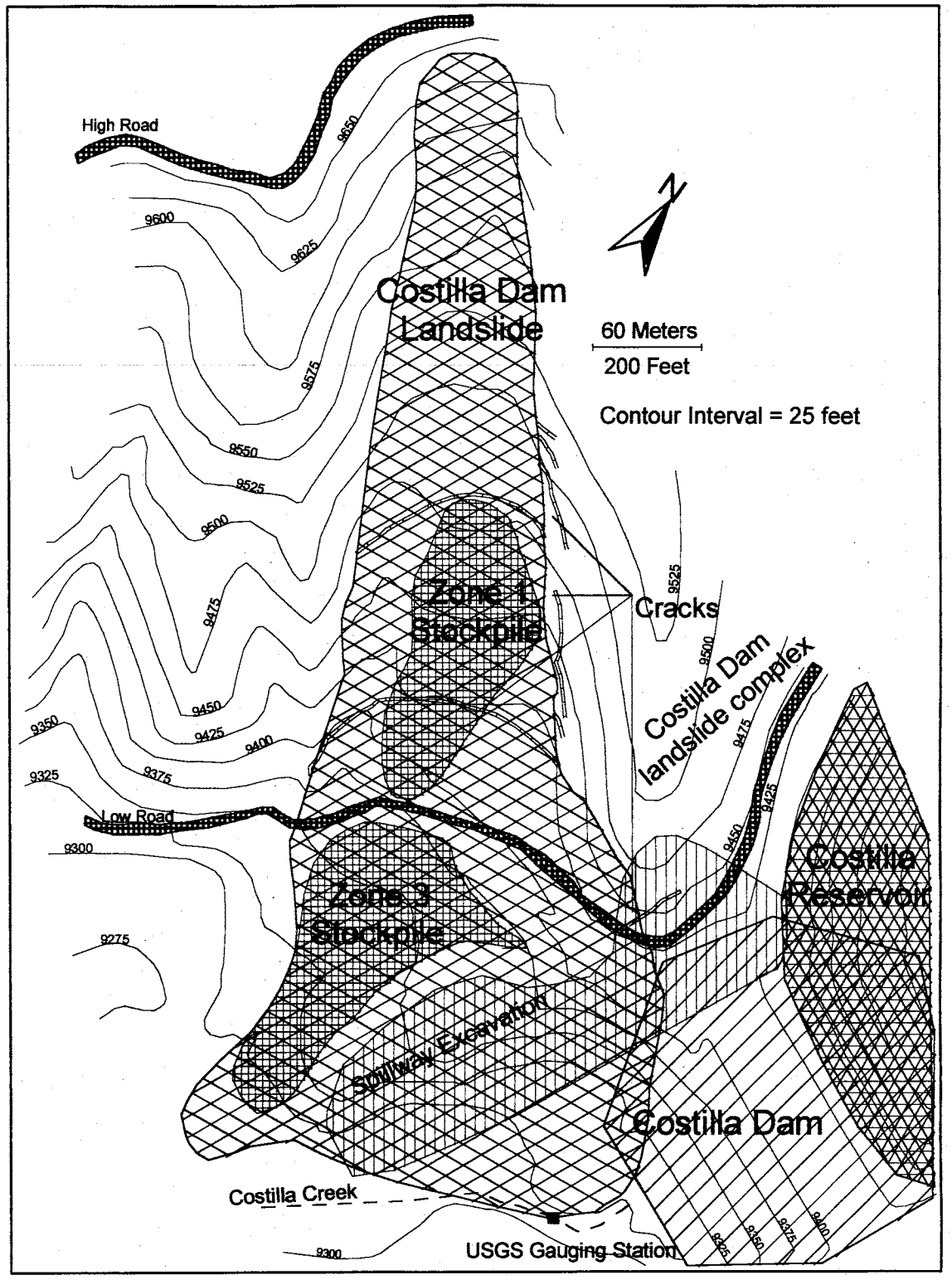

Figure 5 Reactivated Costilla Dam landslide. This figure depicts the significant features noted in the landslide chronology.

By mid-November 1988	Stripped and excavated a portion of the embankment structure and upper part of the spillway chute. Construction ended for season with approximately 60% of the Zone 1 stockpile in place and 75% of Zone 3 stockpile in place. (NMSEO, 1/12/1990)
Winter 1988-1989	Maintenance problems at USGS stream gauge just below Costilla Dam, possibly from pressure ridge development at toe of reactivating landslide. (USBR, 11/1989)
At latest April 2, 1989	Start of construction season. Additional material excavated from embankment and added to stockpiles. (D'Appolonia and others, 11/1992)
April 18, 1989	Cracks first noted in the area upslope of the spillway crest on the eastern side of the stockpiling area by Joseph Bartley of the NMISC. (USBR, 11/1989; USBR, 1/1992)
May 12, 1989	Joseph Bartley (NMISC) and Rich Demlo (USBR) discovered cracks around Zone 1 stockpile and above right abutment of dam. (USBR, 5/18/1989)

May 17, 1989	Series of ground cracks became prominent on north (right) abutment. (NMSEO, 6/20/1989)
May 19-23, 1989	Survey monitoring of surface measurement points started. (USBR, 11/1989)
May 19-25, 1989	Cracks observed extending through Zone 1 stockpile. (USBR, 1/1992)
May 24, 1989	No more material added to the stockpiles. (USBR, 1/92)
May 29-June 2, 1989	Excavation for the spillway stilling basin started this week. (USBR, 11/1989)
June 13-17, 1989	Zone 3 stockpile removed from landslide surface. (USBR, 11/1989)
June 13-29, 1989	Slide cracks filled in with Zone 3 stockpile material. (USBR, 6/22/1989)
June 27-28, 1989	Third slip-circle forming upslope of the Zone 1 stockpile. (USBR, 6/29/1989)

June 29, 1989	Excavation of stilling basin to ~2822 meters (9260 feet) essentially complete. (USBR, 11/1989; USBR 1/1992)
June 30-July 10, 1989	Monitoring of points in the stilling basin invert took place to determine if rate of movement was decreasing and if total movement was within acceptable limits. (USBR, 11/1989; USBR, 1/1992)
July 12, 1989	Cracks extended further upslope to below existing high road, increasing the total length of the slide from about 396 meters (1300 feet) long to 640 meters (2100 feet) long (USBR, 11/1989)
July 14-27, 1989	Stilling basin backfilled to elevation +/- 2838 meters (9310 feet). (USBR, 1/1992; USBR 11/1989)
July 28, 1989	Movement in lower portion of the landslide stops, still some movement higher on the slope. (USBR, 11/1989)
August 4, 1989	Inclinometer I-4 showed a slight deflection at 12.5 meters (41 feet) depth, this is the last movement recorded. (USBR, 11/1989)

August 31-October 16, 1989 Stability berm constructed with 152,911 m^3 (200,000 yd^3) of material. This is about 76,455 m^3 (100,000 yd^3) more material on the toe of the landslide than prior to excavation for the initial spillway ramp and stilling basin (USBR, 11/1989).

After movement of the landslide was recognized, instrumentation proceeded in step with stabilization. Instrumentation of the landslide is described in detail in the following chapter. The landslide was stabilized by placement of the stability berm on the toe of the landslide, and the installation of horizontal drains to discharge groundwater from within and around the landslide. After stabilization of the landslide, construction activities resumed during the summer of 1992. Rehabilitation construction activities were finally completed in June of 1993.

1.6 ARBITRATION

The rehabilitation of Costilla Dam cost approximately $8.79 million more than originally budgeted due to cost overruns associated with the Costilla Dam landslide (Hendron and others, 4/22/1994). The state of New Mexico tried to recover the cost of these overruns from the federal government. The New Mexico congressional delegation was prepared to allocate the necessary federal money to reimburse the state for the extra expense, but the United States Bureau of Reclamation objected to this payment. The United States Bureau of Reclamation felt that the landslide reactivation could not have

been foreseen, and therefore the federal government should not be responsible for any cost overruns associated with it.

On August 4, 1992, after the United States Bureau of Reclamation's objection to federal reimbursement, an independent review team of experts was assembled by the New Mexico Interstate Stream Commission to investigate the reactivation of the Costilla Dam landslide. The New Mexico Interstate Stream Commission independent review team consisted of Elio D'Appolonia, Richard B. Catanach, William C. Haneberg, Robert L. James, and Alan L. O'Neill. This team determined that the United States Bureau of Reclamation should have identified the ancient landslide complex prior to design and construction activities. Prior to reactivation, the deposit forming the right abutment of the dam had been interpreted as a glacial moraine instead of an ancient landslide complex.

On October 1, 1993, the New Mexico Interstate Stream Commission and the United States Bureau of Reclamation entered into an agreement for a fact-finding board to review the arguments and assist in allocating costs to the responsible party. The fact-finding board consisted of three members; one member chosen by each party and a third member chosen by the two selected members. The New Mexico Interstate Stream Commission chose Norbert R. Morgenstern and the United States Bureau of Reclamation chose A. J. Hendron Jr.. Morgenstern and Hendron then chose William F. Swinger to join them on the board. Each side prepared a position paper that was submitted to the other party and the fact-finding board prior to the hearing. The hearing occurred in Denver, Colorado on April 19 and 20, 1994, with each party presenting its case on one day (Hendron and others, 4/22/1994). After the hearing, the fact-finding board weighed the evidence presented by both parties and produced a report of their own. The fact-finding

board determined that the United States Bureau of Reclamation should have identified the ancient landslide complex prior to design and construction activities. However, had the Costilla Dam landslide complex been recognized prior to construction, the New Mexico Interstate Stream Commission would have paid for the construction of the stability berm and spillway ramp essentially as it appears today along with the inclinometers, piezometers, and horizontal drains drilled into the landslide. A general breakdown of costs as recommended by the fact-finding board appears in Table 1 (Hendron and others, 4/22/1994).

Table 1. Distribution of cost overruns related to the Costilla Dam landslide (Hendron and others, 4/22/1994)

Item	Bureau of Reclamation	State of New Mexico
1. Relocate rebar, redistribute zone 3 stockpile, build drill pads, fill cracks, cross section stilling basin, fill stilling basin excavation, relocate batch plant, clear borrow area for stability berm borrow	$410,000	$0
2. Plumb batch plant, relocate fabrication yard, strip stability berm borrow area, haul topsoil, build drill pads, place zone 2 material in stability berm, survey road above slide	$110,000	$0
3. Haul topsoil, fence right abutment, drainage above slide area, and refill cracks	$26,532	$0
4. Construct stability berm	$404,307	$808,613
5. Delete spillway chute, stilling basin, and portion of dam embankment	$0	Paid to State $2,774,478
6. Slide costs and stockpiled material	$1,292,400	$194,446
7. Royalty on material for stability berm and ramp	$0	$119,679
8. Barnard Construction Company contract value	$250,000	$4,063,607
9. Evaluate slide, design stability berm, prepare redesign spillway, prepare change order, design for drains and piezometers, monitor instrumentation, prepare specifications, construction management to complete	$2,333,333	$1,166,666
10. Drilling to install drains, piezometers, and inclinometers	$0	$383,365
Total = $8,788,470	$4,826,572	$3,961,898

2. INSTRUMENTATION

After it was determined that the Costilla Dam landslide was deep-seated, a program was undertaken to instrument the landslide. The goals of instrumentation were to determine the depth of the slide plane, the pore pressure of groundwater in and below the landslide, and to measure whether the horizontal drains were effective in reducing the pore pressure at the slide plane.

2.1 INCLINOMETERS

Five inclinometers (1, 2, 3, 4, and 5) were installed to locate the depth of the slide plane. Figure 6 shows that all of the inclinometers were installed toward the toe of the landslide. Inclinometers are defined by an "I-" preceding the number of the inclinometer. Geologic logs and construction information about the inclinometers are provided in Appendix II. Initially it had been planned to core with HQ wireline, but due to low core recovery and slow drilling rate, the remainder of the inclinometer holes were drilled with a rock bit (USBR, 4/1995). A 3 7/8 inch diameter tricone rock bit was used for drilling all of the holes such that 2.79 inch (outer diameter) inclinometer casings could be installed. Inclinometers two through five had the annuli packed with sand, while inclinometer 1 had a grouted annulus (Appendix II). Inclinometers one through four were installed prior to the drilling of either piezometers or horizontal drains. Inclinometer five was installed after installation of piezometers one through six and at the same time that many of the

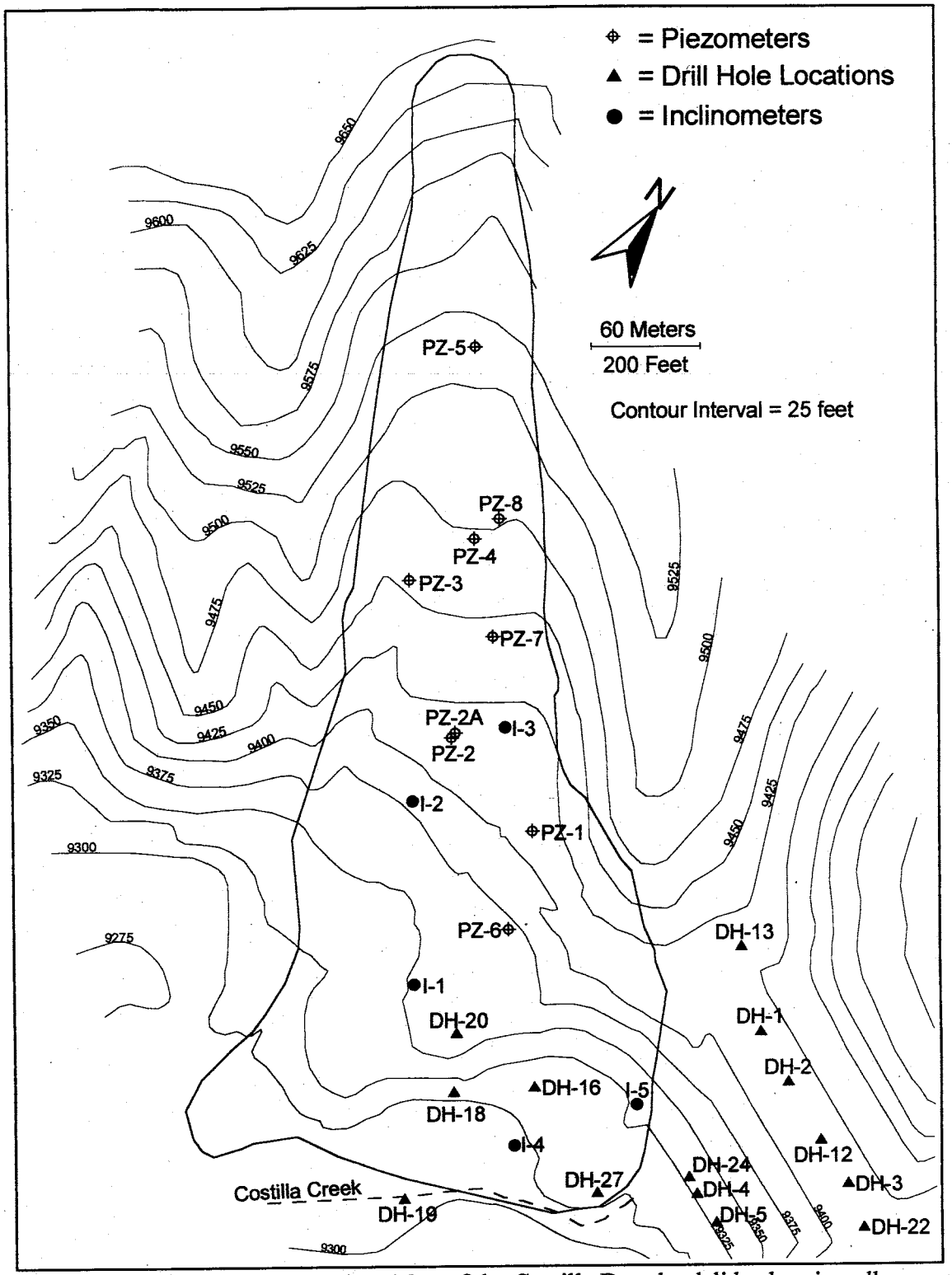

Figure 6 Site Instrumentation. Map of the Costilla Dam landslide showing all instrumentation in the immediate vicinity of the Costilla Dam landslide. Data from many of these instruments were used in geologic and hydrogeologic analyses.

horizontal drains were installed (Figure 7). The inclinometers were used for data collection until the landslide stopped moving, and then were used again during the first fill of the reservoir.

2.2 PIEZOMETERS

Nine piezometer nests (1, 2, 2A, 3, 4, 5, 6, 7, and 8) were drilled on the landslide (Figure 6). The piezometers drilled on the landslide are identified by a "PZ-" preceding the number of the piezometer nest. Seven of the nine nests contain dual completions with one piezometer in the landslide material and another piezometer below the slide plane. Naming convention for the piezometers is as follows; piezometers completed in the landslide mass are followed by a "U" which stands for upper, while piezometers completed below the slide plane are followed by an "L" which stands for lower. The piezometer nests that contain only one piezometer completion are piezometer 2 (PZ-2U), and piezometer 5 (PZ-5L). Geologic logs and construction information on each piezometer are provided in Appendix III. It should be noted that many different types of piezometers were used with varying diameters, open interval lengths, type of openings, and size of sand pack surrounding the open interval. During 1993 and 1994 data was collected daily during the summer field season when driving to the dam site was possible.

2.3 HORIZONTAL DRAINS

The installation and construction of the horizontal drains is poorly characterized. The horizontal drains were originally intended to reduce the pore pressure directly below the slide plane. Observation of water levels during drilling of the drill holes and

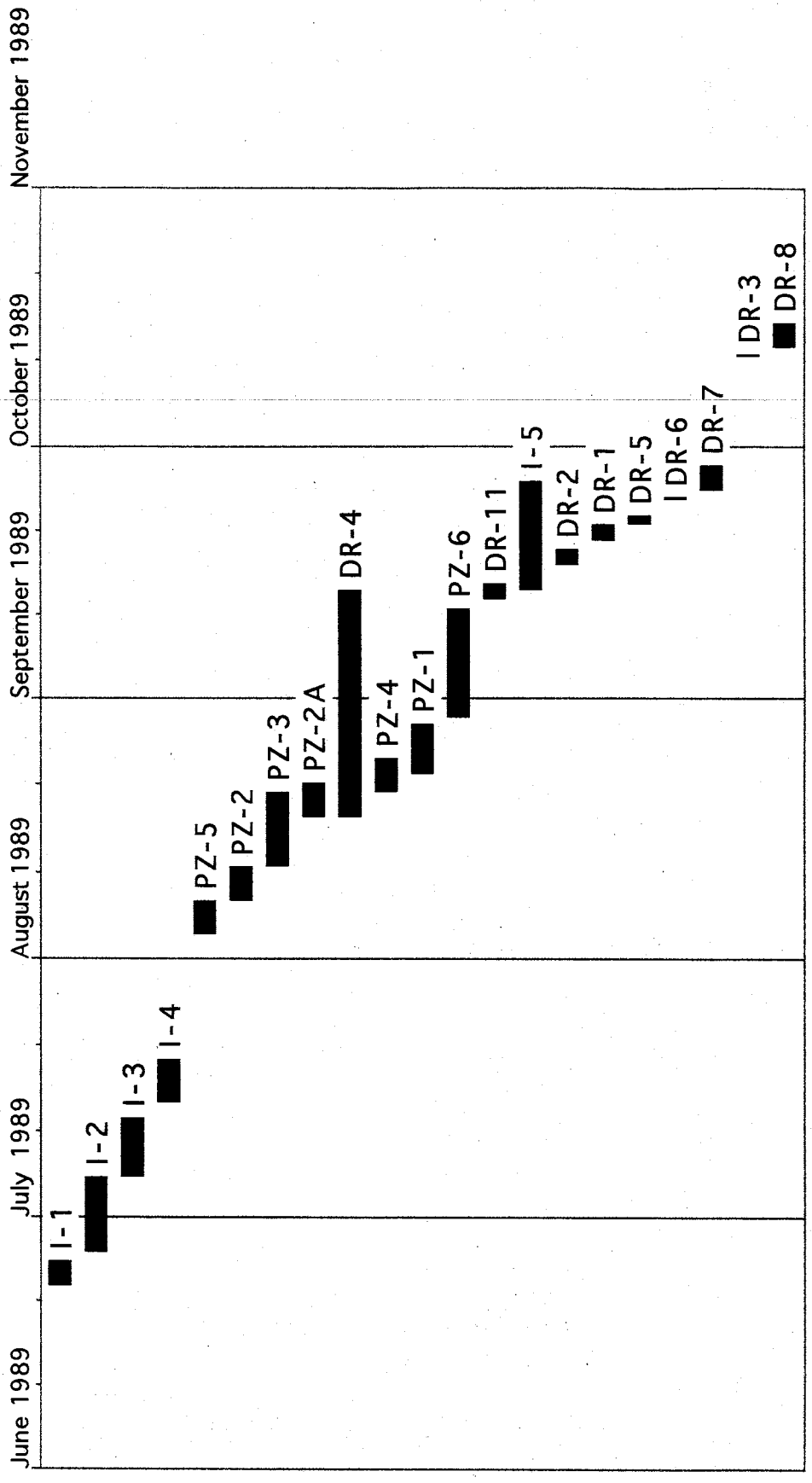

Figure 7 Instrumentation Installation Timeline. Details of the instrumentation installation chronology for the 1989 field season. I- indicates an inclinometer, PZ- indicates a piezometer, DR- indicates a horizontal drain.

piezometers indicated that confined groundwater conditions existed below the slide plane in a number of the holes (DH-18, DH-19, DH-20, DH-24, possibly DH-22 [USBR, 12/1986], I-2, and PZ-2A [USBR, 11/1989]).

No core was logged during this phase of drilling, so the information can not be used to corroborate a three-dimensional model for the geology of the site. The horizontal drains were drilled after most of the piezometers were installed (Figure 7). Water discharged from the hillside through the horizontal drains is removed from the slide surface by means of corrugated drainage channels or unlined surface ditches. Discharge from the drains was measured at the same time as piezometer measurements.

2.4 STREAM GAUGING STATIONS

USGS stream gauging stations are located on the three largest tributary drainages flowing into Costilla Reservoir and on Costilla Creek immediately downstream from the dam. The tributaries contributing to Costilla Reservoir in order of increasing size are Santistevan Creek, Casias Creek, and Costilla Creek. The location of the creeks and stream gauges are depicted in Figure 8. Data for each stream gauge are summarized in Appendix IV. The approximate drainage area for the dam is 141.4 km^2 (54.6 mi^2) (Bovay Engineers, 8/1978; USBR, 9/1985). The three tributary stream gauges cover about 80% of the drainage area contributing to the reservoir. The flow passing the stream gauge on Costilla Creek below the reservoir is controlled exclusively by the amount of water released from the dam. Stream flow is only recorded during the summer field season when the gauges can be driven to.

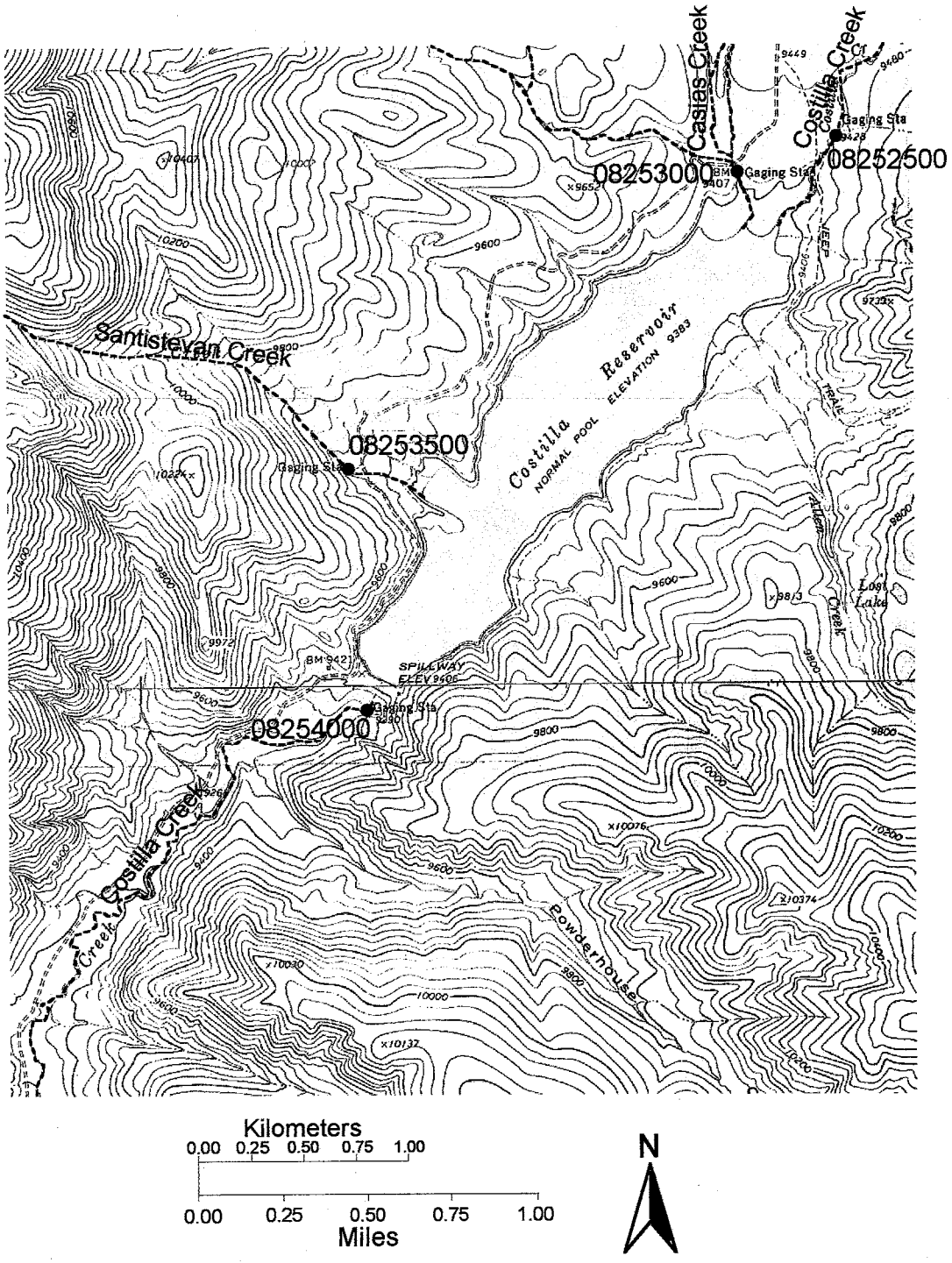

Figure 8 Stream Gauge Locator Map. Shows monitored streams flowing into and out of Costilla Reservoir. The numbers shown are the unique USGS stream gauge identifiers.

2.5 SITE RAIN GAUGE AND NORTH COSTILLA SNOTEL STATION

A manual rain gauge is located just downstream from the dam, near the relocated stream gauging station #08254000 (Figure 8). Fairly complete records exist for the 1989, 1993, and 1994 field seasons. The 1989 and 1994 data were collected on a daily basis over the course of each field season. The early part of the season for 1993 was monitored daily, but toward the end of the season a single reading was made on a weekly basis. In 1994, the rain gauge was missing a funnel located at the top of the collection tube since the first week of observations (McKeen, 8/2/1994). It is assumed that this report meant the first week of the 1994 field season and not the life of the rain gauge. The report also suggested that subsequent readings could have recorded less precipitation than actually occurred.

The North Costilla snotel station (#05N16S) is located at latitude 37 degrees north and longitude 105 degrees 16 minutes west approximately 14 kilometers (9 miles) north of the landslide. The station is at 3230 meters (10600 feet) elevation within the drainage basin of Costilla Reservoir. This station records all forms of precipitation collected daily throughout the year.

3. GEOLOGY

The geologic observations and interpretations included in this chapter are concerned primarily with the geology and hydrogeology of the Costilla Dam landslide. Other geologic observations that were made, but do not directly relate to the Costilla Dam landslide, are included separately in Appendix V.

3.1 REGIONAL GEOLOGY

The Costilla Dam landslide is located in the Sangre de Cristo Mountains of north central New Mexico, which are a southern extension of the Rocky Mountains. Major geologic features in the area include the Rio Grande rift to the west and the Questa caldera to the southwest. Geologic processes related to the rift and caldera are major contributors to deposits in the vicinity of the landslide. Geologic units range in age from Proterozoic basement rock to present alluvium (Lipman and Reed, 1989). Prior geologic mapping in the vicinity of the dam and landslide has been very limited. The first published geologic map of the area was produced by McKinlay (1956), who completed his map based on field work performed from 1947-1950. The stated purpose of McKinlay's investigation was to "delineate any areas of ore mineralization and to gather detailed information on the geology". The map covers the area surrounding the Costilla Dam landslide, but lacks structural detail in many of the units related to it. McKinlay was not concerned about landslides, and did not map any.

A more recent 1:48,000 scale map was completed by Lipman and Reed (1989). Their map ends just south of the dam and does not include the Costilla Dam landslide. Lipman and Reed's map shows glacial moraine deposits just downstream of the dam site, which was later determined to have been misidentified (W.C. Haneberg, pers. comm., 1998). Misinterpretation of the Costilla Dam landslide complex, as a glacial moraine, was what eventually led to the reactivation of the Costilla Dam landslide. So, a new interpretation of these deposits was needed.

During rehabilitation of the dam in the late 1980s, the United States Bureau of Reclamation conducted a limited surface and subsurface geologic investigation of the dam site (USBR, 12/1986). The result was a geologic map that was very similar to McKinlay's map, with the addition of the Costilla Dam landslide complex mapped as glacial moraine deposits.

3.2 DECISION TO PERFORM GEOLOGIC MAPPING

The area around Costilla Dam had never been mapped in detail. Using available subsurface data from the various drilling programs, a more detailed geologic map of the area would assist in the understanding of the dam site geology and hydrogeology. Specifically, the field investigation was undertaken for the following reasons:

1. Create an accurate and detailed geologic map of the area surrounding Costilla Dam and landslide.
2. Gain a better understanding of the subsurface geology.
3. Identify geologic controls on ancient and recent movement of the Costilla Dam landslide.

4. Determine the geologic controls on groundwater flow in and around the landslide.

A map area substantially larger than the Costilla Dam landslide was selected (19.5 km^2, 7.5 mi^2) (Figure 9 and 10). The southern extent of the map area overlapped Lipman and Reed's map so that I could identify their units and then carry them onto my map area. The field area spanned two 1:24,000 scale USGS 7.5-minute quadrangles: the southeast corner of Big Costilla Peak (N. MEX. – COLO.), and the northeast corner of Comanche Point (N. MEX.). Geologic mapping was performed during the summer of 1998, and required under three weeks to complete.

3.3 STRATIGRAPHY

In this section, the geologic map units are arranged and described in a relative stratigraphic order, as opposed to a true chronological order, from the bottom of the section to the top (Figure 10). In a sedimentary section this would also be in chronological order, but because there are sills in this section, the chronological order would be slightly different. The relative order was chosen to minimize confusion associated with examining the units on the geologic map and cross sections.

3.3.1 Older Units

Older units are described here as those units that lie stratigraphically below the units associated with the Questa caldera. Within the map area this includes the Basement Rock and Older Fluvial unit.

Figure 9 Geologic Map of the area surrounding the Costilla Dam landslide. Geologic units are identified on figure 10 and discussed in detail in the text. Topographic lines from the USGS 7.5 minute, 1:24,000 scale Big Costilla Peak and Comanche Point Quadrangles. Elevation is in feet and the contour interval is 40 feet. Cross Section A-A' is located on the map. The queried polygon in the northwest corner of the map is the extent of a possible landslide deposit.

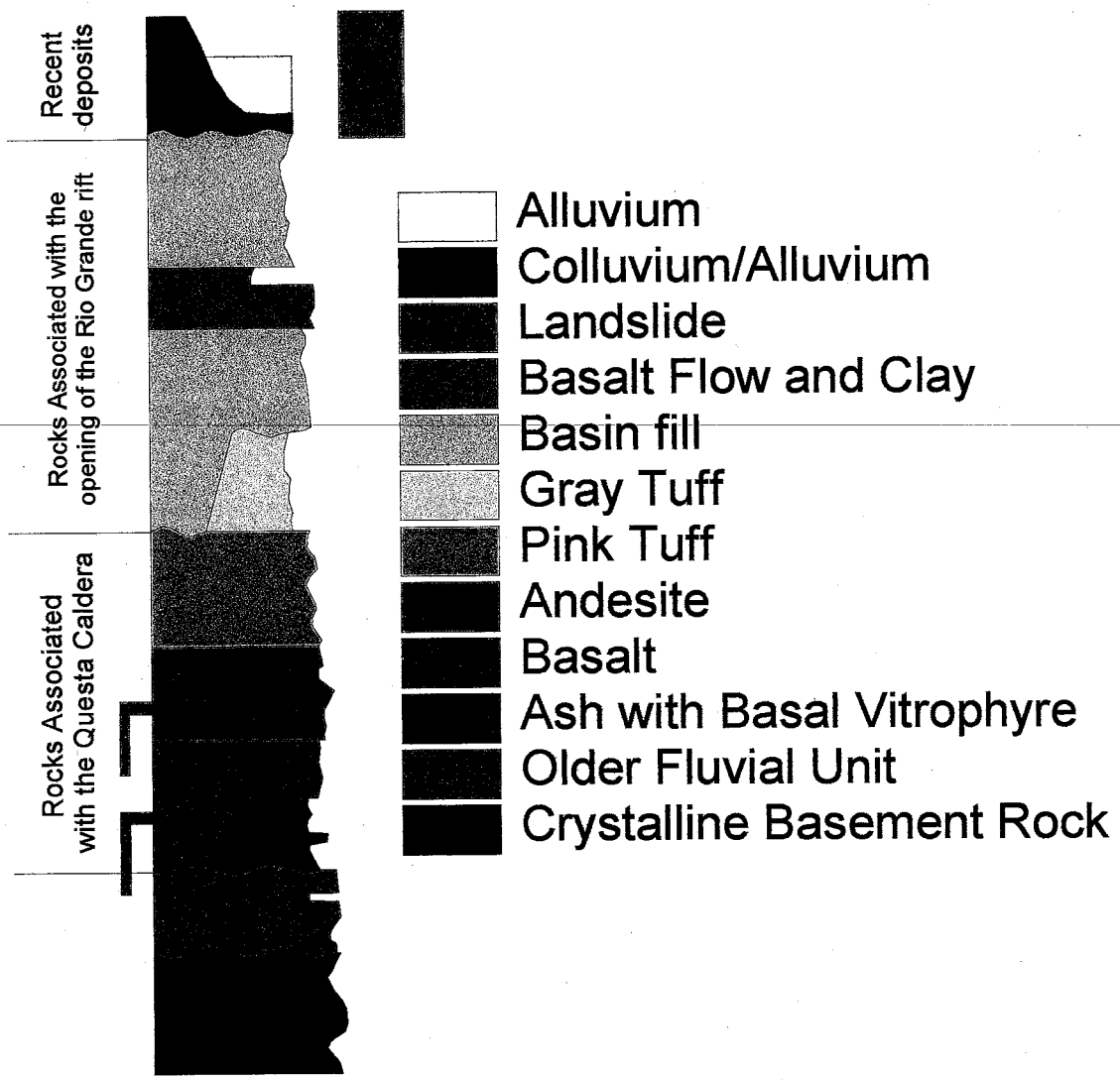

Figure 10 Relative Schematic Stratigraphic Section. Not to scale. The units shown in the stratigraphic section mapped in figure 9 and are described in detail in the text.

3.3.1.1 Basement Rock

Most of the basement rock in this area is Proterozoic crystalline metamorphic rock with some pegmatite (unit Xu of Lipman and Reed, 1989). I identified many different lithologies in the field, but combined them into one unit because of distance from the landslide.

3.3.1.2 Older Fluvial Unit

The Older Fluvial Unit unconformably overlies the basement rock (unit Tps of Lipman and Reed, 1989). This unit is a lower Tertiary (Lipman and Reed, 1989), moderately cemented fluvial unit that contains the following exposed layers:

1. Both a medium and fine-grained quartz-rich sandstone with planar bedding spacings of 2.54 cm (1 inch) to 30.5 cm (1 foot), in some places containing white pumice clasts.
2. A conglomerate with subangular to rounded clasts ranging from sand to 61 cm (2 feet) in diameter. The clasts include granitics, tuff, quartz, ash, gray-green quartzite, and gray-black quartzite.
3. Pistachio green, silty-clay layers.

Lipman and Reed (1984) note that this unit can be identified by the distinctive pale jade-green Precambrian quartzite cobbles, which are the same clasts as the gray-green quartzite clasts described above. The whole outcrop is a distinct light tan-yellow color with areas of rust, mostly in association with the conglomeratic layers. This unit is bounded by unconformities.

3.3.2 Units Associated with the Questa Caldera

The Questa caldera erupted during Oligocene time, and deposited many layers of tuff in the map area. Later, shallowly emplaced sills intruded these tuffaceous layers. The package of units associated with the Questa caldera is bounded by unconformities.

3.3.2.1 Ash with Basal Vitrophyre

The ash is white to light gray with euhedral biotite grains. The unit is partially welded at the base, moving into a ~1.5 m (5 foot) thick basal vitrophyre with about 10% clasts. Up-section from the vitrophyre the unit changes into a welded tuff and finally back into ash. The ash contains a large number of clastic sand-sized grains, and could be mistaken for a sandstone. The vitrophyre is the distinguishing feature of this unit. Lipman and Reed (1984) describe this unit as a thin vitrophyric quartz-latitic welded tuff (unit Twt, Treasure Mountain(?) Tuff of Lipman and Reed, 1989).

3.3.2.2 Basalt

The basalt and andesite units defined in this study were lumped in Lipman and Reed's 1989 map (unit Tai). They describe both units as a shallow sill rather than extrusive rocks. I divided these rocks into two units based on mineral composition. A gradational contact occurs between the two units, suggesting that both were emplaced roughly contemporaneously. The basalt is black on a fresh surface, but greenish-tan-gray on a weathered surface. The unit outcrops as resistant spines in some areas, but usually has a more subdued bulbous form. The resistant spines are near the contact with the Older

Fluvial unit and probably represents a chilled margin of the sill. The unit is non-vesicular, fractured in all directions, and in some places shows a flow banding orientation.

3.3.2.3 Andesite

This unit is light gray in color, massive, and in some places shows faint flow banding (within unit Tai of Lipman and Reed, 1989). This rock has been interpreted as an intrusive sill (Lipman and Reed, 1989), but looks very similar to extrusive andesite. The most noticeable features of this unit are spotty epidote, an unknown brick-red mineral that may be an alteration product, and euhedral hornblende crystals. Some outcrops are very resistant whereas other areas are weak and tend to lie just under the surface cover. An andesitic tuff and maroon colored tuff have been lumped in with the Andesite unit because of their small aerial extent and textural similarities. The individual outcrops of the lumped units are visible in a cliff about 550 meters (1800 feet) WSW of the dam (Figure 9).

3.3.2.4 Pink Tuff

The distinguishing feature of this unit is its pink to brick-red color. This unit can be highly indurated or very friable. The base of this unit is usually a baked contact with the underlying sill of intrusive andesite. Near its basal contact the tuff is very fine-grained with no discernible texture. Higher up in the section, the unit contains plagioclase crystals, quartz crystals, pumice clasts, and vesicles.

3.3.2.5 Gray Tuff

This unit is light gray in color and contains few to many lithic volcanic fragments. No vitrophyre was seen in any of the outcrops, which suggests that it is a different unit than the Ash with Basal Vitrophyre described above. This unit was difficult to place stratigraphically and could be part of an identified or unidentified unit. It crops out at many locations, most commonly lying below the Santa Fe Group deposits (see below).

3.3.3 Units Associated with the Opening of the Rio Grande Rift (Santa Fe Group)

The Santa Fe Group consists of sedimentary and volcanic basin-fill facies deposited during the opening of the Rio Grande rift. Lipman and Reed (1989) correlated the units observed in the field to the Santa Fe Group, and I adopted their terminology for this manuscript. On the geologic map this group is subdivided into a sedimentary facies and a single basalt flow. While both the sediment and basalt flow represent basin-fill deposits, basin fill will from here forth be synonymous with the sedimentary facies of the Santa Fe Group. The package of units comprising the Santa Fe Group is bounded by unconformities.

3.3.3.1 Sedimentary Facies of the Santa Fe Group

This unit is the most common found in the map area (Figure 9). As a whole the unit is very heterogeneous; its deposits are moderately consolidated, weakly stratified, and very rarely cemented with calcite (units Tsc and Tsv from Lipman and Reed, 1989). Grain sizes range from clay to large boulder, with varying degrees of sorting based on depositional environment. Sedimentary facies deposits include: volcaniclastic-rich debris

flow deposits with poorly sorted, angular clasts and very weak stratification (Figure 11); sequences of gravel, with silt and sand layers indicative of channelized flow (Figure 12); silt with cemented coarser-grained sand units; and weakly stratified coarse sand deposits. Lipman and Reed (1989) divided this unit into a volcaniclastic facies and a basement rock-derived facies. I chose not to differentiate these two units due to the lack of outcrop in the study area, the gradational change between the two facies, and the assumption that they have similar hydrogeologic properties. This unit is nonresistant and was identified mainly in road cuts, by examining larger float clasts on the ground surface, and by geomorphologic interpretation. Hydrologically, the unit as a whole probably has a medium hydraulic conductivity from $9x10^{-7} - 6x10^{-3}$ m/sec (Domenico and Schwartz, 1993) and a medium specific storage from $10^{-6} - 10^{-3}$ m^{-1} (Smith and Wheatcraft, 1993).

Two known volcanic deposits are interlayered with the sedimentary deposits, including a thin ash layer and a subaerial basalt flow. The ash layer was lumped in with the sedimentary facies, but the basalt flow is characterized separately as described in the next section. The thickness of the ash layer is 15 to 30 cm (6 inch to 1 foot) and is found east of the andesite outcrop about 550 meters (1800 feet) WSW of the dam (Figure 9). Upstream from the dam-site the contact between the basin fill unit and colluvium/alluvium unit (see below) was difficult to identify. Terraces of the colluvium/alluvium unit in some cases looked like fingers of the basin fill unit, and vice versa.

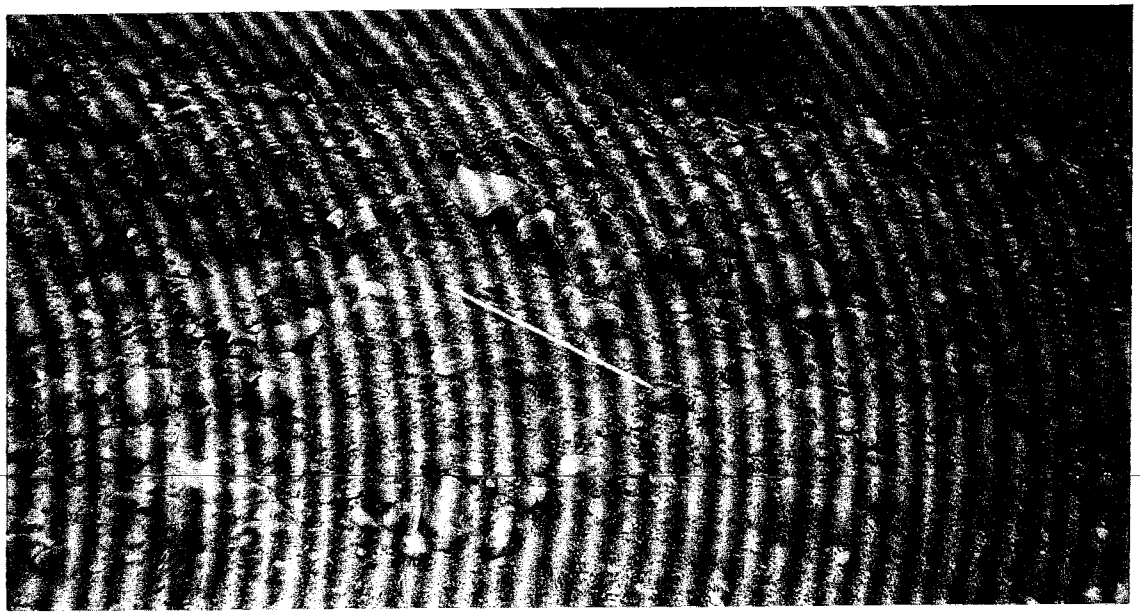

Figure 11 Debris Flow Facies of the Sedimentary Facies of the Santa Fe Group. Deposit is highly heterogeneous and poorly sorted with material ranging from clay to large boulders. Five foot long staff is aligned with very weak stratification.

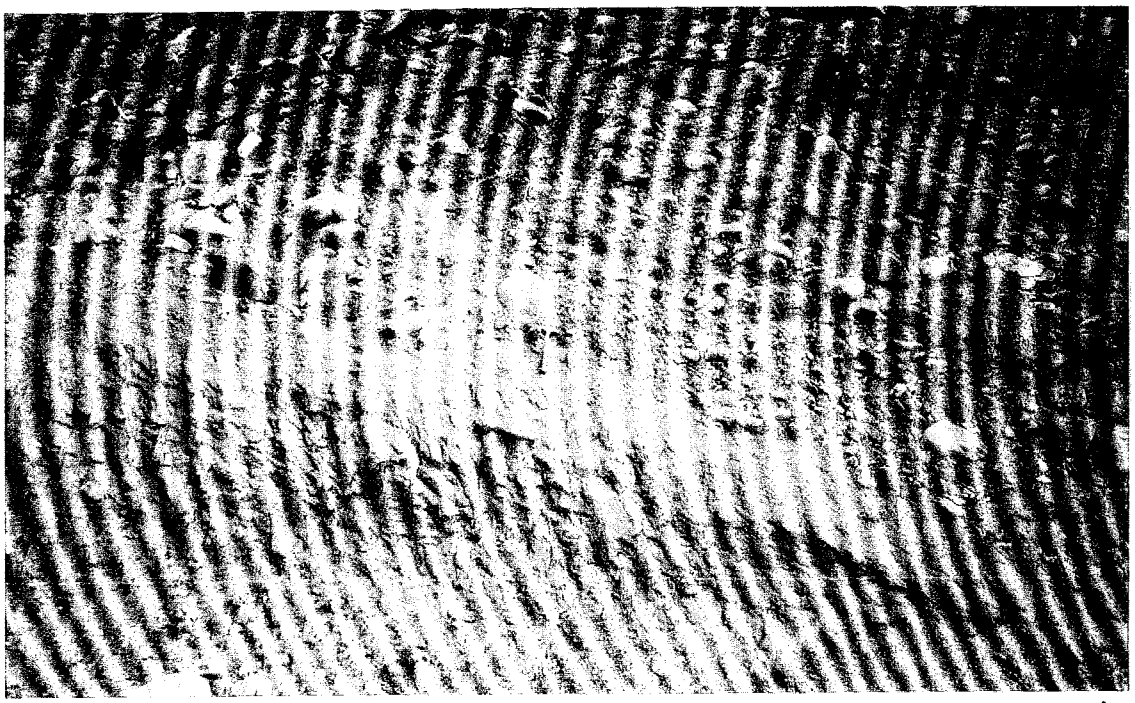

Figure 12 Fluvial Facies of the Sedimentary Facies of the Santa Fe Group. Deposit shows distinct bedding with silt and sand layers overlain by channel gravel. Rounding of the gravel ranges from subrounded to rounded. Rock hammer for scale. Location of photo shown on figure 4.

3.3.3.2 Basalt Flow and Clay within the Santa Fe Group

An approximately 0-14 m (0-45 foot) thick basalt flow occurs within the Santa Fe Group deposits (unit Tbx of Lipman and Reed, 1989). The unit is black to dark gray with different features at different locations. The flow can be vesicular, non-vesicular, scoriaceous, and fresh to highly weathered. The vesicles resemble flattened ellipsoids and some are filled with yellow or white calcite. The unit is highly fractured, mainly parallel and perpendicular to its current orientation strike and dip. An outcrop in a road cut above the top of the Costilla Dam landslide was so fractured and weathered that it could scarcely be identified as a basalt flow. Even though it was not observed in outcrop, many well logs obtained during the previous New Mexico State Highway Department (1984) and United States Bureau of Reclamation (1986) subsurface investigations report a greenish-gray clay directly above the basalt flow. The clay may be a buried paleosol originating from the subareal weathering of the basalt flow. Whatever its origin, the clay zone is an important feature in the geology of the Costilla Dam landslide. The basalt flow is a useful tracer bed for the important but unmappable clay. For this reason the basalt flow and clay are mapped as a single unit. This unit might have two different hydrologic properties. The clay layer likely has a very low hydraulic conductivity from $5x10^{-11}$ – $1x10^{-9}$ m/sec (Domenico and Schwartz, 1990) with a very high specific storage from 10^{-4} – 10^{-2} m^{-1} (Smith and Wheatcraft, 1993). The basalt flow might have a medium hydraulic conductivity from $8x10^{-9}$ – $3x10^{-4}$ m/sec (Domenico and Schwartz, 1990) with a low specific storage from 10^{-5} – 10^{-7} m^{-1} (Smith and Wheatcraft, 1993) due to the highly fractured nature of the outcrop. However, if clay from above the basalt flow has filled the fractures, then this whole unit could have properties similar to the clay layer.

3.3.4 Recent Deposits

Recent deposits are defined as any deposit that was deposited after the conclusion of deposition of the units associated with the opening of the Rio Grande rift. Within the map area this includes the Colluvium/Alluvium, Alluvium, and Landslide Deposit units.

3.3.4.1 Colluvium/Alluvium

This is a very diverse unit containing material that fills tributary valleys in the area (unit Qc of Lipman and Reed, 1989). Geomorphic features that would fall under this category include talus slopes, alluvial fans, older abandoned terraces, and current tributary valley-fill surfaces. The surface of this unit is usually slightly hummocky even though it may be graded like a true alluvial surface. This unit includes all grain sizes up to several meters in diameter, and also organic-rich soil horizons, both current and buried. Most but not the entire unit is unstratified, and the observed stratification suggests an alluvial origin for some of the deposits. The climate of the field area provides around 70 cm/yr (27 in/yr) of precipitation, possibly causing deposited alluvial material to creep downslope, and become colluvium. This unit is bounded by unconformities. Along the Costilla Valley this unit likely has a very high hydraulic conductivity from $1x10^{-5} - 1x10^{-2}$ m/sec (Domenico and Schwartz, 1990) and a low specific storage from $10^{-4} - 10^{-6}$ m^{-1} (Smith and Wheatcraft, 1993).

3.3.4.2 Alluvium

This unit consists of stratified fluvial deposits clay, silt, sand, and gravel up to about 15 cm (6 inch) diameter that are subrounded to rounded in shape (unit Qal of Lipman and Reed, 1989). Sand and gravel deposits are channel facies, while clay and silt deposits represent overbank facies. At the surface, this unit forms the flat valley bottom along the axis of the Costilla Creek valley. This unit unconformably overlies all units in the map area. Hydrologically this unit likely has a high hydraulic conductivity from $9x10^{-7} - 1x10^{-3}$ m/sec (Domenico and Schwartz, 1990), low specific storage from $10^{-6} - 10^{-4}$ m^{-1} (Smith and Wheatcraft, 1993), and low specific yield (0.20 – 0.30).

3.3.4.3 Landslide Deposit

Geomorphically, landslide deposits in the area can be identified by:

1. Hummocky surface features
2. Blunt, steeply-dipping noses
3. Masses of unconsolidated sediment protruding from a valley wall, sometimes forcing streams to the other side of the valley
4. Scarps or hollows from which the material was derived
5. A lower slope angle than surrounding hillsides
6. Vegetation on the shallower dipping surfaces, toward the center of the landslide mass, is usually limited to grasses with no tree growth.

Landslide deposits in this area possess most if not all of the above characteristics (Figures 13 through 15). Withholding the recent reactivation of the Costilla Dam landslide, other landslides in the study area do not reflect evidence of recent movement,

Figure 13 Outlet works slump located across the valley from the Costilla Dam Landslide. The landslide is outlined downstream from the dam by grass vegetation in the midst of the pine forest. Costilla Dam can be seen in this picture. The new spillway lies on top of the toe of the reactivated Costilla Dam landslide and stabilization berm.

Figure 14 Powderhouse Canyon landslide. The landslide located in the center of the picture can be identified by the hummocky surface, blunt nose, protrusion into the valley, and the dominance of grass on the surface of the landslide. For location of the landslide see figure 4.

Figure 15 Landslide east of Costilla Reservoir. The landslide located in the left-center of the picture can be identified by the hummocky surface, blunt nose, protrusion into the valley, and the dominance of grass on the surface of the landslide. For location of this landslide see figure 9.

Figure 16 Outcrop of Costilla Dam landslide complex deposit. This landslide deposit is unstratified, poorly sorted, and contains material derived from the parent sedimentary facies of the Santa Fe Group. Outcrop located just upstream of the dam. Rock hammer for scale. For location of photo see figure 4.

such as fresh surface cracks, pressure ridges, or fresh head scarps and appear dormant under current conditions. The large queried deposit in the northwest corner of the geologic map (Figure 9) has features that suggest it is a landslide deposit, but it was not determined for sure if it was a landslide. All landslide deposits identified in the area were derived from the basin fill unit, as indicated by the geologic map, suggesting its susceptibility to slope instability (Figures 9). The deposits are unstratified and contain material consistent with the parent unit from which they were derived (unit Ql of Lipman and Reed, 1989). The only exposure of landslide material is from the Costilla Dam landslide complex (Figure 16), in a roadcut located just up valley from the right abutment of Costilla Dam. Since the landslide deposits are derived from the sedimentary facies of the Santa Fe Group, their hydrologic properties are likely very similar. Therefore, the landslide deposits could have a medium hydraulic conductivity from $9x10^{-7} - 6x10^{-3}$ m/sec (Domenico and Schwartz, 1990), medium specific storage from $10^{-6} - 10^{-3}$ m^{-1} (Smith and Wheatcraft, 1993), and a medium specific yield (0.20 – 0.40).

3.5 STRUCTURE

Geologic structures in the field area are both simple and complex. Cross section A-A` was located where the structure was very simple to lay the groundwork for the more complex geology of the landslide (Figure 9). The rock units in the field area dip to the east (Figures 9 and 17). Foliation of the metamorphic rocks dips from northwest to southwest, usually around 40 degrees. Because the basement rock crops out on the west side of the map area, the foliation dips into the hillside and away from the landslide.

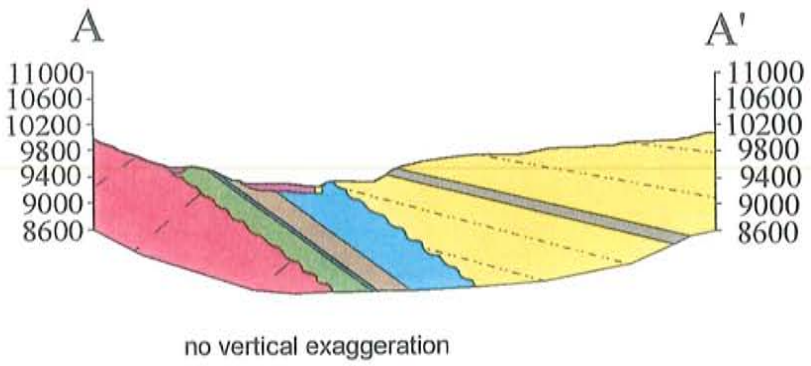

Figure 17 Cross section A-A'. The cross section line is shown on the geologic map (Figure 9), and this figure is to scale. Note the dip of all units to the east. The units can be identified based on their color in figure 10.

Unconformities separate many of the units within the map area, but have little influence on structure and no discernable influence on slope instability; therefore, they will not be discussed further. While rocks associated with the Questa caldera crop out just downstream of the dam, they are not exposed in the vicinity and upstream of Costilla Dam. Upstream of this point the dominant rock unit is the Santa Fe Group. A fault probably separates the Questa caldera and Santa Fe deposits in this location.

As with all other rock units, the Santa Fe Group generally dips to the ENE. The Santa Fe Group was deposited in many different depositional environments by a variety of mechanisms. Adjacent to the andesite outcrop the basin fill unit appears to consist of talus, alluvial fan, and debris flow facies with sub-angular to angular volcanic clasts up to large boulder size. At this location the deposit dips 40 degrees, which is the steepest dip observed for the Santa Fe Group in the map area. Farther to the northeast, on the north side of the Costilla Dam landslide complex, the unit changes from debris flow facies to well-stratified fluvial deposits (Figure 9 and star on Figure 4). The dip of the deposit generally decreases with distance from the andesite outcrop. Santa Fe Group deposits on the ridge north of Powderhouse Canyon (Figure 9) are horizontal and appear to be fluvial channel and overbank deposits. Approximate paleocurrent directions obtained using the orientation of channel deposits suggests that the river system was aligned in a NNE-SSW orientation (which is the same as the current drainage). The flat-lying fluvial deposits found at the top of the ridge could be the deposits of a fledgling through-flowing drainage for the valley. When through-flowing drainage was established, incision marked the end of Santa Fe Group deposition and began to form the present day valley. This same pattern is observed along the Rio Grande rift with the ancestral Rio Grande (Lozinsky, 1994).

Since Costilla Creek drains into the Rio Grande rift, fluctuations in the level of the ancestral Rio Grande may have influenced the ancestral fluvial system in the valley.

3.6 GEOLOGY OF THE LANDSLIDE

The arbitration panel (chapter 1) determined that the Costilla Dam landslide complex should have been identified during pre-rehabilitation geologic investigations. This study has the advantage of hindsight along with information gathered by inclinometers, additional well logs, syn-movement observations, and the findings of post-movement reports. A conceptual geologic model was assembled using aerial photo interpretation, geologic mapping, analysis of well logs, interpretation of hydrogeologic data, and review of prior work on the landslide.

As with all landslides identified in the area, the Costilla Dam landslide complex is derived solely from the sedimentary facies of the Santa Fe Group. A number of landslides were mapped in the field area with two in the immediate vicinity of Costilla Dam (Figure 9). The Costilla Dam landslide complex is located to the NW of the dam and forms the dam's right abutment. A slump is visible in aerial photos across the valley from the Costilla Dam landslide complex (Figure 4). A vegetation change from trees to grass highlights the old lateral and head scarps. This landslide will be referred to as the outlet works slump. The history of the outlet works slump is likely related to that of the Costilla Dam landslide complex and will be explored later in more detail.

Three detailed cross sections of the Costilla Dam landslide were constructed from surficial geology and well logs (Figure 18). Cross section B-B` (Figure 19) coincides

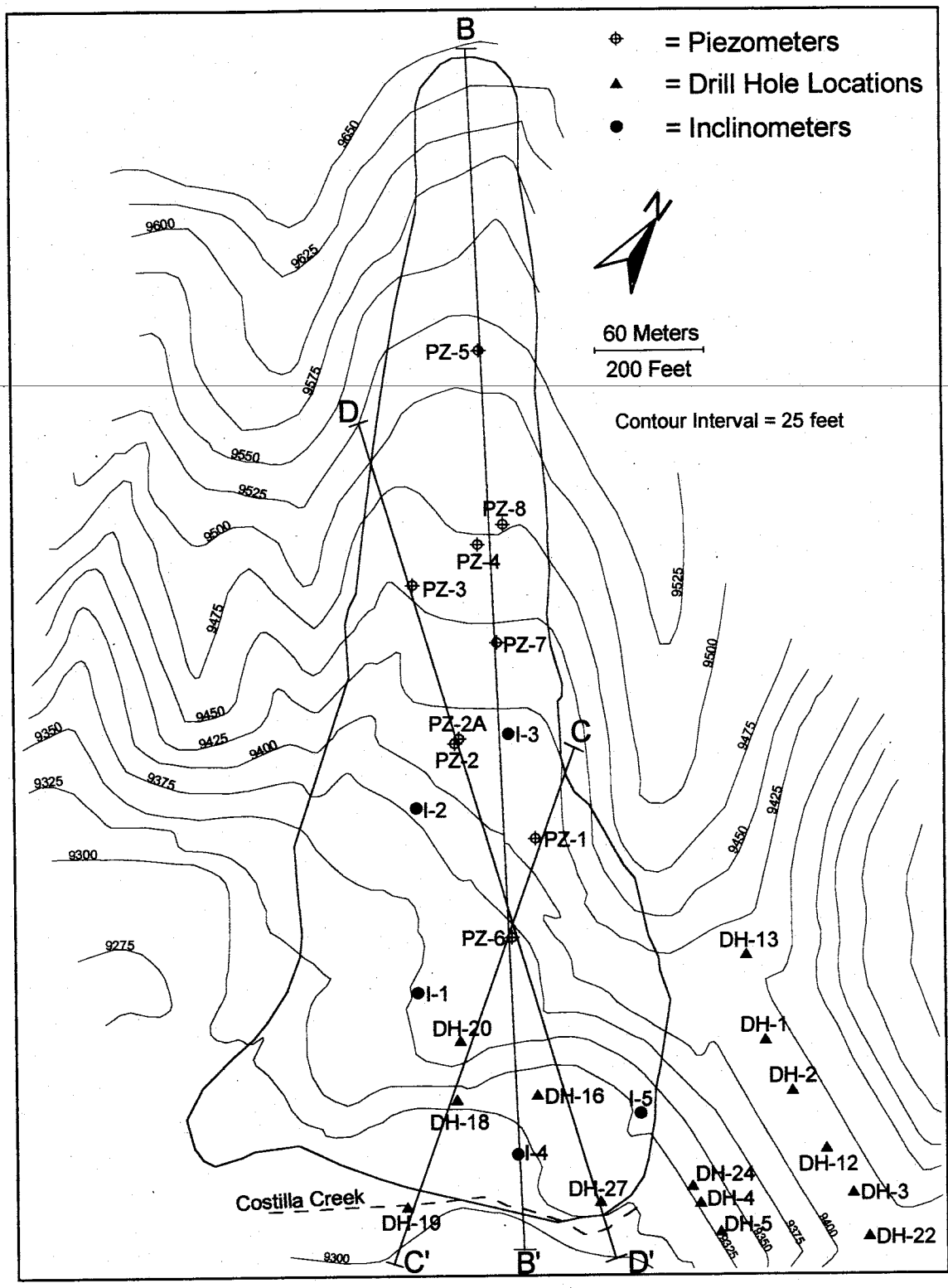

Figure 18 Site topographic map with cross section lines. This figure shows the location of landslide instrumentation and cross section lines on the Costilla Dam landslide.

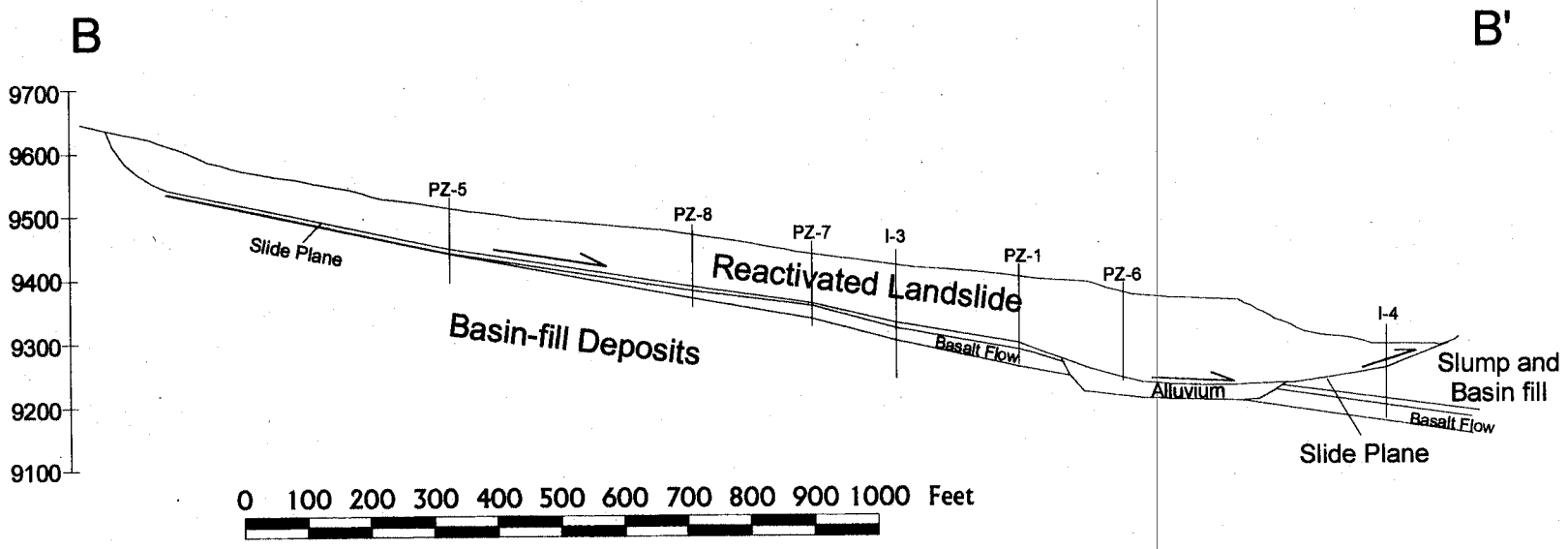

Figure 19 Cross Section B-B'. This cross section shows the longitudinal profile of the Costilla Dam landslide. Note the dip of the basalt flow and associated clay approximately parallel to the ground surface.

with the axis of the landslide while cross sections C-C` and D-D` (Figures 20 and 21) are oblique to the landslide to help examine the lateral margins. The rest of this section is devoted to the detailed examination of the Costilla Dam landslide complex.

Two old arcuate head scarps of the landslide complex are evident at the crest of the hillside, in aerial photos. The western scarp is a full arc while the eastern scarp is partial (Figure 4). This cross cutting relationship suggests that the eastern landslide moved first and its head scarp was subsequently truncated by activation of the western landslide. The toe of the landslide complex has been obscured by Costilla Creek through erosion and fluvial reworking. However, during movement of the Costilla Dam landslide, a pressure ridge developed near the opposite side of the valley bottom (Figure 18). The location of the landslide toe suggested correctly that the landslide was deep-seated. The northeastern (left) lateral margin of the complex was identified through both topography and geologic mapping. The topography of the valley changes abruptly where the landslide protrudes onto the otherwise broad valley floor (Figure 9 and 4). Also, a small gully has formed at this location (Figure 22). In road cuts on the lower road, the gully separates an unstratified landslide deposit (Figure 16) from a well-stratified basin-fill deposit (Figure 12).

Outcrops of the Basalt Flow with Clay Layer Unit define the southwestern (right) lateral margin for both the Costilla Dam landslide and landslide complex. At the surface, the basalt flow dips around 30 degrees to the east, which is both down the hill and under the landslide (Figure 9).

Inclinometers 1 through 4 provide valuable information about the properties and mechanics of the Costilla Dam landslide. Inclinometer 5 was installed after landslide

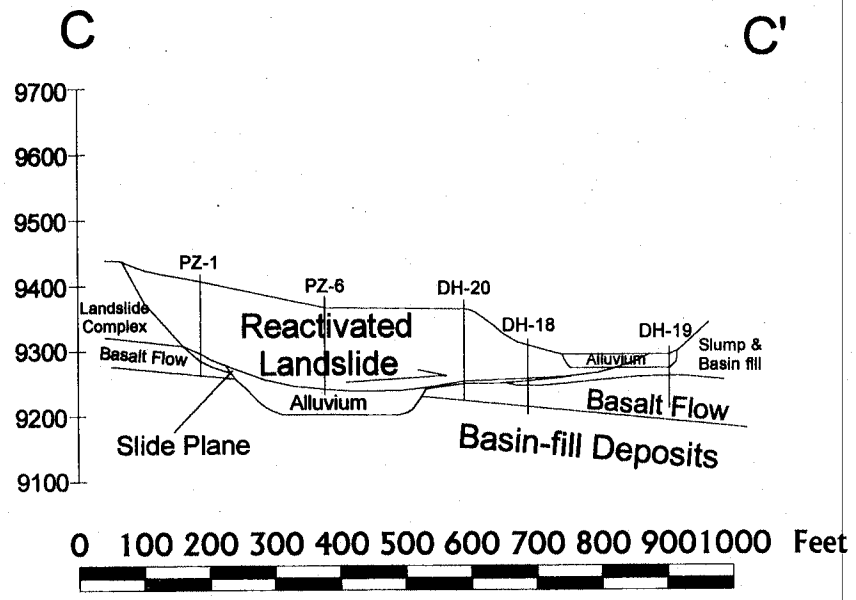

Figure 20 Cross Section C-C'. This cross section shows the northeast (left) lateral margin of the Costilla Dam landslide. The lateral margin is fairly steep as compared to the right lateral margin in figure 21. Note how PZ-6 should identify the basalt flow but does not.

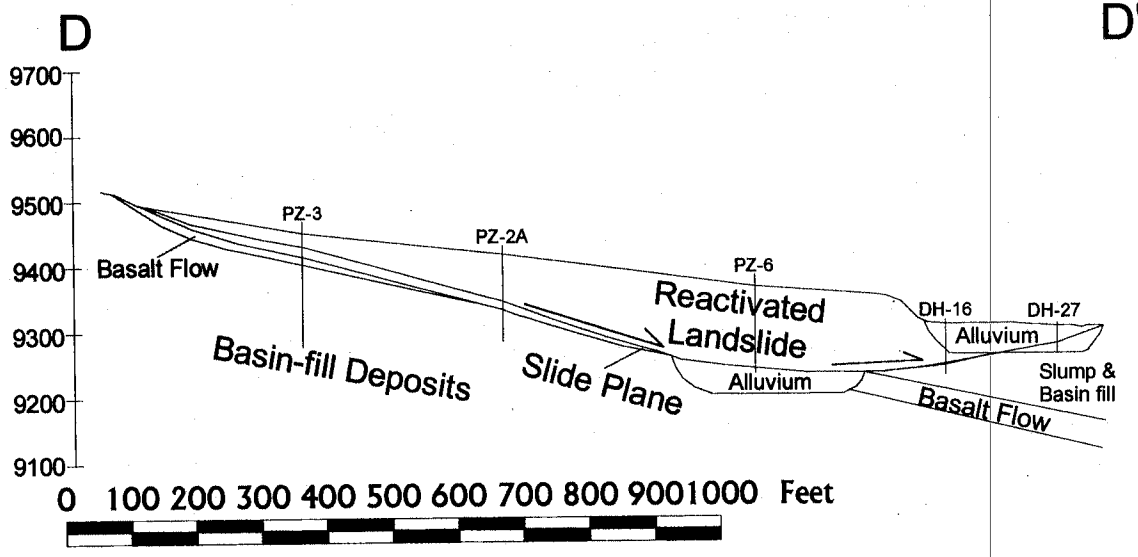

Figure 21 Cross Section D-D'. This cross section shows the southwest (right) lateral margin of the Costilla Dam landslide and landslide complex. Note how the basalt flow is folded near the edge of the landslide and the thin nature of the landslide deposit at this margin as compared to the left lateral margin in figure 20.

Figure 22 Gully defining lateral extent of Costilla Dam landslide complex. The gully located in the center of the picture is the northeastern lateral margin of the Costilla Dam landslide complex at the location of the star in figure 4. To the left of the gully when looking uphill is the landslide deposit photographed in figure 16, while to the right is the fluvial facies deposit of the Santa Fe Group photographed in figure 12.

movement ceased and therefore does not directly identify the slide plane as did inclinometers 1 through 4. Appendix VI contains plots of data obtained from the monitoring of the inclinometers. The term "slide plane" is actually incorrect for the base of the landslide, because the inclinometers show it to be from 6 to 10 ft thick, but it will be used with this understanding. The inclinometers show that the landslide is translational with deformation occurring solely within the slide plane (Appendix VI). The geology of the inclinometer logs show that the clay layer above the basalt flow is the basal slide plane when it is present (Appendix II).

Contouring the base of the basalt flow from well logs shows the basalt flow dipping roughly 15 degrees to the east. The dip of the basalt flow in the subsurface is half of that measured at the surface. Multiple measurement points of the basalt's dip indicate that the basalt flow is folded below the Costilla dam landslide near its southwestern (right) lateral margin (Figure 23). This also suggests that low shear strength clay forms the basal and southwestern (right) lateral shear surface of the Costilla Dam landslide.

Contours for the base of the reactivated landslide were estimated using subsurface data collected from the well logs and inclinometers (Figure 24). The landslide is generally thicker toward the left lateral margin than it is toward the right due to the dip of the basalt flow and clay layer. The thickest portion of the landslide lies just downhill from PZ-6, and from this location the landslide thins rapidly toward the toe and gradually toward the head.

The basalt flow is positively identified in a number of the well logs (PZ-1, PZ-7, PZ-8, I-4, DH-18, and DH-19), but not in all. The reason why the basalt flow was not identified could be due to a number of factors. First, the basalt flow may not have been

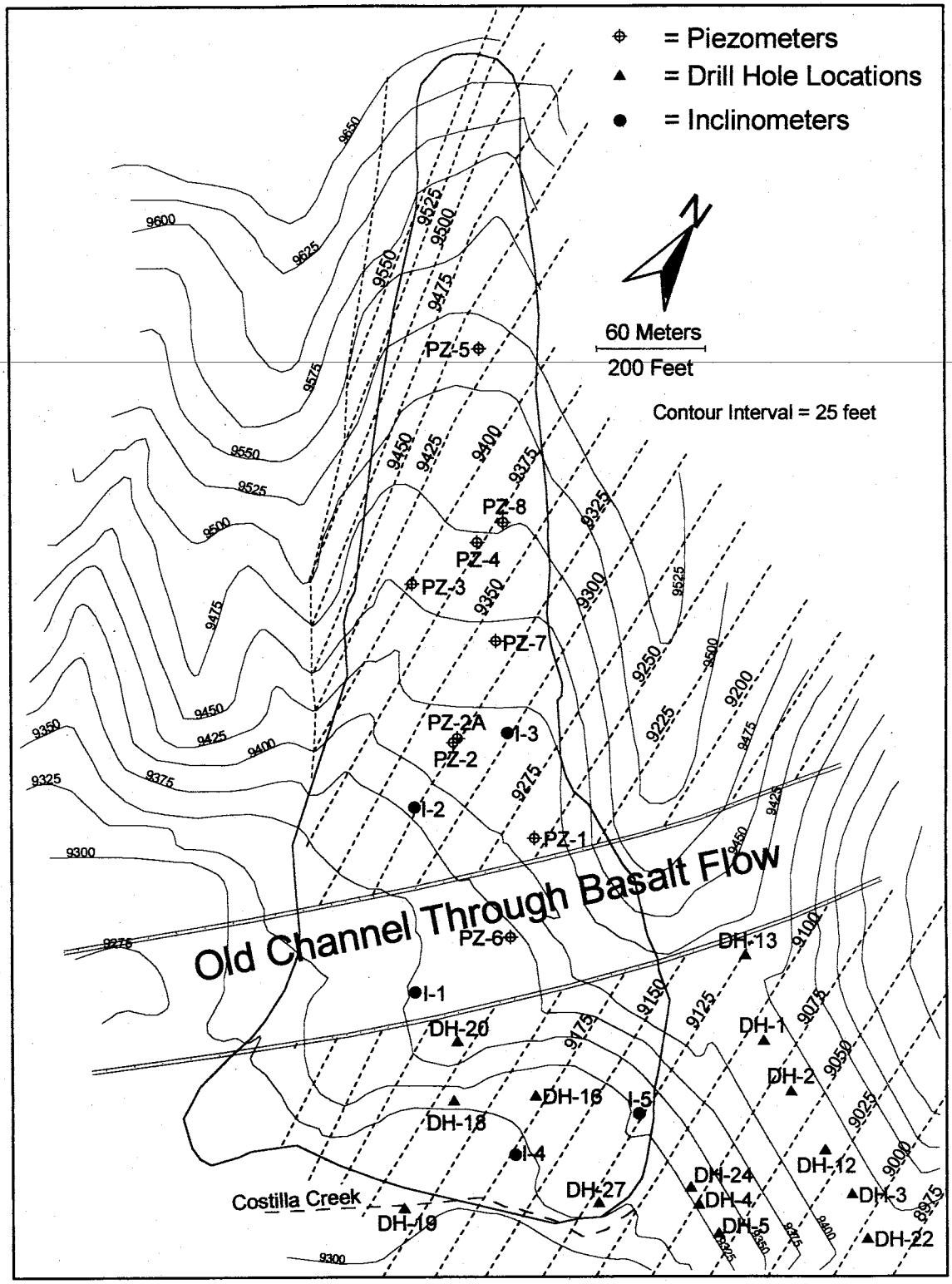

Figure 23 Contours for the base of the basalt flow. The dashed contours are elevations in feet and were created using the location of the basalt flow as determined by outcrop and well log identification. The basalt flow generally dips ~15 degrees to the east, except near the southwestern lateral margin of the landslide where the dip increases to ~30 degrees. The buried channel is likely filled with alluvium and has an important influence on the hydrogeology of the landslide. The solid lines are topographic contours.

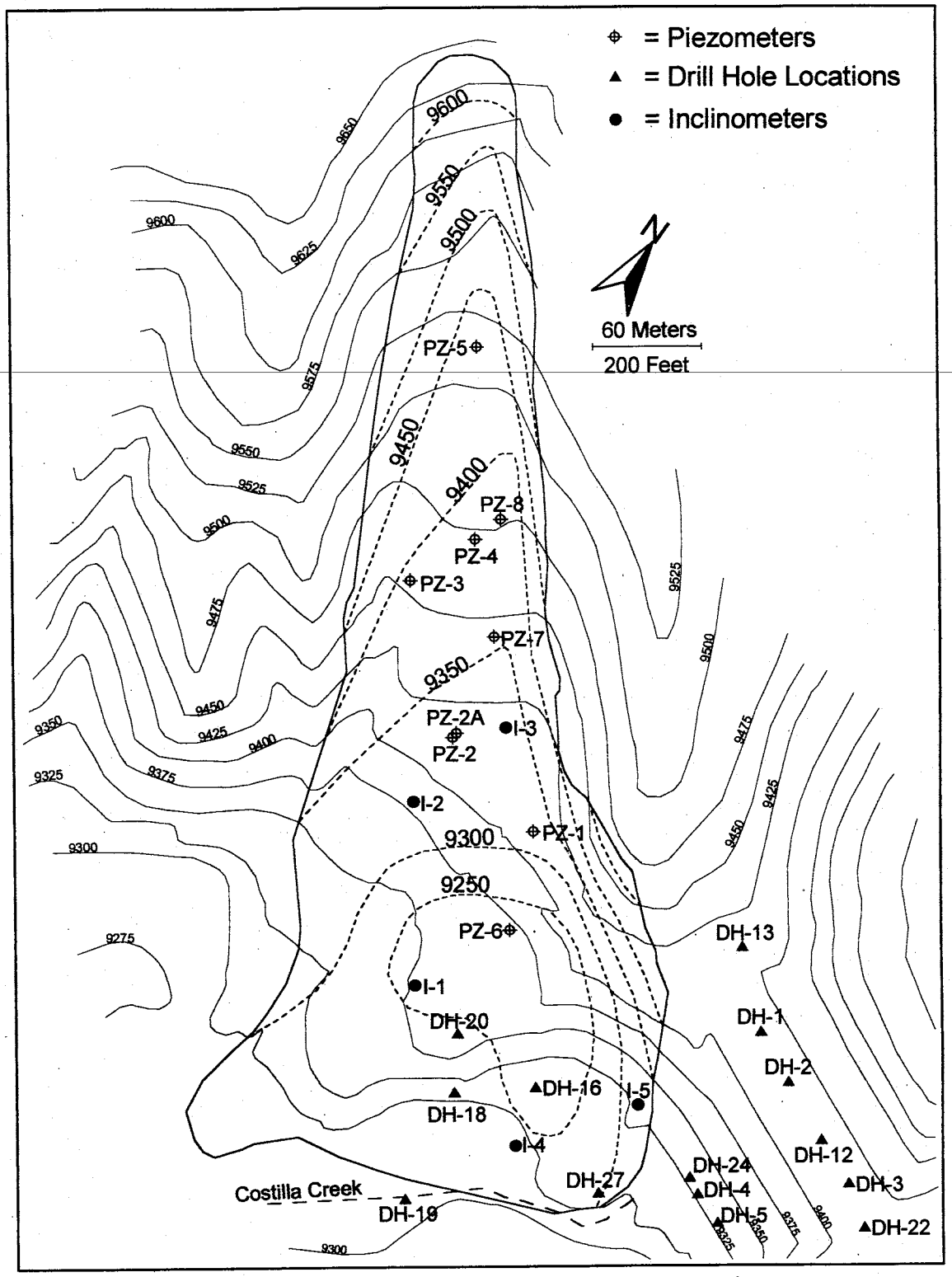

Figure 24 Contours for the base of the Costilla Dam landslide. The contours were created using inclinometer and other well log data. The dashed contours indicate the elevation of the slide plane in feet and the solid lines are topographic contours.

recognized when drilling with the rock bit or was undistinguishable from the basin fill unit or slide plane (probably I-2, I-3, PZ-2A, PZ-3, PZ-4, PZ-5, and possibly DH-20). Second, the basalt flow may have been eroded and does not exist at the location of drilling (PZ-6, I-1, and possibly DH-20). Finally, the well may not have penetrated to the depth of the basalt flow (DH-12, DH-13, DH-16, DH-22, DH-24, DH-27, PZ-2, and I-5).

In all three of the site cross sections (B, C, and D), PZ-6 should penetrate or at least encounter the basalt flow as projected from other spatial basalt flow identifications. Even though the hole was cored through the depth that the basalt flow was projected to be located (Appendix III), no basalt flow was evident. When examining the topography of the valley north of the dam, one can see the Costilla Dam landslide complex projecting out from the otherwise linear valley wall profile (Figures 9 and 4). The current valley profile just downstream of the landslide suggests that the former edge of the valley probably fell between PZ-1 and PZ-6, very near to PZ-1. I infer that Costilla Creek eroded the basalt flow around PZ-6 and I-1 prior to activation of the Costilla Dam landslide complex. On figure 23 I have drawn the approximate location of the buried channel that cuts through the basalt flow. As will be discussed in the hydrogeology chapter, PZ-1L and PZ-6L behave differently than all other lower piezometer completions. Fluctuations in both peak at the same time as the reservoir and they are almost identical to each other. The identical and nearly immediate response of the piezometers to reservoir fluctuations suggests they are in the same hydrogeologic system and that it includes the reservoir. The alluvium that fills the buried channel through the basalt flow and weathered clay would likely have a higher hydraulic conductivity and

lower specific storage than the overlying landslide deposit or underlying basin-fill deposits.

The main factors contributing to the initial activation of the Costilla Dam landslide complex appears to be:

1. The existence of moderately consolidated, and landslide susceptible, basin-fill deposits dipping into the valley.
2. The clay zone above the basalt flow, within the basin-fill deposits, providing a plane of low shear strength for the basal and right shear zones.
3. The clay zone above the basalt flow acting as a hydrologic barrier to infiltration.
4. The removal of material from the toe of the slope by the lateral incision of Costilla Creek.

3.6.1 Geologic History of the Costilla Dam landslide complex

Much of the chronology of events prior to the reactivation of the Costilla Dam landslide agrees with the chronology proposed by United States Bureau of Reclamation geologist Louis Frei (USBR, 11/1989). Figure 25 schematically depicts the events as they are presumed to have occurred.

Costilla Creek followed a meandering as it flowed through the very wide, flat-bottomed Costilla Valley. As the creek laterally incised the northern valley wall in the present day location of Costilla Dam, the Costilla Dam landslide complex was probably activated as two large failures that projected into the valley. As discussed previously, aerial photo interpretation suggests that the northeast failure likely occurred first, followed by the southwest failure (Figure 18). The protrusion of landslide debris into

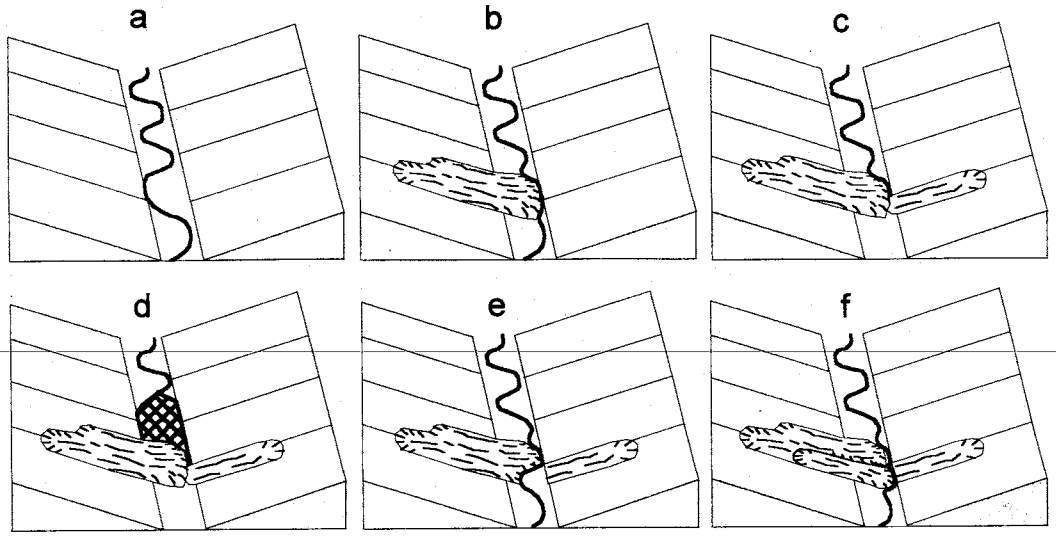

Figure 25 Possible chronology for development of deposits identified near Costilla Dam.

a) Costilla Creek meanders down the valley, laterally incising the valley wall which will be the location of the Costilla Dam landslide complex.
b) The Costilla Dam landslide complex is activated and protrudes into the valley. The landslide deposit forces Costilla Creek against the opposite valley wall.
c) Lateral incision of the redirected Costilla Creek causes the outlet works slump across the valley to activate. The slump does not protrude very far into the valley because it is buttressed against the Costilla Dam landslide complex.
d) A temporary landslide dammed lake possibly formed behind the landslide deposits.
e) After drainage of the temporary lake, Costilla Creek would have probably reassumed its original gradient. Lateral incision proceeded to transport some of the toe of both landslides out of the area. Removal of material at the toe of the landslide reactivates a portion of the Costilla Dam landslide complex. The landslide moves in a translational manner. The portion of the landslide that reactivated was probably very similar to that reactivated through construction activities in the late 1980s.

the valley likely diverted Costilla Creek, causing it to develop a new channel around the toe of the deposit. Thus, lateral incision was focused on the opposite side of the valley. As material was removed from the toe of the opposite slope, instability followed. The outlet works slump was activated but did not travel very far because it was buttressed against the toe of the Costilla Dam landslide complex. Movement of the slump might have created a temporary landslide-dammed lake, but any evidence would be submerged below the current Costilla Reservoir. Drainage of any lake, if it had formed, would proceed and the creek would have attempted to regain its original gradient. The Costilla Dam landslide complex was then stable until once again Costilla Creek laterally eroded the toe of the landslide reducing stability and causing translational reactivation of the southwestern portion of the landslide complex. The landslide that reactivated during this movement is the same as the modern day Costilla Dam landslide. A topographic hollow supports this idea and also indicates that the Costilla Dam landslide was contained within the Costilla Dam landslide complex deposit (Figure 18). The cyclic behavior discussed above probably produced a very complex interfingering of alluvial and landslide deposits in the valley bottom. The reconstruction activities of the late 1980s that led to the reactivation of the Costilla Dam landslide were outlined in Chapter A.

3.6.2 Summary of Factors Contributing to Reactivation of the Costilla Dam Landslide During Construction Activities

In summary, the factors contributing to the reactivation of the Costilla Dam landslide during construction activities were:

1. The existence of moderately consolidated, and landslide susceptible, basin-fill deposits dipping into the valley.
2. The clay zone above the basalt flow, within the basin-fill deposits, providing a plane of low shear strength for the basal and right shear zones.
3. The clay zone above the basalt flow acting as a hydrologic barrier to infiltration.
4. Loading of the landslide surface with stockpiles of building material, which covered existing springs.
5. Excavation at the toe of the landslide to build the concrete emergency spillway and stilling basin. This excavation likely mimicked lateral incision of Costilla Creek.
6. Since this was a dormant landslide, the shear strength of the clay within the slide zone could have been at its reduced residual strength, which would be even weaker than the pre-deformation clay.

4. HYDROGEOLOGY

4.1 INTRODUCTION

The hydrogeology of deep-seated landslides, such as the Costilla Dam landslide, has been studied less than shallow landslides (Haneberg, 1991a, 1991b; Haneberg and Gökce, 1994; Iverson and Major, 1987; Jackson and Cundy, 1992; Sidle, 1984; Sidle and Tsuboyama, 1992; Stephenson and Freeze, 1974). Reasons for this discrepancy may include the ease of instrument installation, difference in response times between shallow and deep landslides to infiltration events, and more feasible characterization of subsurface geology.

The elevation of the Costilla Dam landslide is around 9400 feet (2865 meters). As a result, most precipitation falling between October and May is in the form of snow. Generally the area accumulates a thick snow pack during these winter months. Late spring is usually dry and temperatures increase. Monitoring of stream gauges begins in time to observe the large increase in stream flow, presumably due to snowmelt (Figure 26; Appendix VII). The reservoir collects this runoff with little release until the irrigation season begins around the beginning of June. As a result, the reservoir levels rise until irrigation demands exceed inflow to the reservoir, which in turn decreases the reservoir level to meet demands. During the summer, the southwest monsoon causes an increase in precipitation, mainly in the form of afternoon thundershowers. The storms are usually intense, but short-lived. Much of the precipitation falling during this period is recycled

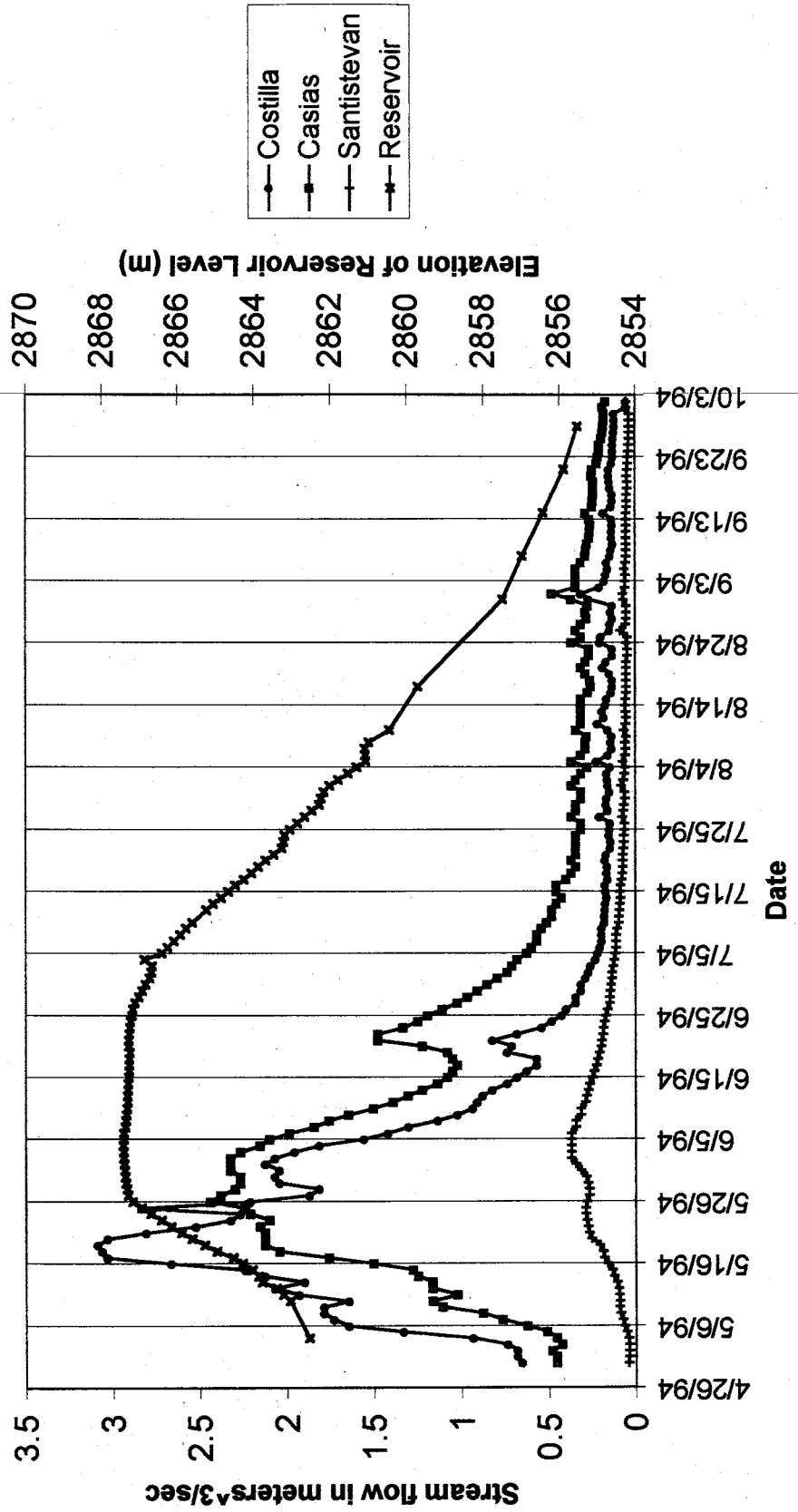

Figure 26 Stream gauge runoff data for 1994. Large peak is from snowmelt runoff, while small peaks after 7/25/1994 are likely from summer thundershowers. For gauge locations see figure 8. Note how the reservoir level rises with the increasing stream flow, but then remains elevated and lowers well after the stream flow has decreased.

through evapotranspiration. The small peaks in runoff after Julian Day 190 (July 9) represent runoff from summer monsoon thundershowers (Figure 26; Appendix VII). The peak flows, caused by snowmelt runoff, are 10 to 70 times larger than the late summer peaks in flow caused by thundershowers. Fall marks the end of the irrigation season, and the return of cooler temperatures and snowfall to the mountains. Each year this cycle repeats with slight variations.

4.2 HYDROLOGY OF THE COSTILLA DAM LANDSLIDE

The nested piezometers record head data for groundwater both within the landslide and below it. The head in the upper piezometers is always higher than in the lower piezometers, indicating the presence of a downward vertical hydraulic gradient. However, when potentiometric surfaces are created for the upper and lower flow domains, groundwater flow is dominantly down the axis of the landslide (Figures 27 and 28).

One difficulty with examining the hydrogeology of the Costilla Dam landslide is that the system has been disturbed by human intrusion. Inclinometers 2-5 had their annuli packed with sand which could increase hydrologic communication across an otherwise impermeable slide plane toward the toe of the landslide (Figure 6 and Appendix II). According to the United States Bureau of Reclamation, piezometer 4 has a leaky bentonite seal at the slide plane (USBR, 11/1989). Piezometer 7 may also have a leaky bentonite seal because it behaves similarly to PZ-4. Finally, 18 horizontal drains were drilled into and through the landslide.

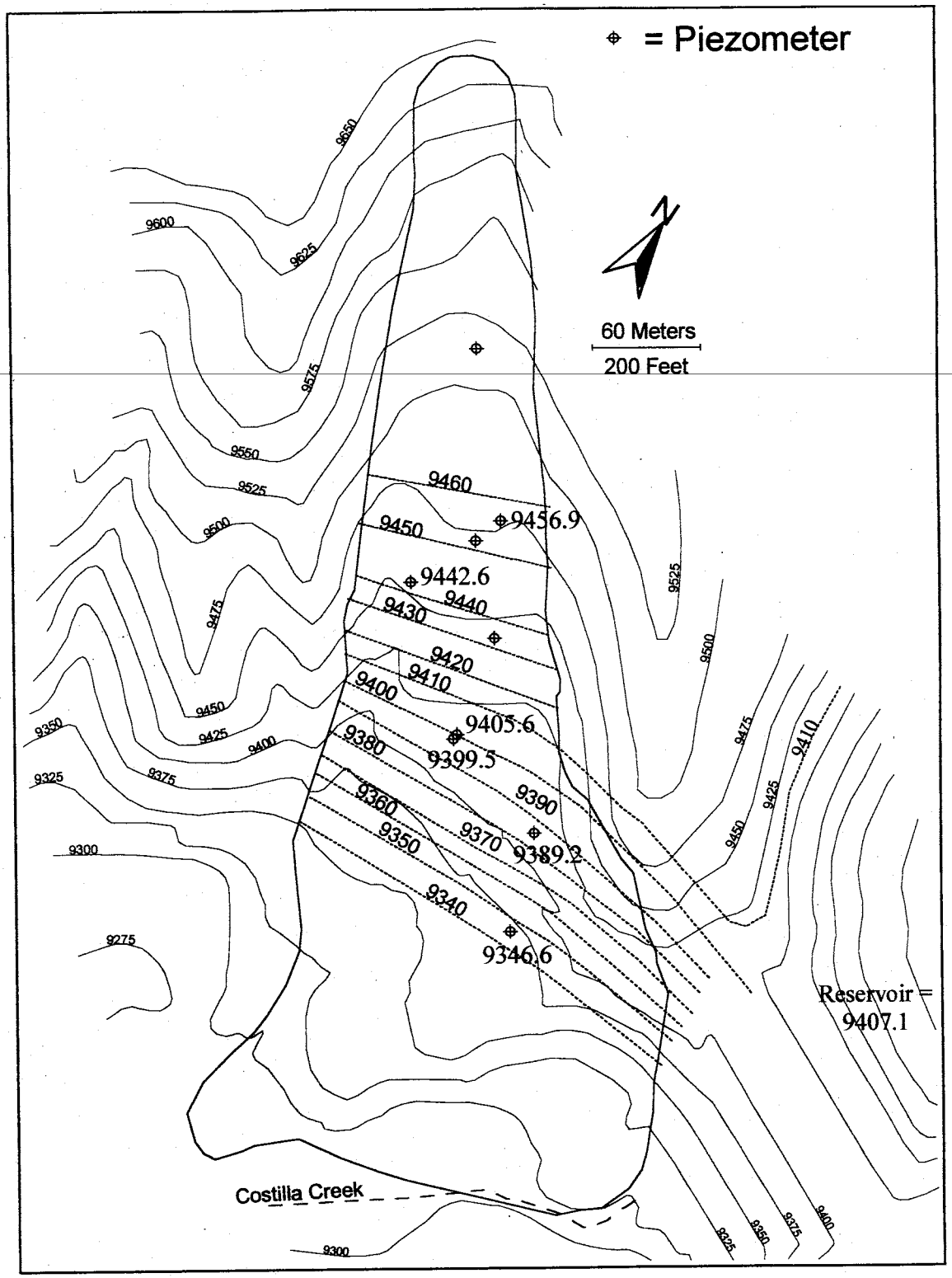

Figure 27 Potentiometric surface for the upper flow domain. This flow domain is within the landslide deposit, as recorded by the upper piezometers. The contours were made for head levels recorded on June 15, 1994 (shown next to each piezometer); excluding piezometers 4U and 7U. The dashed contours show the elevation of the potentiometric surface, and the solid lines show the topographic contours, in feet.

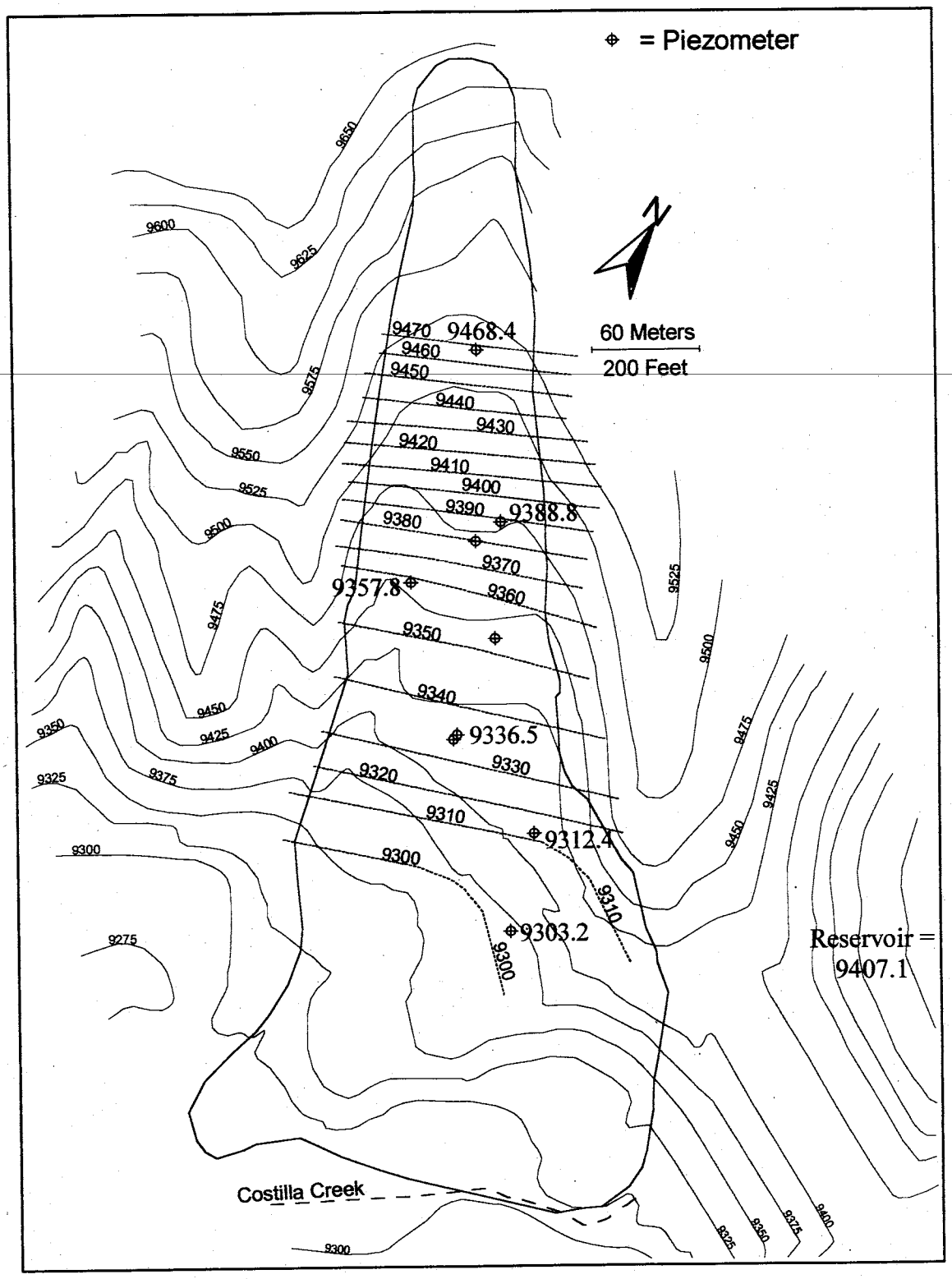

Figure 28 Potentiometric surface for the lower flow domain. This flow domain is below the landslide deposit, as recorded by the lower piezometers. The contours were made for head levels recorded on June 15, 1994 (shown next to each piezometer); excluding piezometers 4L and 7L. The dashed contours show the elevation of the potentiometric surface, and the solid lines show the topographic contours, in feet.

The data from PZ-4 and PZ-7 were neglected in this study because they are believed to be unreliable. With regard to the horizontal drains, they may effect the groundwater flow field by creating fast paths for flow but due to uncertainties associated with them, they are not considered in this study. During mapping in the summer of 1998, a minimal amount of water was produced from the drains. Most of the water draining from the landslide ponded on the surface in overgrown drainage channels to either leave the system through evapotranspiration or re-enter it through infiltration.

The time of day of data collection was not always the same, nor was the collector. In addition, no correction was made for barometric pressure fluctuations, or other background noise. Because data were collected daily, any fluctuation whose period was less than one day could not be identified. However, since data collection proceeded for the whole field season, longer period fluctuations were identified.

4.2.1 Surface Water

The reservoir and stream gauges record the fluctuations of the surface water in the study area. All streams and the reservoir have one dominant fluctuation with one to multiple peaks occurring during the summer field season (Figures 26 and Appendix VII; Figure 29 and Appendix VIII). Many smaller fluctuations are superimposed on the dominant feature. The stream gauges record increases in runoff in all streams flowing into Costilla Reservoir during the spring and early summer. This water is most likely from snowmelt, and could be a good indicator of when groundwater levels in the Costilla Dam landslide might rise. The reservoir level is dependent on natural snowmelt runoff within the drainage basin, but is also manipulated by humans. The rapid rise in reservoir

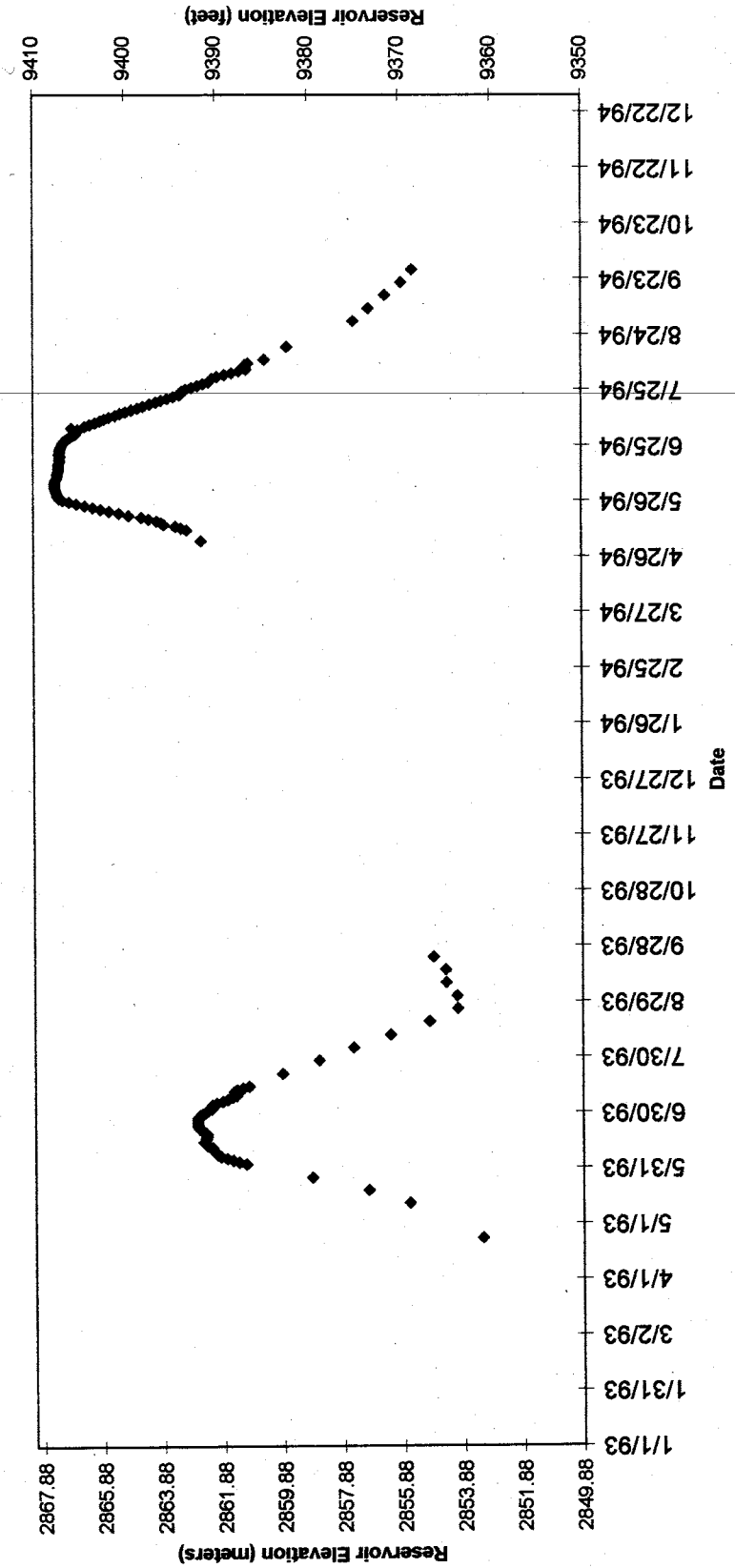

Figure 29 Reservoir fluctuations. This plot shows the fluctuation of the Costilla Dam reservoir for the 1993 and 1994 field seasons.

level in late spring and early summer is related to the increase of stream flow into the reservoir due to snowmelt (Figure 26). As irrigation demands increase and inflow to the reservoir decreases, the reservoir level peaks and then falls throughout the irrigation season. The reservoir level typically falls slightly more slowly than it rose (Figure 29).

In 1993, much of the snowpack sublimated and the Office of the State Engineer was not able to fill the reservoir to capacity. During this year the reservoir reached a level of about 2863 meters (9392 feet). The magnitude of the recorded fluctuation for 1993 was 9 meters (31 feet), but the actual fluctuation might have been up to 11 meters (37 feet). In 1994 the reservoir attained the level necessary to spill (>2867 meters or >9406 feet), which allowed the New Mexico State Engineer Office to test the newly completed spillway ramp. The magnitude of the recorded fluctuation for 1994 was 12 meters (40 feet), but the actual fluctuation might have been up to 14 meters (45 feet).

The temporal center (roughly near peak) of the reservoir fluctuation usually falls within the second half of June. The 1993 fluctuation has a distributed peak, which would be expected during most years. The 1994 fluctuation has a flat peak, which was caused by the first time the reservoir had spilled through the emergency spillway. The loss of water through the spillway halted the rise of the reservoir and created the flat-peaked fluctuation (Figure 29; Appendix VIII).

4.2.2 Precipitation

Precipitation was identified in chapter 1 as a possible source of the observed groundwater fluctuations. Annual precipitation recorded at the North Costilla snotel station averages about 70 centimeters (27 inches) (Figure 30). As noted before, the

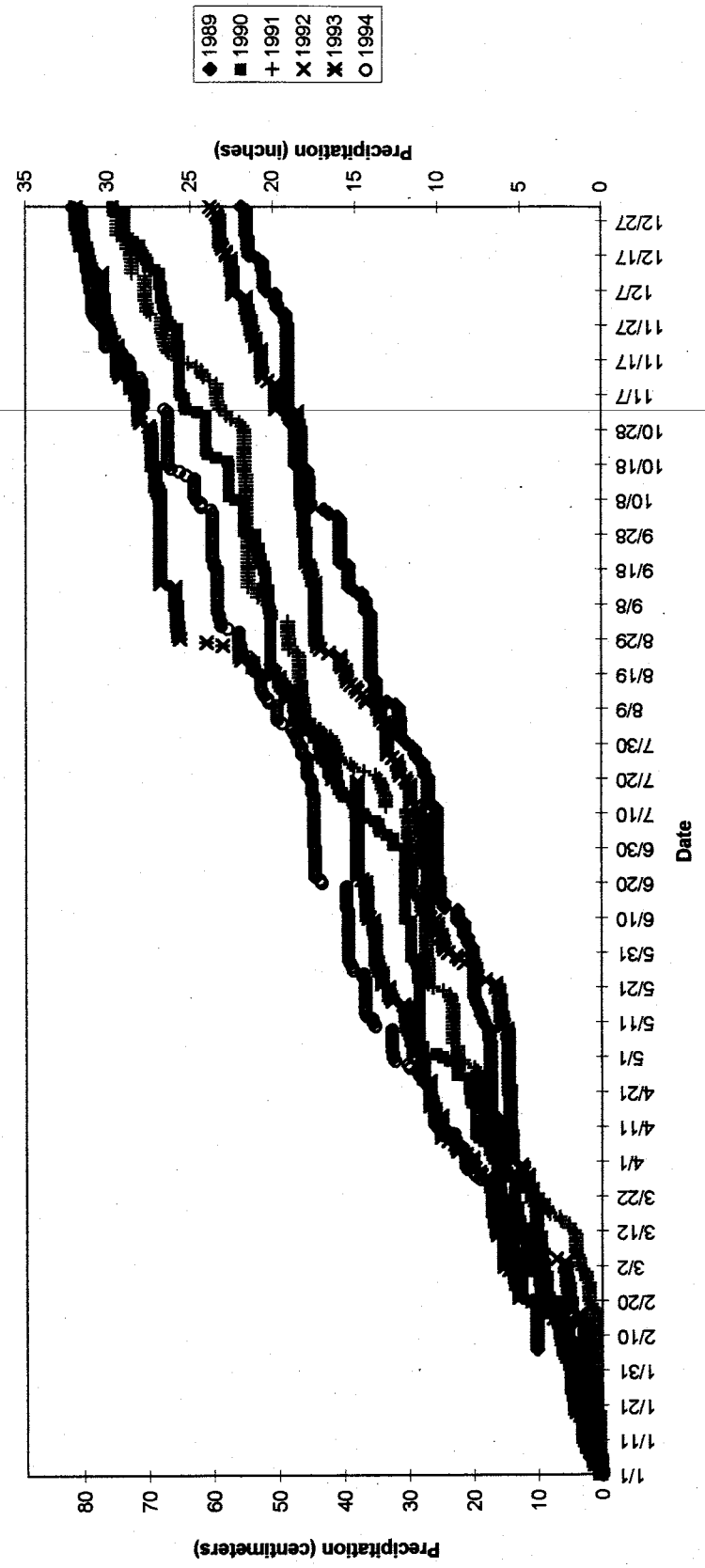

Figure 30 North Costilla snotel site precipitation data. This data is from the North Costilla snotel station (#05N16S) located approximately 14 kilometers (9 miles) north of the Costilla Dam landslide at an elevation of 3230 meters (10600 feet). The data is presented as the cumulative for each calendar year from 1989 to 1994. This snotel site measures the total daily-accumulated precipitation. These data suggest that the annual precipitation at the landslide is approximately 70 centimeters (27 inches).

head in the upper completions are always higher than in the lower completions of the same piezometer. When the fluctuations observed in the upper and lower completions are compared, usually the upper fluctuation occurs first and is the larger of the two (Appendix IX). Both of these characteristics could support precipitation recharge, or any other kind of infiltration from the surface, as the driving mechanism for the fluctuations. However, in piezometers 1 and 6 the lower fluctuations occur simultaneously with the upper fluctuations and are larger in magnitude (Appendix IX). A numerical model of the 1-D pore pressure diffusion equation was used to verify that it was unrealistic to get amplification of a pore pressure fluctuation at depth within the subsurface. Precipitation data from the site rain gauge was compared to head levels, and while precipitation recharge might be responsible for some of the smaller fluctuations superimposed on the larger fluctuation (ex. PZ-2U, PZ-2AU), it can not be the driving mechanism for all of the large annual fluctuations (Figure 31 and Appendix IX).

4.2.3 Upper Flow Domain

The upper flow domain is mainly limited to groundwater flow within the landslide. Head data was contoured using the reservoir level along with piezometers 1U, 2U, 2AU, 3U, 6U, and 8U. Examination of data collected in 1993 and 1994 for the previously mentioned piezometers was used to characterize the height and timing of groundwater fluctuations within the landslide. Graphs of the data are in Appendix IX.

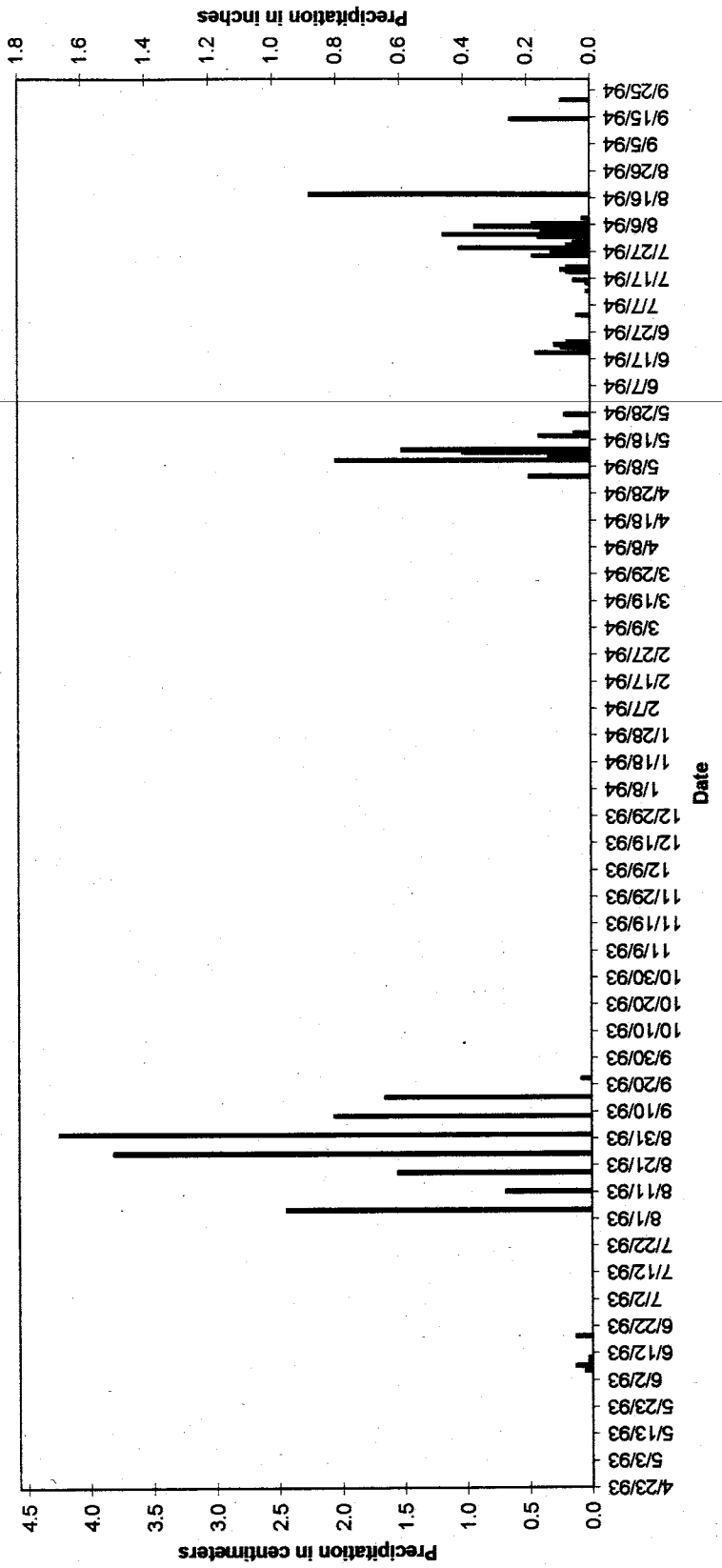

Figure 31 Site 1993-1994 precipitation data. This precipitation data was collected during the 1993 (6/4 to 9/22) and 1994 (5/4 to 9/28) field seasons at a manual rain gauge near Costilla Dam. Data was collected daily during the first half of the each field season, then was collected weekly from 7/15 to 9/22 in 1993, and from 8/11 to 9/28 in 1994.

4.2.3.1 General

Groundwater within the landslide is unconfined. The contoured water table surface indicates that groundwater flow is mainly down the axis of the landslide (Figure 27). There were reports of at least three springs on the surface of the landslide prior to the construction activities in the late 1980's, one of which may have been used as a water supply during construction of the original dam (Hendron and others, 4/22/1994). The springs, which were covered over with stockpile material, were produced from the intersection of the water table with the ground surface. The location of the springs halfway down the landslide helps support some of the geologic interpretations of the previous chapter. The springs were located on a gently sloping section of the landslide, but none are located on the steep face closer to the toe of the landslide. The cut for the spillway excavation contained only small areas of perched groundwater, and was dry for the most part (USBR, 4/1995). The only significant water encountered in the spillway excavation was entering the excavation on the southeast side. This groundwater originated from Costilla Creek and flowed through alluvium to the excavation. Figure 32 shows the location of the spillway cut in relation to the landslide. It is likely that the alluvium in the buried channel underneath the landslide deposit acts like a drain and collects water flowing within the landslide. The highly permeable alluvium then carries the water downstream, out from under the landslide deposit and into the broad valley bottom. Figure 32 also shows my interpretation of the cross sectional profile of the water table within the landslide.

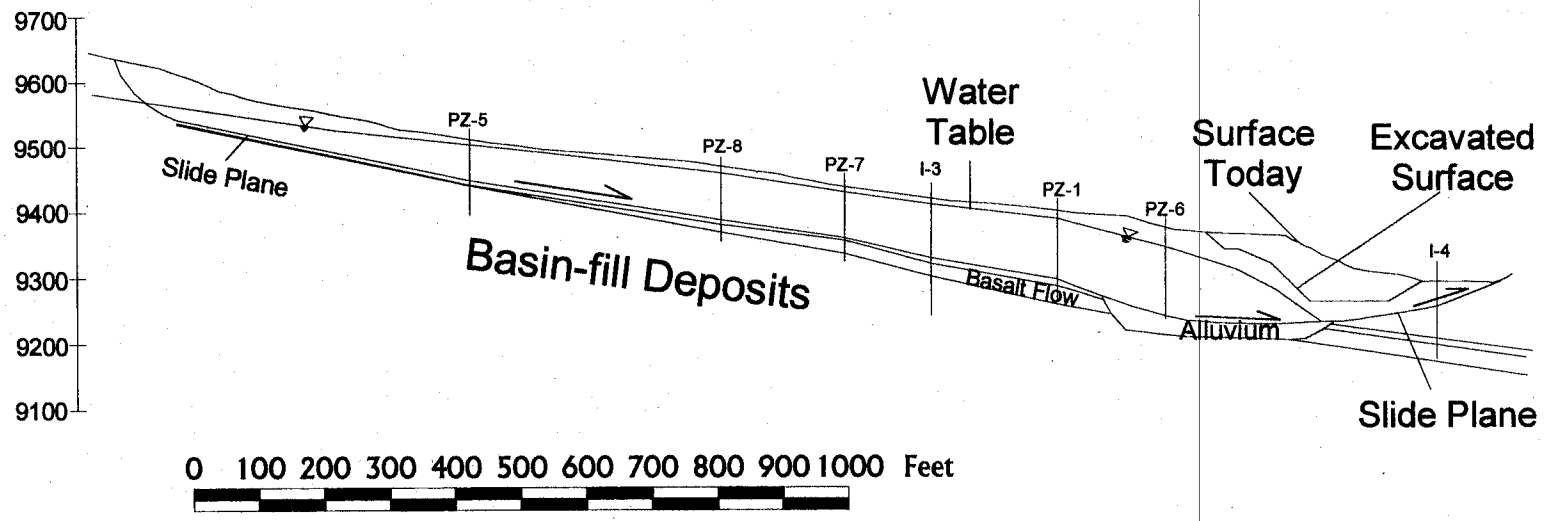

Figure 32 Cross section showing water table and spillway excavation. The spillway ramp and stilling basin excavation is labeled on the figure. The water table profile is nearest to the ground surface around I-3, which is where springs were located before construction activities. The buried channel acts like a drain and captures all water flowing within the landslide.

4.2.3.2 Fluctuation Magnitude

Piezometers in the upper flow domain have been lumped into groups based on the magnitude of their fluctuations. The reservoir is the largest fluctuation that is in contact with the upper flow domain. The largest piezometer fluctuations are observed in PZ-2U, PZ-2AU, and PZ-3U. The second largest are observed in PZ-8U and PZ-1U. Finally, the smallest fluctuations are observed in PZ-6. The piezometer fluctuation magnitude appears to increase with distance from the reservoir. This pattern is also consistent with depth to the slide plane. However, if the piezometers were lumped based on this variable, they would not match the fluctuation magnitude groups listed above.

4.2.3.3 Fluctuation Timing

The fluctuations observed in the unconfined aquifer in piezometers 1U, 2U, 2AU, 3U, 6U, and 8U are controlled by snowmelt infiltration recharge. All of the fluctuations in these piezometers occur either before or at the same time as the reservoir fluctuation (Figure 33). This timing is consistent with the increase in runoff shown at the stream gauges (Figures 26). It also eliminates the reservoir fluctuations as the driving force for the fluctuations within most of the landslide. The piezometers are greater than 150 meters (500 feet) from the edge of the reservoir. In addition, the specific yield of an unconfined aquifer would be expected to dampen out the fluctuations in a much shorter distance.

4.2.4 Lower Flow Domain

The lower flow domain is limited to groundwater flow below the landslide. Head data were contoured using piezometers 1L, 2AL, 3L, 5L, 6L, and 8L. Data collected in

1993 and 1994 for these piezometers was used to characterize the height and timing of groundwater fluctuations below the landslide (Figure 34). Graphs of the data are contained in Appendix IX.

4.2.4.1 General

The clay-rich slide plane confines groundwater below the landslide. In all lower piezometers the head is higher than the elevation of the slide plane. Groundwater flows through basin-fill deposits and possibly the basalt flow above it. The heads at PZ-1L and PZ-6L are very similar and suggest a much larger downstream gradient than heads observed higher on the slope. This change in gradient direction may be interpreted as the flow of groundwater from the reservoir, within the buried channel of alluvium, under the landslide. When the piezometric surface was contoured for the lower piezometers, it showed that flow would be dominantly down the landslide, except in the vicinity of PZ-6, and PZ-1 (Figure 28). The piezometric contours near the toe of the landslide show flow dominantly from the reservoir, parallel to the axis of the valley. Also, the fluctuations seen in PZ-6L and -1L are almost identical and support the idea of a buried channel of alluvium below the toe of the landslide (Figures 35 & 23).

4.2.4.2 Fluctuation Magnitude

Fluctuations in the lower flow domain are similar to the magnitude of fluctuations in the upper flow domain. The reservoir is the largest fluctuation in contact with the lower flow domain. In general, PZ-1L and PZ-6L fluctuations are about the same magnitude, especially during 1994, and are the largest of the lower piezometers. The next

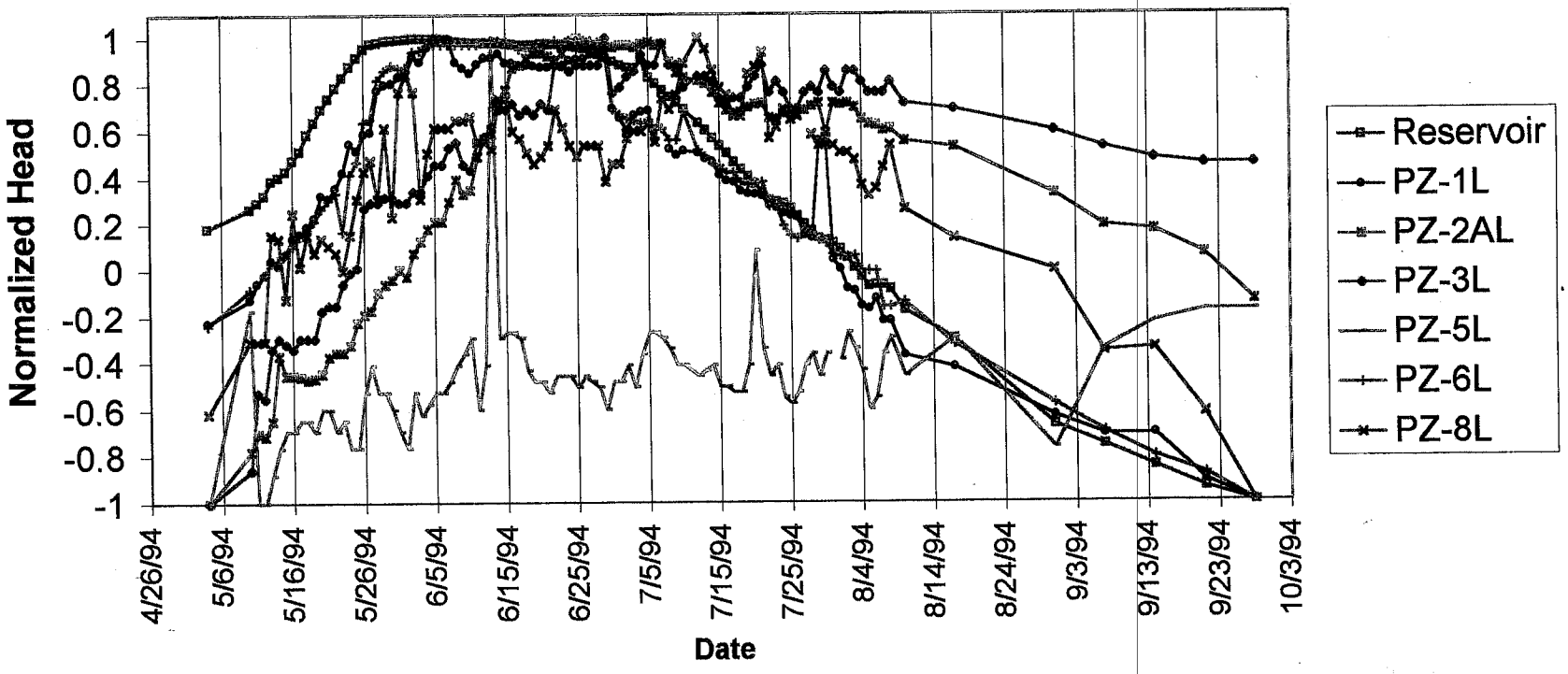

Figure 34 Comparison of the timing of fluctuations observed in the lower piezometers and reservoir (1994). This plot is of scaled data with the maximum observed water level equal to 1 and the minimum equal to -1 at each location. This scaling is done to allow comparison of fluctuation timing regardless of fluctuation magnitude. Note how all piezometer fluctuations occur after or at the same time as the reservoir fluctuation. This supports the idea that the reservoir is the driving mechanism for the lower piezometer fluctuations.

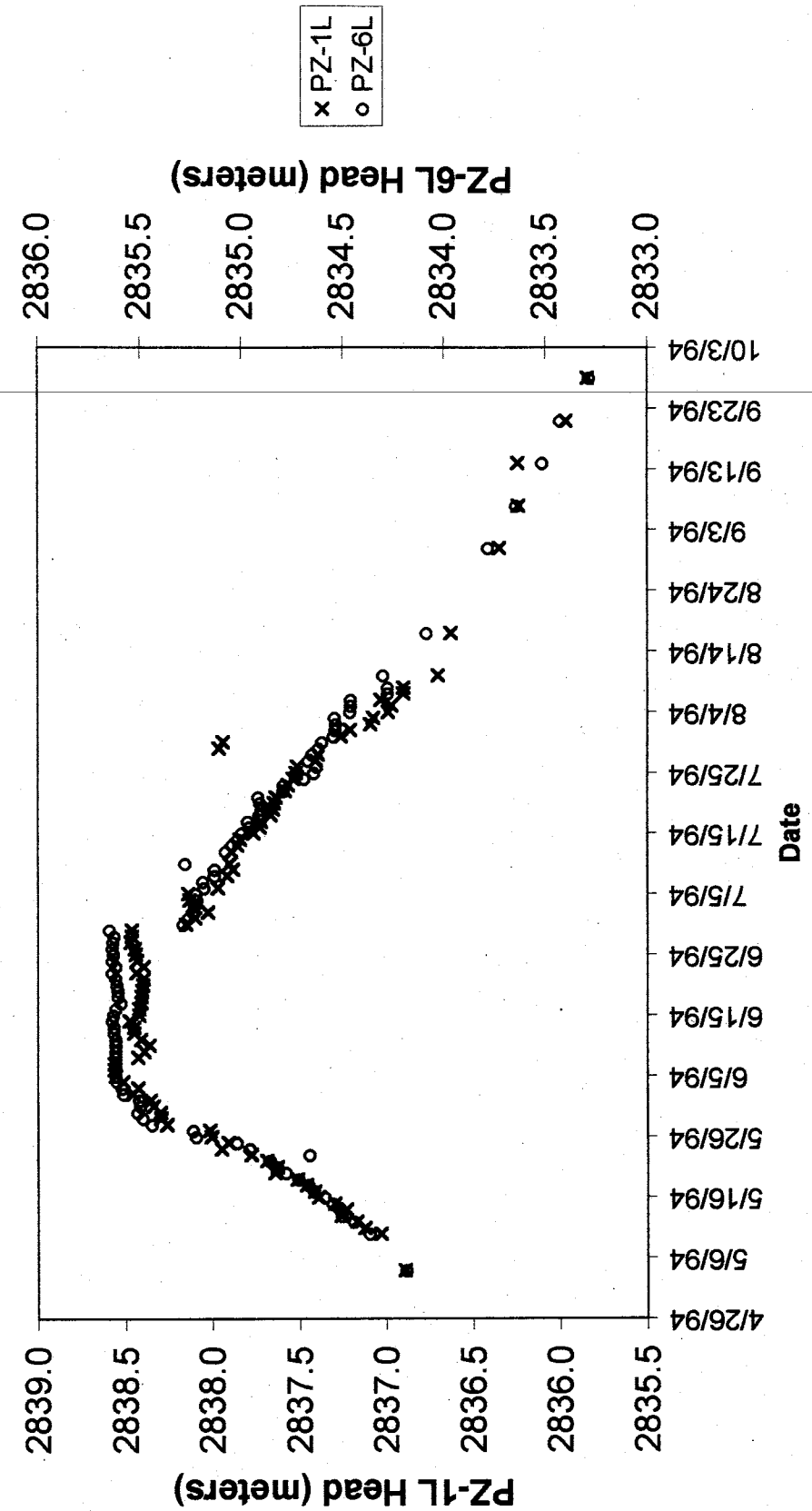

Figure 35 Comparison of PZ-1L and PZ-6L (1994). These two piezometers are located toward the toe of the landslide, with PZ-6L being within the buried channel, and PZ-1L being very close to the edge of the channel. The vertical scales are different, but the shape of the fluctuations is nearly identical. This shape is also very similar to the reservoir fluctuation, as discussed in the hydrogeology section.

largest fluctuation is in PZ-2AL and the third largest fluctuation is in PZ-8L. Finally, PZ-3L and -5L show little to no fluctuation, respectively. This order shows that the fluctuation magnitude decreases both uphill and away from the reservoir (Figure 6). The fluctuation pattern suggests that the reservoir could be the driving force behind the fluctuations in the lower piezometers.

4.2.4.3 Fluctuation Timing

Figure 34 shows the normalized reservoir and piezometer fluctuations for 1994. Although the data for 1993 and 1994 are similar, differences exist that can not be explained using the current understanding of the system. I will limit my discussion here to the 1994 data because 1994 represents a year with more infiltration recharge, higher reservoir levels, and a constant peak reservoir elevation during the planned spill through the recently completed spillway.

The reservoir was the first fluctuation to peak. The two toe piezometer (PZ-6L and PZ-1L) fluctuations occurred just a few days behind that of the reservoir. Piezometers 8L and 2AL peaked at roughly the same time. Next, piezometer 3L peaked. Finally, piezometer 5L did not peak during the summer field season. It may have a weak annual fluctuation, or may fluctuate later in the year after the conclusion of monitoring. The temporal distribution of the fluctuations indicates that the piezometer fluctuations occur later both uphill and away from the reservoir. The head at PZ-5L could be a relative indicator of how much recharge has reached the lower flow domain from further upslope. The difference between the head in PZ-5L for 1993 and 1994 is only approximately 0.3 meters (1 foot), but a definite increase in head is observed (Figure 36).

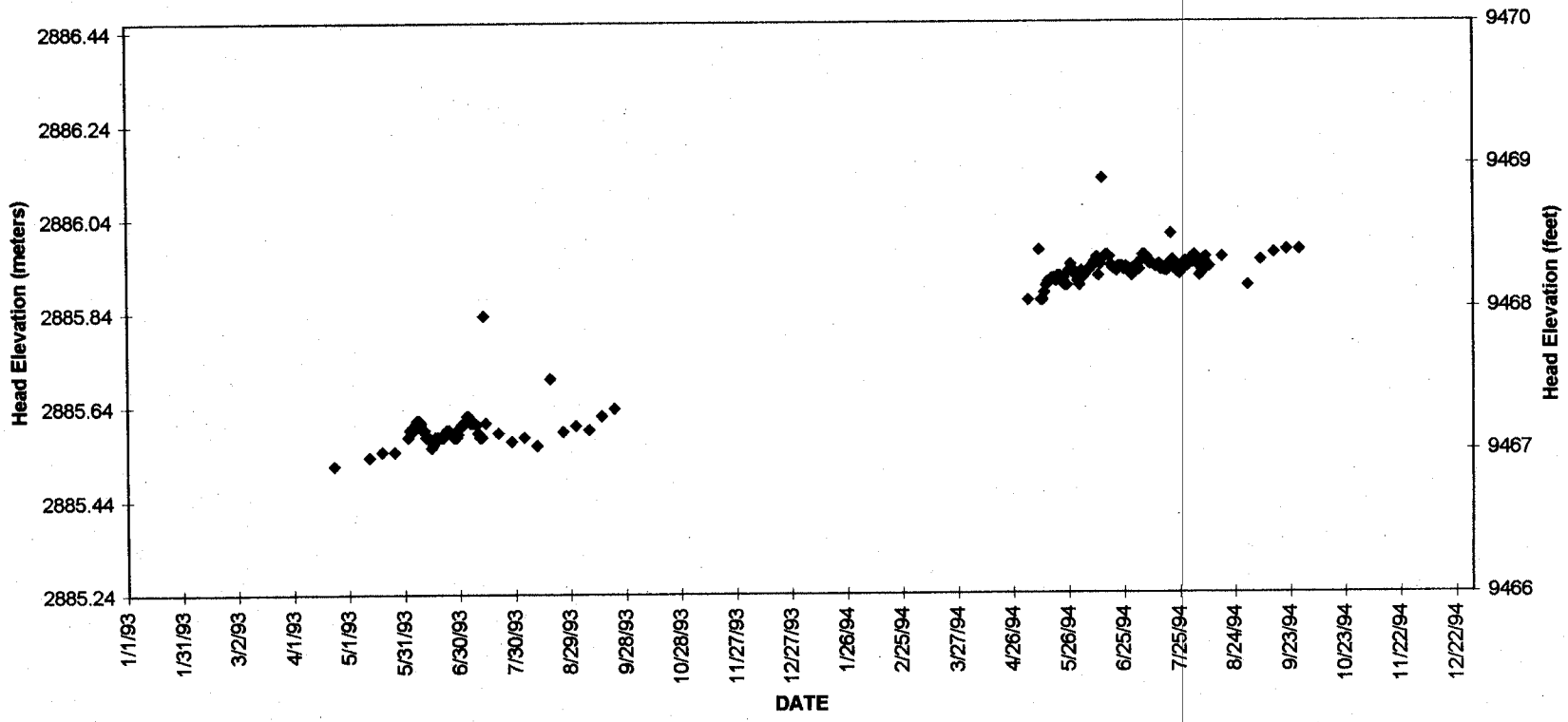

Figure 36 PZ-5L head data. This plot shows the head measured at PZ-5L for the 1993 and 1994 field seasons. There is no discernable fluctuation, but the head is higher overall during the 1994 field season. This piezometer may be used as an indication of the amount of recharge that has reached the lower flow domain.

Based on the stream gauge and reservoir level data, it appears the period of time before the 1994 field season was wetter than the same time in 1993.

4.2.5 Transient Hydrogeology

The upper and lower flow domains are hydraulically connected in the buried channel of alluvium beneath the toe of the landslide complex. At other locations, where the slide plane may be thin or has been penetrated by the various drilling programs, there may be communication between the upper and lower flow domains. However, this communication is probably minor compared to the buried channel. The buried channel is also the most influential connection between the two flow domains with the reservoir.

The fluctuations within the upper piezometers are controlled by the timing and volume of water recharged to the water table through snowmelt recharge. The input of snowmelt recharge causes the water table to rise and fall both before and at the same time that the reservoir level fluctuates. The fluctuation of water in the upper flow domain does not propagate to the lower flow domain due to the thick clay slide plane.

Heads in piezometers 1L and 6L rise and fall at the same time as the reservoir level and mark the largest fluctuations observed in the lower flow domain. As time passes, the fluctuation propagates uphill and away from the reservoir and the magnitude of the fluctuation decreases. This pattern indicates that the large fluctuations observed within the lower flow domain are controlled by the fluctuation of the reservoir.

The only transient influence of the reservoir on the upper flow domain is likely related to the head in the buried channel. As the reservoir level increases and the head in the buried channel increases (as observed in PZ-6L), the head difference between the

upper and lower flow domains becomes smaller and flow to the buried channel from uphill would decrease slightly.

4.3 MODFLOW MODELING

Groundwater modeling was performed to determine if the qualitative hypotheses presented through observation of hydrologic data could be realistic. The geology and hydrogeology of the area surrounding the Costilla Dam landslide are very complicated and hydrologic testing has not been performed on any of the geologic units in the vicinity of the study area. Assumptions can be made about the behavior of the reservoir, piezometers, stream flow, and precipitation, along with appropriate ranges of values for specific yield, storage coefficients, hydraulic conductivity, and transmissivity. Even if one were able to produce a model that reacted close to what is observed, it would still be non-unique. The model constructed for this study was not intended to be a site-specific model, but instead a more generic model aimed at identifying trends and behaviors.

4.3.1 Conceptual Model

In order to produce a conceptual model, a simplified geologic interpretation of the area surrounding the Costilla Dam landslide was created. The geologic and hydrogeologic features that are deemed important and are in the groundwater model include:

1. The dip of geologic units into the valley
2. The buried channel of alluvium connecting the reservoir with the upper and lower flow domains

3. A nearly impermeable clay layer between the upper and lower flow domains
4. The valley bottom acting as an outlet because of water being removed by Costilla creek and evapotranspiration on the floodplain
5. The fluctuation of the reservoir
6. The likely pulse of snowmelt recharge

MODFLOW-96 was selected because of its 3-dimensonal capabilities, ability to handle fluctuating specified head nodes, and its established record of application. MODFLOW had also been used previously to model dipping bed simulations (Jones, 4/26/1996). Jones (1996) formulation for dipping bed simulations was slightly different than what was required for the model used in this study, requiring a slightly different formulation that is described in Appendix X.

The conceptual geology of the site is represented by a three-layer model. Layer 1 consists of landslide deposits (upper piezometers), layer 2 consists of clay and the buried alluvium channel, and layer 3 is basin-fill deposits (lower piezometers). Each layer of the model dips 10° into the valley. This dip was determined from the average dip of the landslide slide plane, down the axis of the landslide (Figure 17). Ten degrees is not the same as the dip of the geologic units in the area (~15°), but this was chosen to align the dip of the model layers perpendicular to the axis of the valley. Figures 37 - 39 show each individual model layer with areas of interest noted. The hydrologic properties of each material are listed in Table 2. Layer 1 is unconfined with the free surface being limited to this layer, while layers 2 and 3 are confined. "Actual" and "model" values are described in Appendix X and relate to transformations to input data necessary when calculating dipping layer simulations. Actual values would normally be the value of

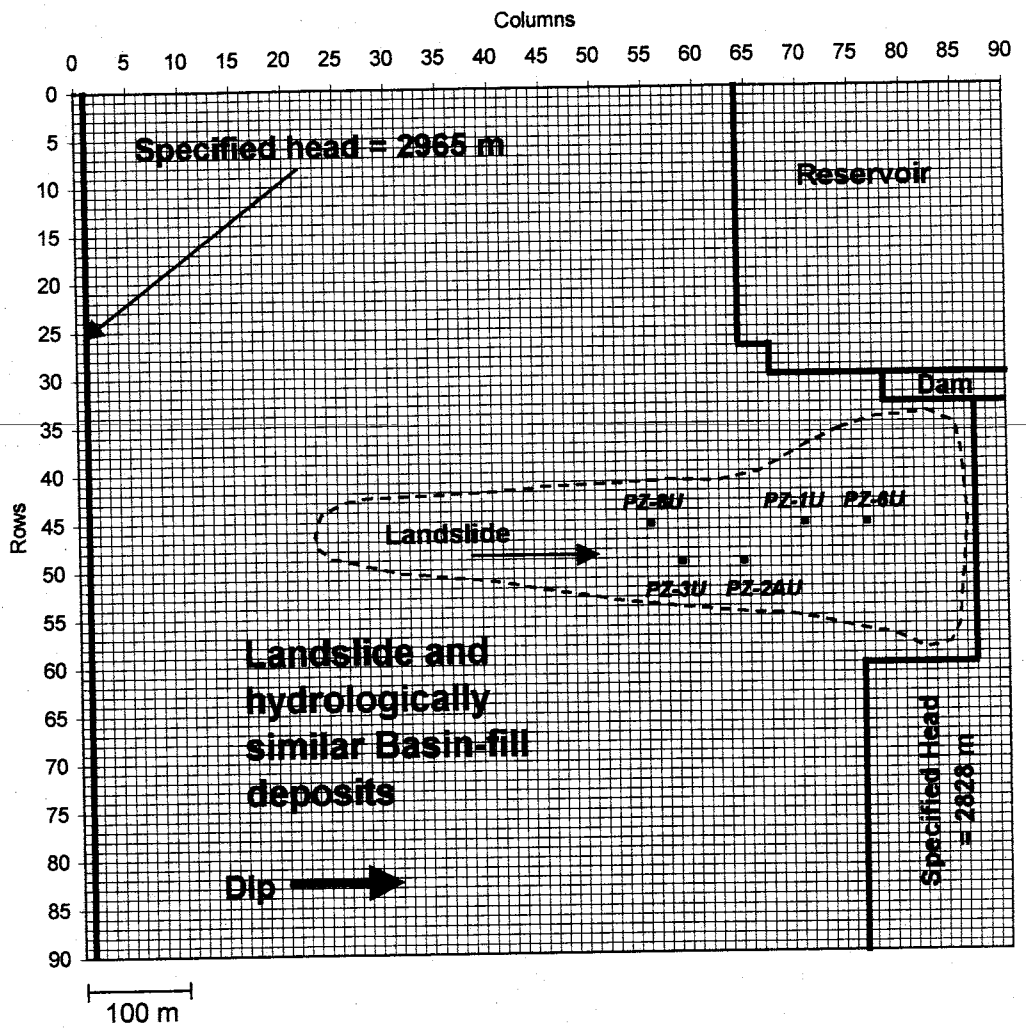

Figure 37 Layer 1 model setup. Layer 1 is an unconfined model layer. Hydrologic properties of all variable cells are consistent with landslide deposits (Table 2). Cells in column 1 are specified at 2965 meters. No-flow cells represent the dam. The reservoir cells are specified, but are not always constant depending on the simulation. The specified head cells in the bottom right corner represent the valley alluvium where water is discharged from the system through evapotranspiration or stream flow. The nodes that were compared to piezometer observations are located within the outline of the landslide.

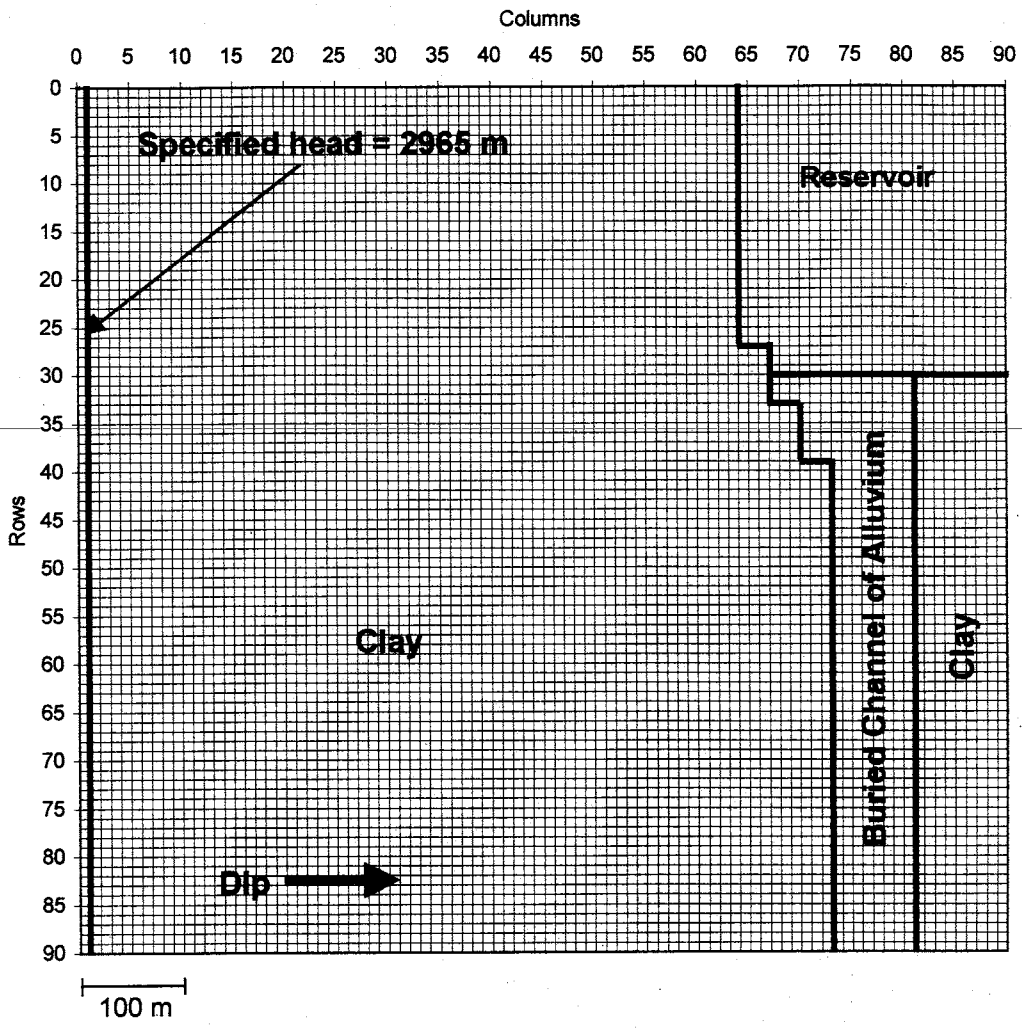

Figure 38 Layer 2 model setup. Layer 2 is a confined model layer that is 5 meters thick. Hydrologic properties of variable cells are either for clay or if within the buried channel, alluvium (Table 2). This layer represents the slide plane beneath the landslide. Cells in column 1 are specified at 2965 meters. The reservoir cells are specified, but are not always constant depending on the simulation.

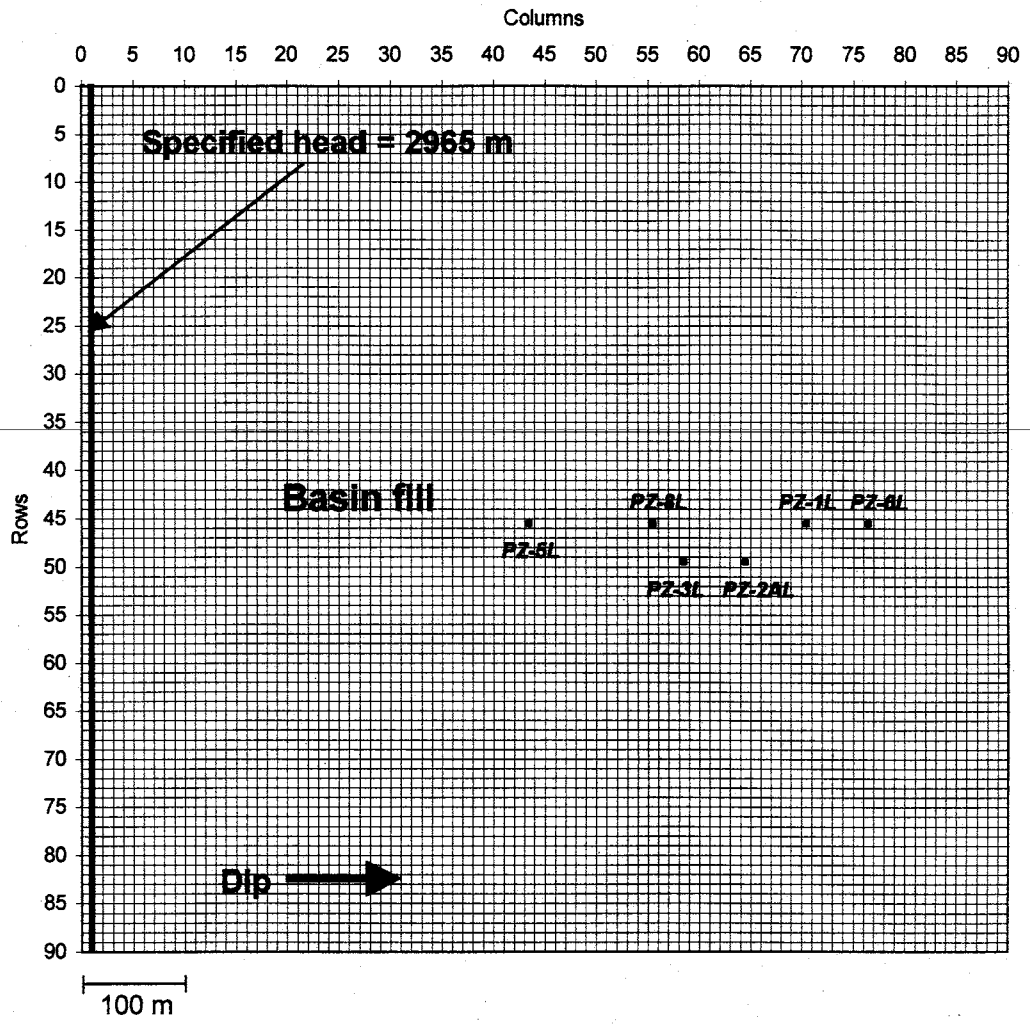

Figure 39 Layer 3 model setup. Layer 3 is a confined model layer that is 30 meters thick. Hydrologic properties of variable cells are all represented by basin-fill deposits (Table 2). Cells in column 1 are specified at 2965 meters. The nodes that were compared to lower piezometer observations are identified.

Table 2. Generic MODFLOW model parameters

	Layer Physical Properties	Actual Hydraulic Conductivity (m/sec)	Flat Layer Transmissivity (m^2/sec)	Model Hydraulic Conductivity (m/sec)	Model Transmissivity (m^2/sec)	Actual Specific Storage (m^{-1})	Flat Layer Storage Coefficient (unitless)	Model Storage Coefficient (unitless)
Layer 1	Unconfined; Roughly 30 m thick							
Landslide		1.00E-06	Variable with head	1.00E-06	na	na	0.15	0.15
Layer 2	Confined; 5 m thick							
Clay		1.00E-10	5.00E-10	na	4.92E-10	1.00E-03	5.00E-03	5.08E-03
Buried Channel		1.00E-04	5.00E-04	na	4.92E-04	1.00E-04	5.00E-04	5.08E-04
Layer 3	Confined; 30 m thick							
Basin fill		1.00E-06	3.00E-05	na	2.95E-05	1.00E-04	3.00E-3	3.05E-03

Vertical Conductance	Layer 1 Actual Hydraulic Conductivity (m/sec)	Layer 2 Actual Hydraulic Conductivity (m/sec)	Vertical Hydraulic Conductivity (m/sec)	VCONT (sec^{-1})
Layer 1 to 2				
Landslide to Clay	1.00E-06	1.00E-10	7.00E-10	4.06E-11
Landslide to Buried Channel	1.00E-06	1.00E-04	1.16E-06	6.76E-08
Layer 2 to 3				
Clay to Basin fill	1.00E-10	1.00E-06	7.00E-10	4.06E-11
Buried Channel to Basin fill	1.00E-04	1.00E-06	1.16E-06	6.76E-08

Model Anisotropy	1.031	

Dip of Layers	10	degrees

hydrologic properties measured in the field or lab, but in this case they are estimated based on geologic medium. Model values are the values which need to be input into a MODFLOW simulation based on the formulation for a dipping bed simulation described in Appendix X. An average recharge rate of $8*10^{-9}$ m/sec (10 inches/year) was used. Constant specified head nodes equal to 2965 meters (9728 feet) were placed at the top of the slope in all model layers. The solution for a dipping bed simulation is very sensitive to the grid spacing of the model. Initially a 30 meter grid spacing was simulated, but the cross sectional of the water table unrealistic. Therefore, a 10 meter grid spacing was used which produced a more realistic water table profile.

Four simulations were performed on the model described above, one steady state simulation and three transient simulations. The steady state simulation was run to produce starting heads for the three transient simulations, and to be compared to potentiometric surfaces created from piezometer data. The steady state model had a constant reservoir elevation of 2854 meters (9364 feet) and an average recharge rate of $8*10^{-9}$ m/sec (10 inches/year). The distribution of heads produced from this simulation is plotted in Figure 40. One transient simulation was run in which the reservoir fluctuation replicated the observed fluctuation in the 1994 field season, and the recharge rate was held constant (Figure 41). In the second transient simulation, the reservoir elevation was held constant at 2854 meters (9364 feet) and I redistributed the $8*10^{-9}$ m/sec (10 inches/year) recharge to match the timing of the increase in runoff in the local streams (Figure 42). The third transient simulation combined the fluctuating reservoir and fluctuating recharge rate in an attempt to represent all identified driving mechanisms, which could then be compared to trends in the observed data.

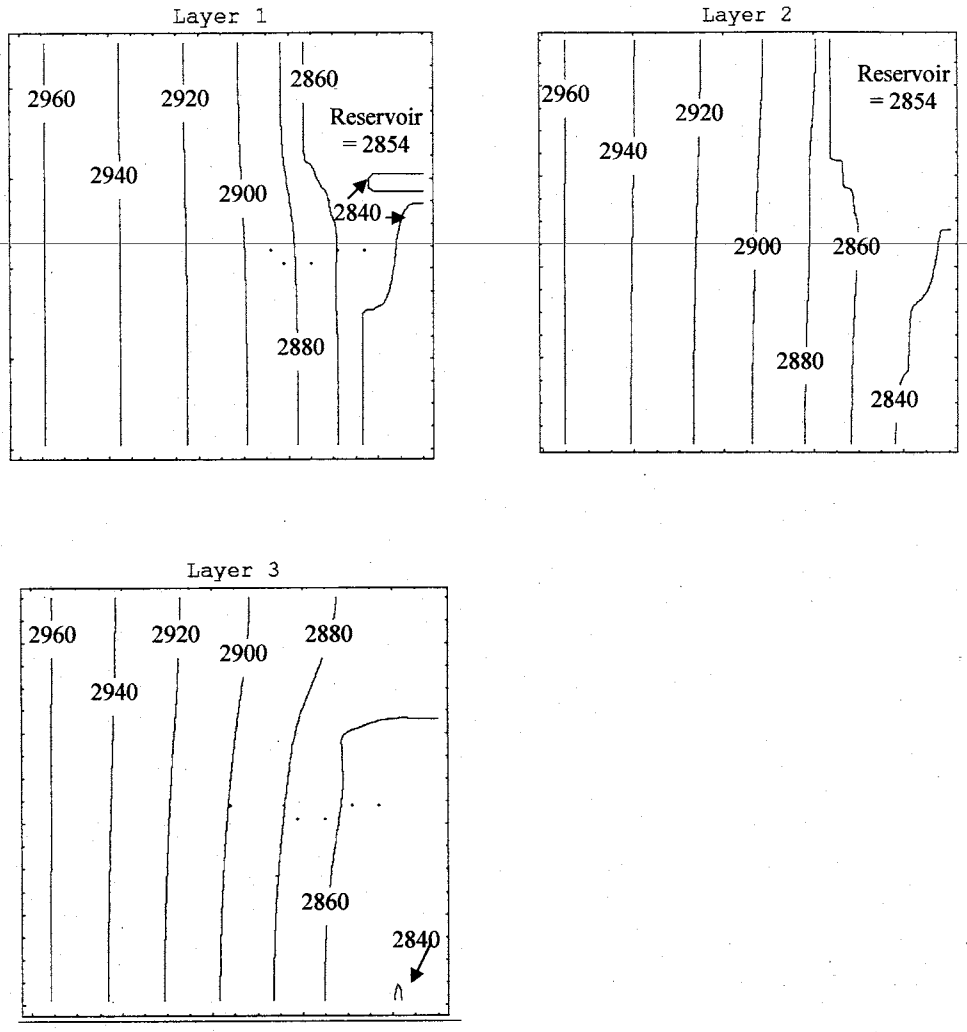

Figure 40 Model layer steady state heads. Piezometer cells are marked by points. For model layer setup or identification of individual piezometers see figures 37 and 39. Head is given in meters.

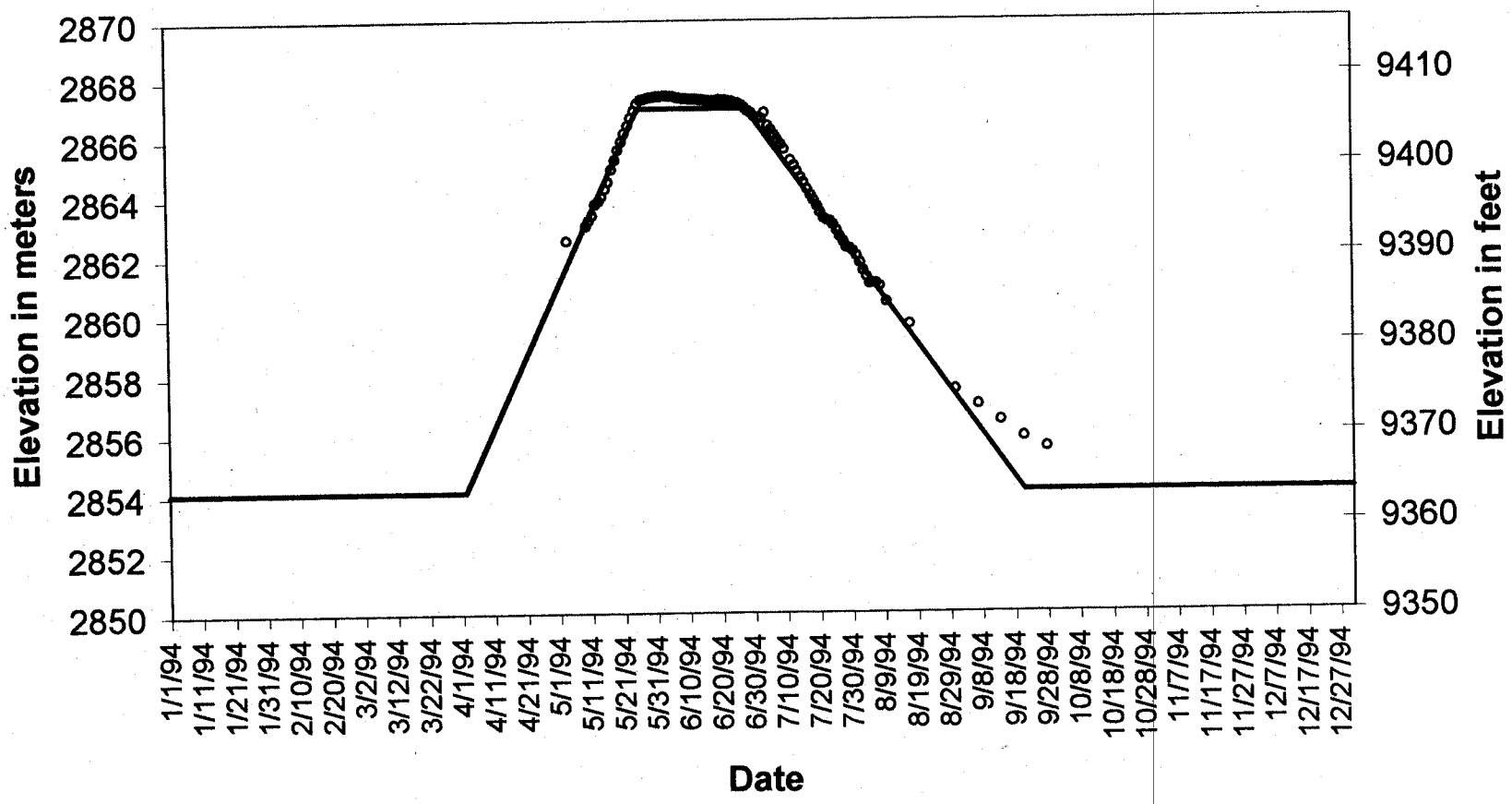

Figure 41 Actual 1994 Reservoir Fluctuation vs. Model Reservoir Fluctuation. The actual data is represented as points by the circles, while the model reservoir fluctuation is represented by the continuous line.

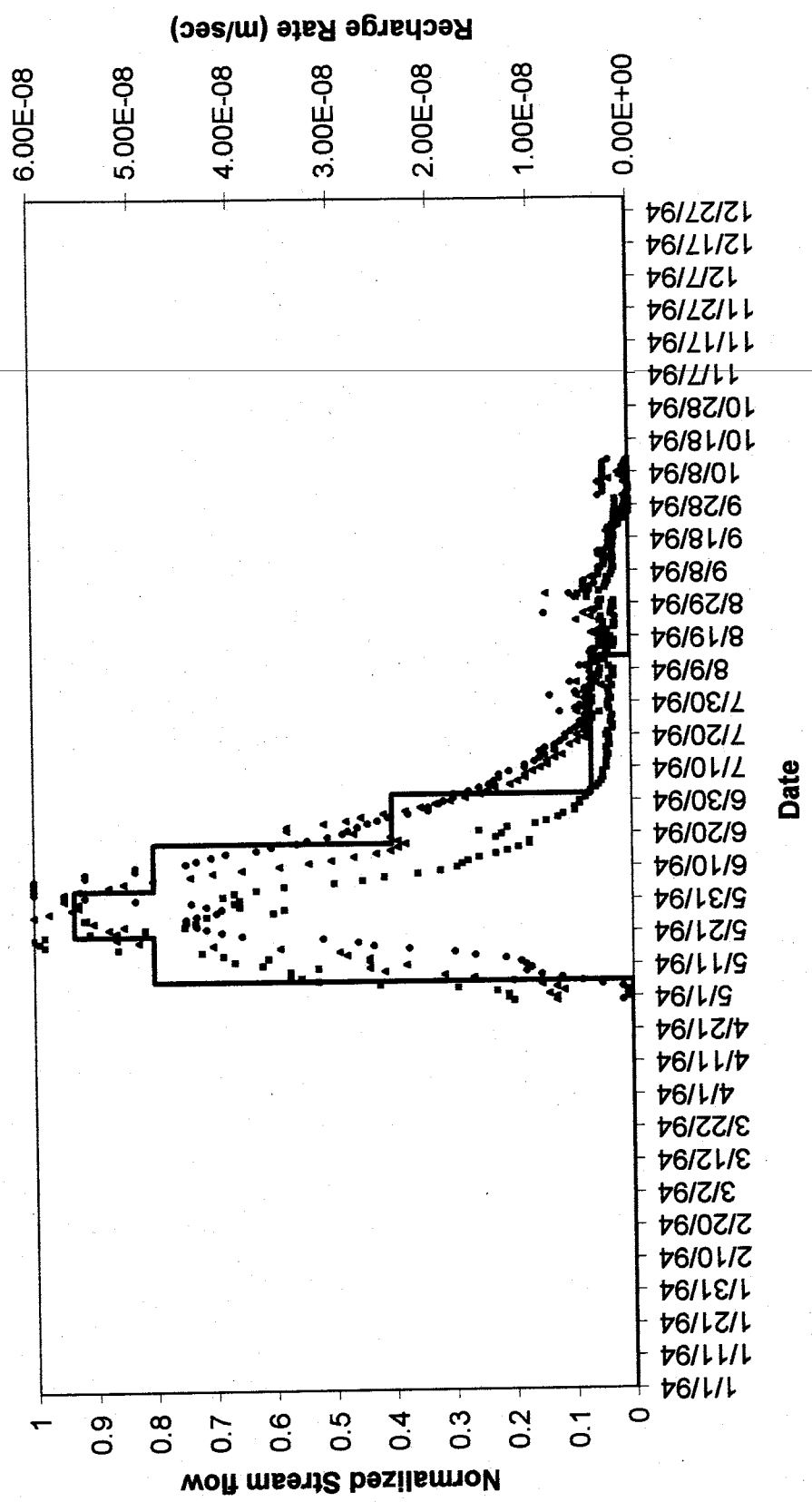

Figure 42 Model Recharge Rate Fluctuation Mimicking Observed Stream flow Fluctuation. Points represent normalized stream flow data from the three streams monitored above the reservoir. The continuous line represents the modeled recharge rate. For actual stream flow data see figure 26.

4.3.2 Comparison of Model to Observed Data

The generic model results are compared with observed data to determine if the MODFLOW modeling can replicate observed groundwater flow and transient behavior. The model results are compared to the general flow field, and the relative timing and magnitude of modeled groundwater fluctuations are compared to observed groundwater fluctuations.

4.3.2.1 Steady State

The steady state head distribution used as the starting heads for the transient simulations very closely resembles the observed data. Both the upper and lower model layers show flow down the axis of the landslide. Layer 3 also shows a component of flow from the reservoir down-valley under the landslide that is present in the observed data (Figure 40). Overall, the model appears to predict a similar flow field to the observed data using the conceptual geologic outlined in this study.

4.3.2.2 Transient

The three transient simulations lend insight into the driving mechanisms for fluctuations in both layer 1 and 3. The simulation with only the reservoir level changing shows very little fluctuation in most of the upper piezometer nodes, with the largest fluctuations occurring near the buried channel. The simulation with only recharge varying shows that all upper piezometers peak at about the same time with about the same fluctuation magnitude (Table 3). This behavior was identified by Haneberg and Gökce (1994) and is consistent with hillside flow domains that are much longer than they are thick. When both the reservoir level and recharge rate fluctuate, the piezometer cell fluctuations more

closely match that of the recharge only simulation, and support the idea that recharge rate fluctuation is the main driving force behind the upper piezometer fluctuations (Figure 43; Table 3). However, the actual upper piezometer data within the landslide have a variety of fluctuation magnitudes and timings. This difference could be related to the oversimplified model of the geology, spatially and temporally variable recharge rates over the landslide, or variations in hydrologic properties.

The layer 3 model results match the observed lower piezometer data much better than the layer 1 model results. For the lower piezometer nodes, the reservoir fluctuating only model most closely matches the model with both the reservoir and recharge rate fluctuating. This suggests that the reservoir is the main driving force behind the lower piezometer fluctuations. The magnitude of fluctuation decreases both upslope and away from the reservoir. Also, the timing of a fluctuation is directly related to the magnitude of the fluctuation (Figure 44; Table 3 and 4). The earlier the fluctuation, the larger the fluctuation. The fluctuation in layer 3 of the model is mainly controlled by the reservoir fluctuation. The recharge rate fluctuation simulation produced small fluctuations in layer 3 with the largest fluctuations occurring below the buried channel of alluvium. Outside of this area the recharge pulse was much smaller than the fluctuations driven by the reservoir.

4.4 HYDROGEOLOGIC CONCLUSIONS

The hydrogeology of the Costilla Dam landslide can be divided up into an unconfined upper flow domain within the landslide, and a confined lower flow domain below the landslide. The two flow domains are connected at the buried channel of

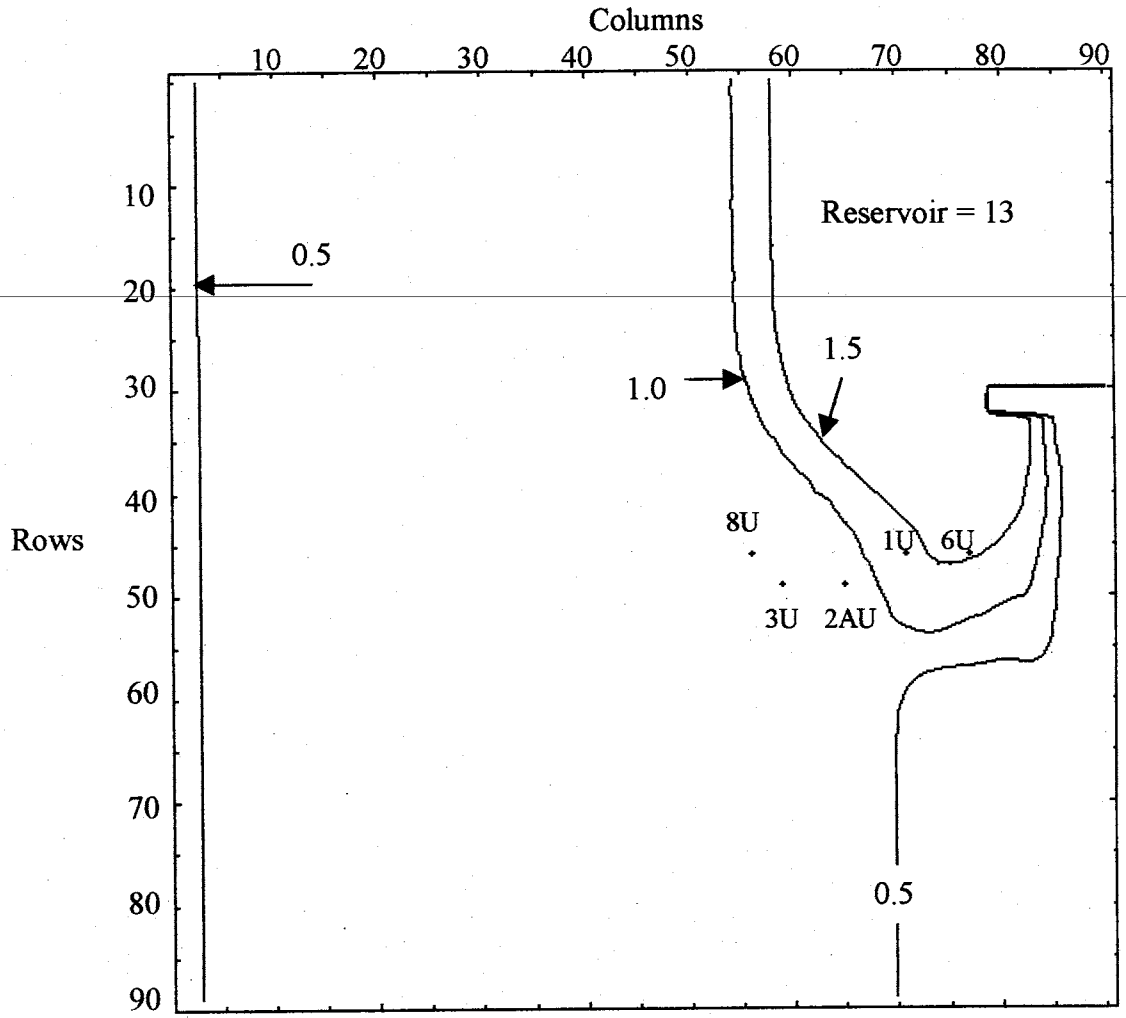

Figure 43 Layer 1 magnitude of fluctuation due to recharge pulse and reservoir level fluctuation. Magnitude is in meters. Upper piezometer cells that were compared with real piezometers in this study are shown. For model layer 1 setup see figure 37.

Table 3 Fluctuation Magnitude Comparison

First number represents height of fluctuation in meters, while the number in brackets arranges the fluctuations in order of magnitude with [1] being the largest.

Piezometers	Actual 1994 Fluctuation Data (meters)	Simulation of Reservoir Level Fluctuation Only (meters)	Simulation of Recharge Rate Fluctuation Only (meters)	Simulation of Both Reservoir Level and Recharge Rate Fluctuations (meters)
Reservoir	13	13	0	13
1U	1.9 [4]	0.52 [2]	1.27 [1]	2.28 [2]
2AU	2.9 [2]	0.12 [3]	1.26 [2]	1.93 [3]
3U	3.2 [1]	0.03 [4]	1.26 [2]	1.90 [4]
6U	0.9 [5]	1.02 [1]	1.10 [3]	2.55 [1]
8U	2.5 [3]	0.02 [5]	1.26 [2]	1.90 [4]
1L	3.5 [1]	1.12 [2]	0.74 [2]	2.24 [2]
2AL	1.4 [3]	0.87 [3]	0.49 [3]	1.62 [3]
3L	0.5 [5]	0.76 [5]	0.35 [4]	1.31 [4]
5L	0 [6]	0.53 [6]	0.19 [6]	0.82 [6]
6L	3.15 [2]	1.13 [1]	0.89 [1]	2.46 [1]
8L	0.75 [4]	0.78 [4]	0.33 [5]	1.29 [5]

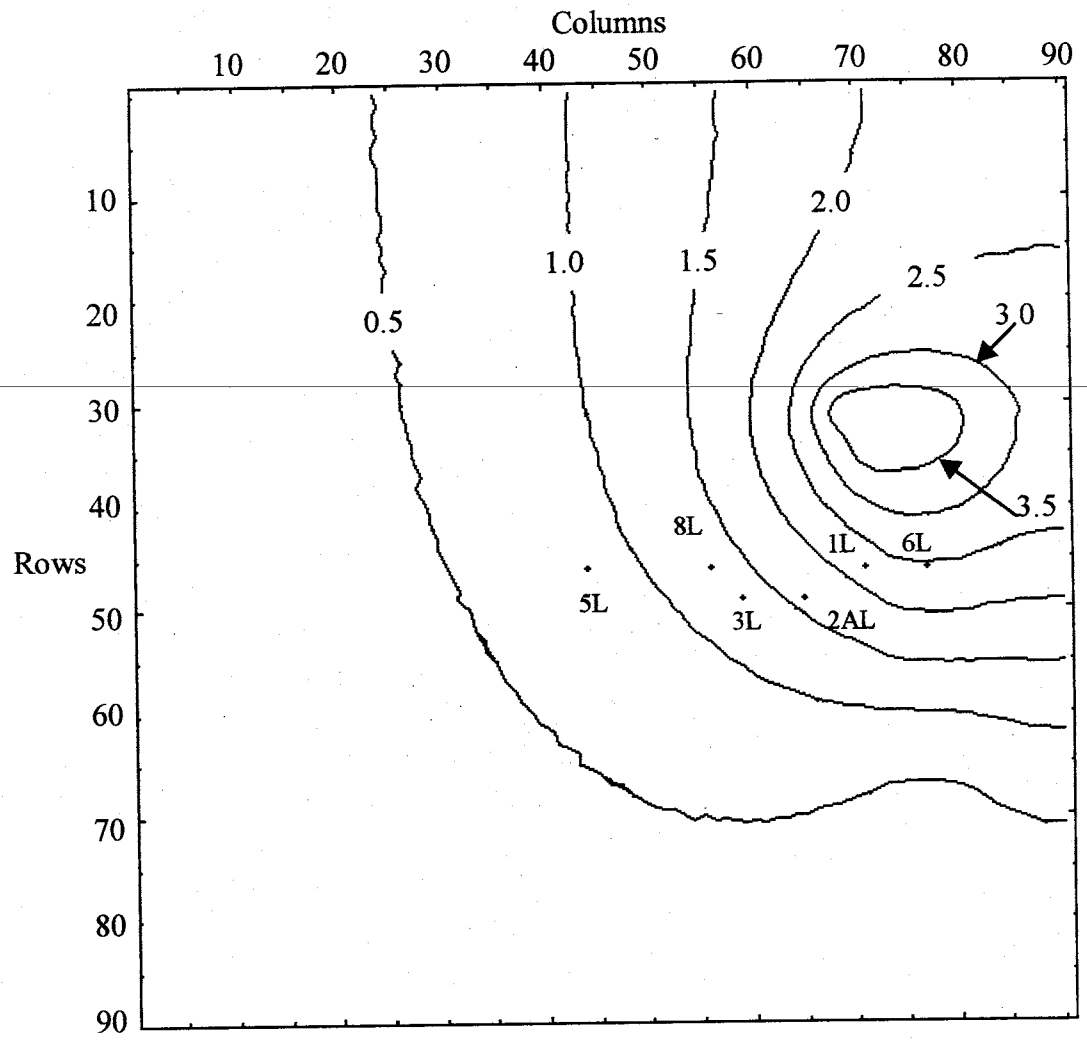

Figure 44 Layer 3 magnitude of fluctuation due to recharge pulse and reservoir level fluctuation. Lower piezometer cells that were compared with real piezometers in this study are shown. Note how the magnitude of fluctuation decreases both away from the reservoir and upslope in the vicinity of the piezometer cells, as was observed with the actual piezometers. For model layer 3 setup see figure 39.

Table 4. Comparison of Fluctuation Peaks in Time

Piezometers arranged in order of fluctuation in time. Piezometers in square brackets represent multiple peaks, or uncertain peak timing.

Timing	Actual Fluctuation Data (1994)	Simulation of Reservoir Level Fluctuation Only	Simulation of Recharge Rate Fluctuation Only	Simulation of Both Reservoir Level and Recharge Rate Fluctuations
UPPER				
Earliest	8	Reservoir	1, 2A, 3, 6, 8	Reservoir
	3	6		2A, 3, 6, 8
	1	1		1
	Reservoir	8		
	2A	3		
Latest	6	2A		
LOWER				
Earliest	Reservoir, [8]	Reservoir, 1, 6	1, 6	Reservoir
	1	2A, 3, 8	2A	1,6
	6	5	3	2A
	2A		8	3,8
	3		5	5
	[8]			
Latest	5			

alluvium, which penetrates the confining layer and is also connected to the reservoir. Groundwater flow in the upper flow domain is mainly down the axis of the landslide, with the buried channel acting like a drain that collects all of the water flowing down the landslide and removes it. The large fluctuations in groundwater level within the landslide, observed during the summer months, are caused by an influx of snowmelt recharge. The groundwater fluctuations observed within the landslide occur before or at the same time as the reservoir fluctuation. Large fluctuations in groundwater levels, similar to the upper flow domain, were also observed in the lower flow domain. However, the mechanisms behind the fluctuations are completely different. In the lower flow domain, the reservoir fluctuations control the timing and magnitude of groundwater fluctuations. All groundwater fluctuations occur after, or nearly synchronous with the reservoir fluctuation. The largest and earliest groundwater fluctuations occur toward the toe of the landslide, in proximity to the buried channel of alluvium. As the reservoir fluctuation propagates uphill and away from the reservoir, the fluctuations decrease in magnitude until they are not observed. A generic MODFLOW dipping bed simulation was run to see if the qualitative observations could be verified quantitatively. Model results within the landslide failed to mimic observed groundwater behavior, but modeled results of flow below the landslide matched observed groundwater behavior much better. The inability of the model to match the fluctuations seen in the upper piezometers could be due to spatially and temporally variable recharge, and spatially variable hydrologic properties within the landslide. The model does support the idea that the reservoir is the main driving mechanism for the fluctuations seen in the lower piezometers, and that a recharge rate fluctuation is the likely driving mechanism behind the upper piezometer fluctuations.

5. SUMMARY AND CONCLUSIONS

The Costilla Dam landslide is a reactivated portion of the Costilla Dam landslide complex located just downstream of the right abutment of Costilla Dam. Costilla Dam is an earth-fill dam completed in 1921 whose right abutment is the Costilla Dam landslide complex. The Costilla Dam landslide was reactivated in 1988 or 1989 when construction activities on the dam decreased slope stability. After reactivation the landslide was instrumented, monitored, and stabilized.

Geology of the landslide site consists of dipping deposits of the Santa Fe Group. All landslides identified near the Costilla Dam landslide are derived from the moderately consolidated basin-fill deposits of the Santa Fe Group, suggesting its susceptibility to slope instability. Geologic control on movement of the Costilla Dam landslide complex and Costilla Dam landslide includes the ~10 degree dip of basin-fill deposits into the valley. Interbedded with these deposits is a basalt flow with a weathered clay-rich surface. This clay zone is the slide plane for both the Costilla Dam landslide and part of the landslide complex. The basalt flow and overlying clay zone is absent in the subsurface near the toe of the landslide. The ancestral Costilla Creek probably eroded the basalt flow prior to the initial activation of the Costilla Dam landslide complex. The buried channel of alluvium is likely located beneath the landslide deposits where they protruded into the valley.

Nested piezometers allow observation of groundwater both within the landslide and below the slide plane. The upper flow domain is unconfined and flows within the landslide deposit. Groundwater flow in the upper flow domain is generally down the axis of the landslide. The lower flow domain is confined beneath the slide plane and flows in basin-fill deposits beneath the landslide. Groundwater flow in the lower flow domain is generally down the axis of the landslide, except near the toe of the landslide where there is a larger component of down-valley flow. In all cases the head in the upper flow domain is always higher than the head in the lower flow domain. Most piezometers, the reservoir, and the stream gauges show one large fluctuation peak in head, elevation, and flow respectively during the summer field season. Fluctuations within the upper flow domain are controlled most likely by snowmelt recharge and occur before, or are synchronous with the reservoir fluctuations. Fluctuations within the lower flow domain are controlled by the fluctuation of the reservoir level and occur synchronous, or after the reservoir fluctuation. The magnitude of piezometer groundwater fluctuations decreases, while the time lag increases, both uphill and away from the reservoir. The upper and lower flow domains are connected in the buried channel of alluvium beneath the landslide deposit, within the valley. This coarse grained alluvium acts as a drain that captures all flow within the landslide before it gets to the toe and directs it down valley out from beneath the landslide. Lower flow domain piezometers completed within this buried channel react almost instantaneously to fluctuations of the reservoir. A generic MODFLOW dipping bed simulation supported the idea that the lower flow domain groundwater fluctuations are controlled by the reservoir level fluctuation, but was inconclusive about driving

mechanisms within the upper flow domain. Whereas the upper and lower flow domains have similar looking seasonal fluctuations, the driving forces behind them are different.

APPENDIX I. DRILL HOLE LOGS

The drill hole well logs are to scale vertically. The number on the left is the elevation of each particular feature in feet, while the number on the right is the depth from the surface in feet. The geologic interpretation of the log is contained outside of the box.

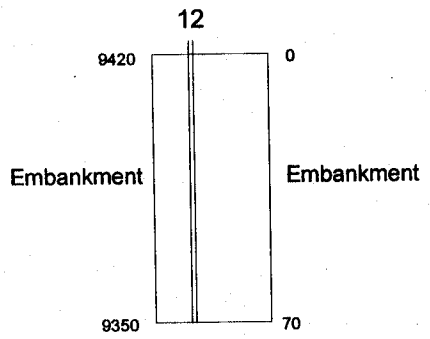
12
9420
0
Embankment
Embankment
9350
70

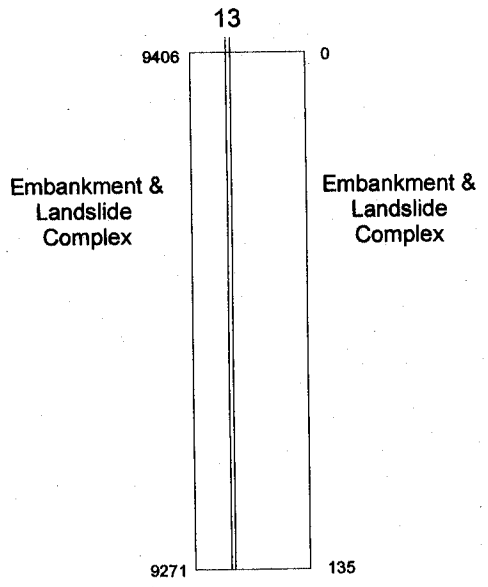
13
9406
0
Embankment &
Landslide
Complex
Embankment &
Landslide
Complex
9271
135

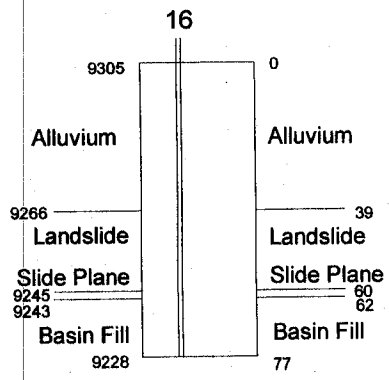
16
9305
0
Alluvium
Alluvium
9266
39
Landslide
Landslide
Slide Plane
Slide Plane
9245
60
9243
62
Basin Fill
Basin Fill
9228
77

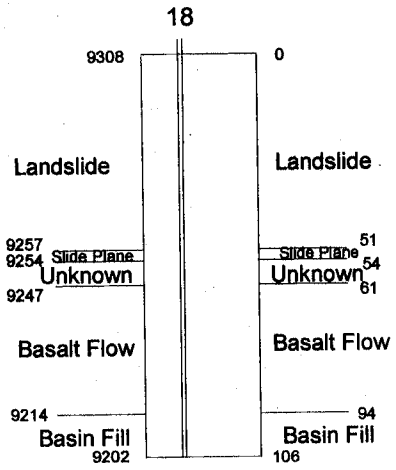
18
9308
0
Landslide
Landslide
9257
9254
Slide Plane
Unknown
9247
Slide Plane
51
Unknown
54
61
Basalt Flow
Basalt Flow
9214
Basin Fill
9202
94
Basin Fill
106

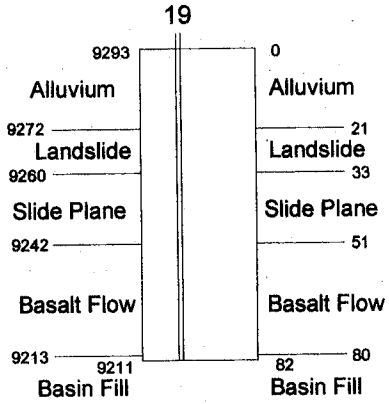
19
9293
0
Alluvium
Alluvium
9272
Landslide
21
Landslide
9260
33
Slide Plane
Slide Plane
9242
51
Basalt Flow
Basalt Flow
9213
9211
Basin Fill
82
80
Basin Fill

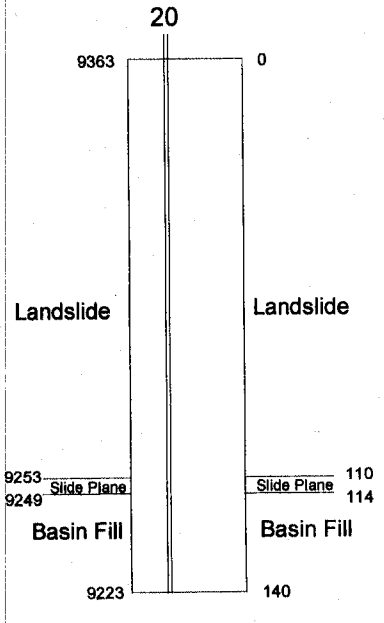
20
9363
0
Landslide
Landslide
9253
Slide Plane
9249
Basin Fill
Slide Plane
110
114
Basin Fill
9223
140

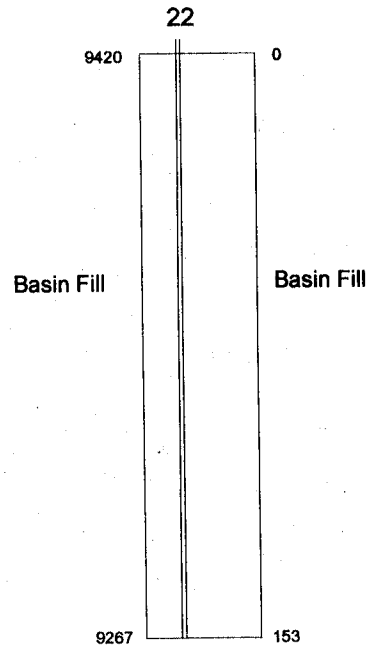
22
9420
0
Basin Fill
Basin Fill
9267
153

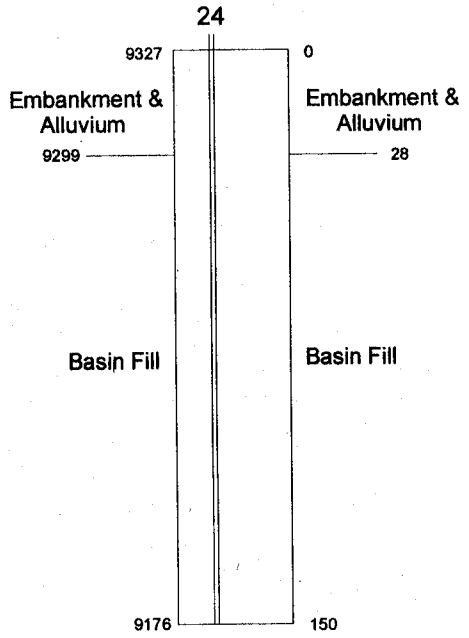
24
9327
0
Embankment &
Alluvium
Embankment &
Alluvium
9299
28
Basin Fill
Basin Fill
9176
150

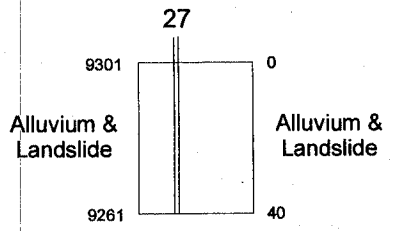
27
9301
0
Alluvium &
Landslide
Alluvium &
Landslide
9261
40

APPENDIX II. INCLINOMETER LOGS

The inclinometer well logs are to scale vertically. The number on the left is the elevation of each particular feature in feet, while the number on the right is the depth from the surface in feet. Divisions within the box are related to the construction of the instrument, while geologic interpretation of the log and inclinometer data (Appendix VI) is contained outside of the box.

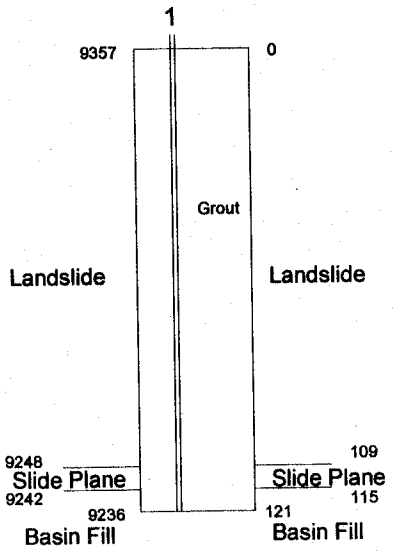
1
9357
0
Grout
Landslide
Landslide
9248
Slide Plane
9242
9236
109
Slide Plane
115
121
Basin Fill
Basin Fill

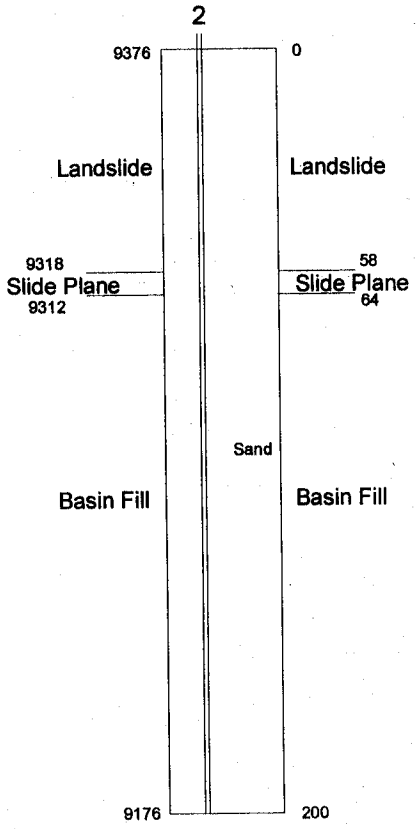
2
9376
0
Landslide
Landslide
9318
Slide Plane
9312
58
Slide Plane
64
Sand
Basin Fill
Basin Fill
9176
200

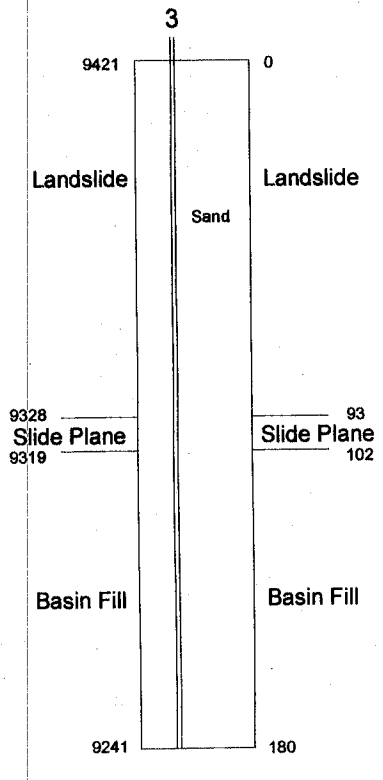
3
9421
0
Landslide
Landslide
Sand
9328
Slide Plane
9319
93
Slide Plane
102
Basin Fill
Basin Fill
9241
180

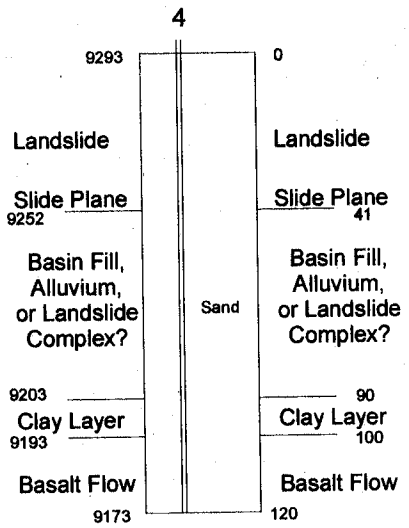
4
9293
0
Landslide
Landslide
Slide Plane
9252
Slide Plane
41
Basin Fill,
Alluvium,
or Landslide
Complex?
Sand
Basin Fill,
Alluvium,
or Landslide
Complex?
9203
90
Clay Layer
9193
Clay Layer
100
Basalt Flow
9173
120
Basalt Flow

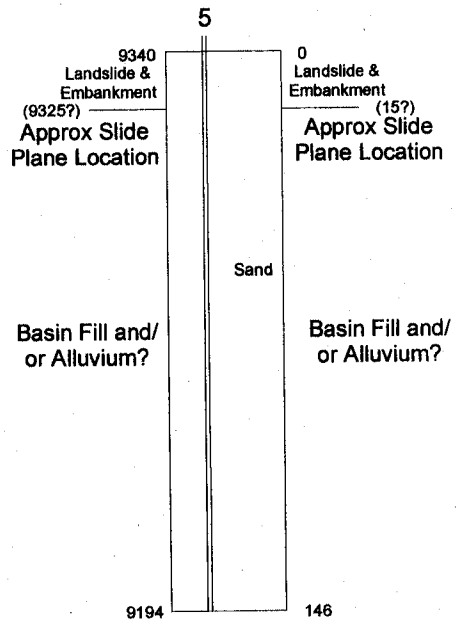
5
9340
Landslide &
Embankment
(9325?)
Approx Slide
Plane Location
0
Landslide &
Embankment
(15?)
Approx Slide
Plane Location
Sand
Basin Fill and/
or Alluvium?
Basin Fill and/
or Alluvium?
9194
146

APPENDIX III. PIEZOMETER LOGS

The piezometer well logs are to scale vertically. The number on the left is the elevation of each particular feature in feet, while the number on the right is the depth from the surface in feet. Divisions within the box are related to the construction of the instrument, while geologic interpretation of the log is contained outside of the box. More data that was left off of the logs, but may be important is the diameter of the piezometer and the type of openings. The following table contains construction information not contained on the graphic well logs for the landslide piezometers.

PIEZOMETER	STANDPIPE	TYPE OF OPENINGS
1U	Unknown size?	Porous tube
1L	¾ inch diameter PVC pipe	0.020 inch slots in PVC pipe
2U	2 inch diameter PVC pipe	0.020 inch slots in PVC pipe
2AU	¾ inch diameter PVC pipe	Porous tube
2AL	2 inch diameter PVC pipe	0.020 inch slots in PVC pipe
3U	¾ inch diameter PVC pipe	Porous tube
3L	2 inch diameter PVC pipe	0.020 inch slots in PVC pipe
4U	¾ inch diameter PVC pipe	Porous tube
4L	2 inch diameter PVC pipe	0.020 inch slots in PVC pipe
5L	2 inch diameter PVC pipe	0.020 inch slots in PVC pipe
6U	¾ inch diameter PVC pipe	Porous tube
6L	¾ inch diameter PVC pipe	Porous tube
7U	1 ½ inch diameter PVC pipe	0.020 inch slots in PVC pipe
7L	¾ inch diameter PVC pipe	0.010 inch slots in PVC pipe
8U	1 ½ inch diameter PVC pipe	0.020 inch slots in PVC pipe
8L	¾ inch diameter PVC pipe	0.010 inch slots in PVC pipe

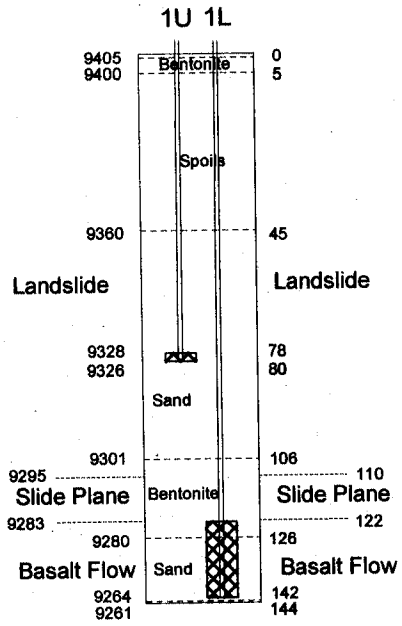
1U 1L
9405
9400
Bentonite
0
5
Spoils
9360
45
Landslide
Landslide
9328
9326
78
80
Sand
9301
106
9295
110
Slide Plane
Bentonite
Slide Plane
9283
122
9280
126
Basalt Flow
Sand
Basalt Flow
9264
9261
142
144

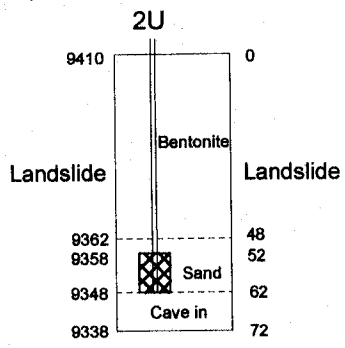
2U
9410
0
Bentonite
Landslide
Landslide
9362
9358
48
52
Sand
9348
62
Cave in
9338
72

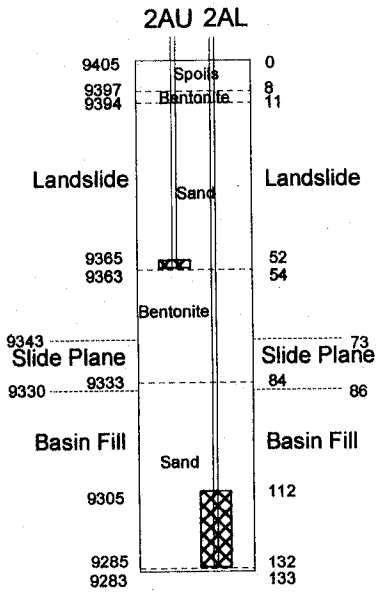
2AU 2AL
9405
Spoils
0
9397
9394
Bentonite
8
11
Landslide
Landslide
Sand
9365
9363
52
54
Bentonite
9343
Slide Plane
73
Slide Plane
9330
9333
84
86
Basin Fill
Basin Fill
Sand
9305
112
9285
9283
132
133

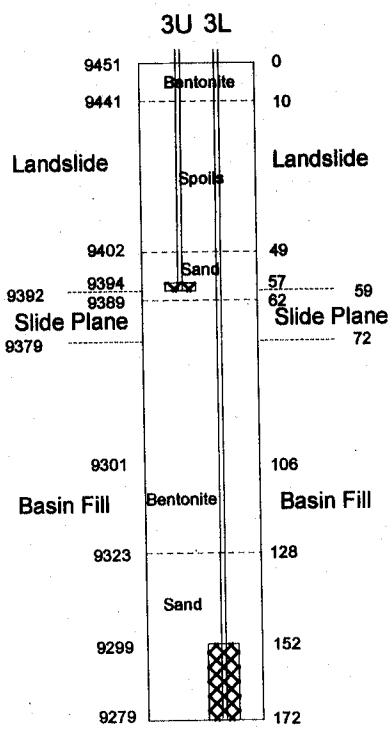
3U 3L
9451
0
Bentonite
9441
10
Landslide
Landslide
Spoils
9402
49
Sand
9394
57
9392
9389
62
59
Slide Plane
Slide Plane
9379
72
9301
106
Basin Fill
Bentonite
Basin Fill
9323
128
Sand
9299
152
9279
172

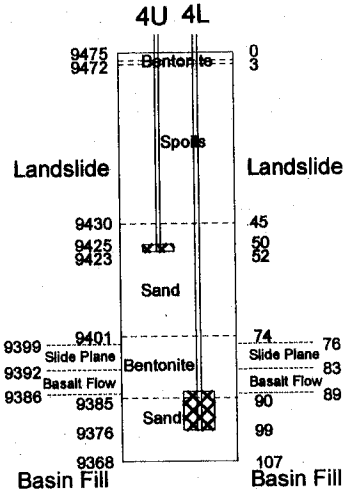
4U 4L
9475
9472
0
3
Bentonite
Spoils
Landslide
Landslide
9430
45
9425
9423
50
52
Sand
9401
74
76
9399
Slide Plane
Slide Plane
9392
Basalt Flow
Bentonite
Basalt Flow
83
9386
9385
90
89
Sand
9376
99
9368
107
Basin Fill
Basin Fill

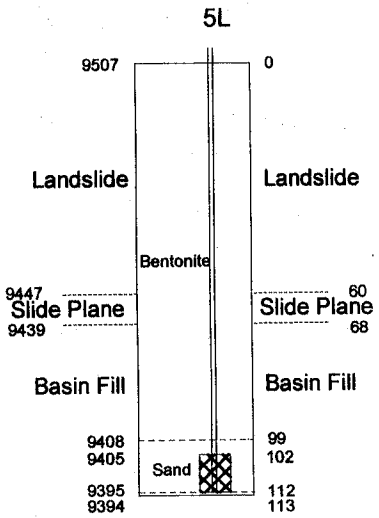
5L
9507
0
Landslide
Landslide
Bentonite
9447
60
Slide Plane
Slide Plane
9439
68
Basin Fill
Basin Fill
9408
99
9405
102
Sand
9395
112
9394
113

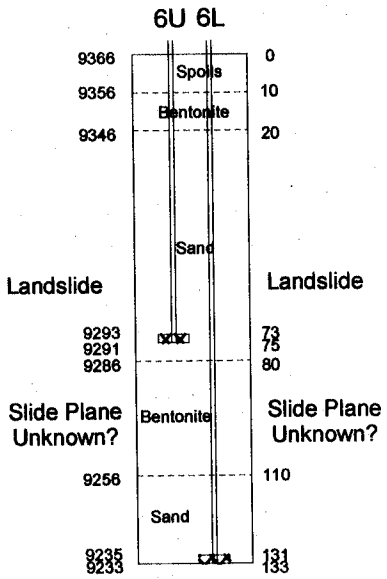
6U 6L
9366
0
Spoils
9356
10
Bentonite
9346
20
Sand
Landslide
Landslide
9293
73
9291
75
9286
80
Slide Plane
Unknown?
Bentonite
Slide Plane
Unknown?
9256
110
Sand
9235
131
9233
133

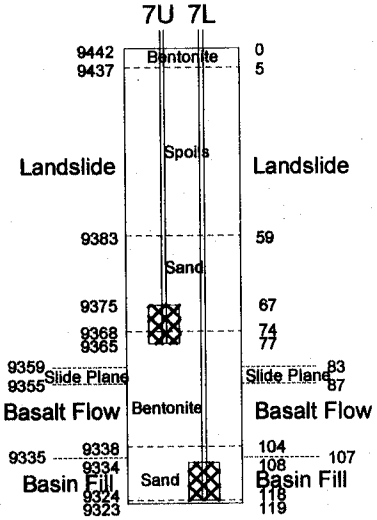
7U 7L
9442
0
Bentonite
9437
5
Landslide
Spoils
Landslide
9383
59
Sand
9375
67
9368
74
9365
77
9359
83
9355
Slide Plane
Slide Plane
87
Basalt Flow
Bentonite
Basalt Flow
9338
104
9335
9334
107
108
Basin Fill
Sand
Basin Fill
9324
118
9323
119

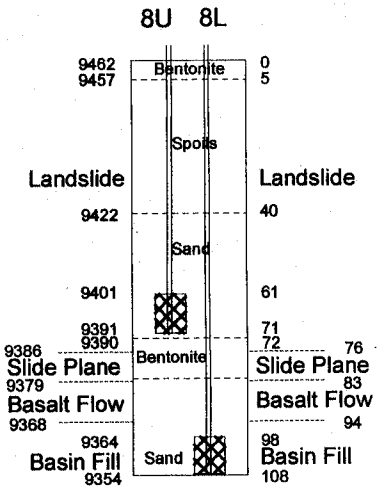
8U 8L
9462
0
9457
5
Bentonite
Spoils
Landslide
Landslide
9422
40
Sand
9401
61
9391
71
9390
72
76
9386
Bentonite
Slide Plane
Slide Plane
9379
83
Basalt Flow
Basalt Flow
9368
94
9364
98
Basin Fill
Sand
Basin Fill
9354
108

APPENDIX IV. STREAM GAUGE INFORMATION

Information on USGS Stream Gauges near Costilla Reservoir			
Gauging Station	**USGS Station Number**	**Drainage Area (km^2)**	**% of Total Reservoir Drainage Area**
Santistevan Creek	08253500	5.57	4
Casias Creek	08253000	42.99	30
Costilla Creek above Reservoir	08252500	65.01	46
Costilla Creek below Reservoir	08254000	141.40	100

APPENDIX V. OTHER GEOLOGIC OBSERVATIONS

A decision was made to discuss the following information in an appendix instead of the main text to maintain fluidity within the body of the report. The information presented here may be useful to the larger understanding of the geology of the area, but it does not directly impact the Costilla Dam landslide. The ideas presented here are based on reconnaissance geologic mapping, and would need to be looked at in greater detail by other investigators in order to be supported or rejected.

V.1 ABANDONED AND CURRENT COLLUVIUM/ALLUVIUM

As mentioned previously, the colluvium/alluvium unit is lumped due to difficulties in separating out the two facies. In general, this unit fills all side valleys where tributary drainages flow into Costilla Creek. There may be as many as four different fluvial geomorphic surfaces within the Costilla Creek drainage, but only the two surfaces seen in the vicinity of the Costilla Dam landslide will be discussed. The two surfaces have been termed "current" and "abandoned". The current surfaces are the most prevalent, and are located adjacent to tributary streams, or form the surface found at the axis of unchannelized tributary valleys. The grain-size distribution for the current surfaces range from small gravel to clay. The abandoned surfaces are generally located adjacent to bedrock outcrops at the mouths of the largest tributary valleys. Away from the axis of Costilla Valley, both the current and abandoned surfaces have the same slope.

Close to the axis of Costilla Valley, the abandoned surfaces tend to a gentler slope than the current surface. The abandoned surfaces also contain a much different range of clast sizes. The material deposited to construct this surface ranges from boulder to clay. The large fraction of boulder- and gravel-sized material catches the eye, and suggests that deposition occurred under a higher-energy environment than the current surface. Although measurements were not taken, the abandoned surface probably ranges from 3 to 6 meters (10 to 20 feet) higher than the current surface.

The abandoned surface can be seen best at the following four locations:

1. The south side at the mouth of Powderhouse Canyon, on the east side of the andesite outcrop (Figure 45).
2. On the north side of the road to the dam, just south of the mouth of Powderhouse Canyon. The larger overall clast size can be observed in the road cut. On the north side of this deposit, the current and abandoned surfaces have the same slope.
3. The mouth of Blind Canyon adjacent to the ash with basal vitrophyre and basalt units (Figure 46).
4. At the mouth of Santistevan Creek upvalley from the dam.

It could be argued that the colluvium/alluvium unit on this geologic map is in fact just a younger portion of the basin-fill unit. I think that my previous conclusions are correct for the following reasons: the abandoned unit is commonly found at the mouths of tributary valleys, independent of what geologic unit outcrops in the area. This association with the mouths of tributary streams and the fact that some of the units are stratigraphically removed from the basin-fill unit suggests that the units are different. The location of these deposits can be explained easier geomorphically than stratigraphically.

Figure 45 Colluvium/Alluvium unit at the mouth of Powderhouse Canyon. The current colluvium/alluvium unit is located at the bottom of Powderhouse Canyon to the right in the photograph. The abandoned colluvium/alluvium unit is the planar surface that is seen on the far left hand side of the photograph. Vertical difference between these two surfaces is from 3 to 6 meters (10 to 20 feet).

Figure 46 Colluvium/Alluvium unit at the mouth of Blind Canyon. The current colluvium/alluvium unit is seen adjacent to the small tributary stream that flows into Costilla Creek which it the larger stream flowing from right to left. The abandoned colluvium/alluvium deposit is the planar surface that is seen at the base of the hill in the foreground. Trees grow on the steep sides and grass grows on top. The surface is roughly triangular in shape.

Speculation as to the origin of these surfaces is beyond the scope of this investigation, but contributing factors may have been:

1. Periodic incision of the Rio Grande
2. Wetter climate during the Pleistocene, depositing high-energy material to the level of the abandoned surfaces seen today.
3. Alpine glaciation of tributary valleys at higher elevations within the Costilla Creek drainage basin.

V.2 FAULTS

Two faults were positively identified in the map area. Other faults could be interpreted from the location of different geologic units with respect to one another. Both of the faults that could be seen in outcrop occurred on the northern side of the large andesite outcrop on the downstream right side of the dam. The movement along these faults can be identified by slickensides, but both show different types of movement.

V.2.1 Small Faults

This fault is located on the northern side of the contact between the pink tuff and andesite. At this side of the outcrop the contact changes from what was seen on the southern side of the outcrop to a strike and dip of N40E/57SW. Striations can be seen best on promontories of the rock, and could possibly also be caused by extreme folding on this side of the outcrop. The trend and plunge of the southern fault striations is N50E/15. These striations are located on the base of the pink tuff at the top of the andesite unit. Striations at this location suggest largely strike-slip movement.

In the same outcrop on the downstream right hand side of the dam there is another small fault. The fault lies just upstream from the andesite outcrop and within an andesitic tuff. The fault plane is vertical with a strike of N55E. The trend and plunge of the striae is N55E/4. The striations suggest that at least the last movement along the fault was strike-slip. The offset of the outcrop indicates that the fault is a right lateral strike-slip fault with a small offset of approximately 4.5 meters (15 feet).

V.2.2 Major Faults

Major faults cannot be seen in outcrop, but can be inferred from stratigraphic relationships. Lipman and Reed (1989) have the Older Fluvial unit in depositional contact with the basement rock, and I did not find any evidence to suggest otherwise. No outcrops exist that show basin-fill deposits adjacent to the basement rock unit. The contact between these units is everywhere concealed by the colluvium/alluvium unit. The andesite unit, which forms the large outcrop to the downstream right side of the dam, abruptly ends and is not seen in the valley above this point. Basin-fill deposits can be seen dipping steeply at that contact, but no striations were seen on the andesite at that point. Based on the above observations it is likely that two large basin-bounding faults exist within the map area. One major fault likely separates the basement rock and basin-fill units in the northwest portion of the geologic map. The second major fault runs just southwest of the Costilla Dam landslide juxtaposing the basin-fill unit next to the andesite unit. It could be possible that only one major fault cuts the end of the andesite outcrop before proceeding to the NW to form the contact between the basin-fill and basement rock.

APPENDIX VI. INCLINOMETER DATA

This appendix contains inclinometer data that was collected and plotted by United States Bureau of Reclamation personnel (USBR, 11/1989). Only inclinometers one through four are included because movement of the Costilla Dam landslide ceased prior to installation of inclinometer five. My general interpretation of the location of the slide plane as indicated by the data is identified as the italicized numbers on each plot.

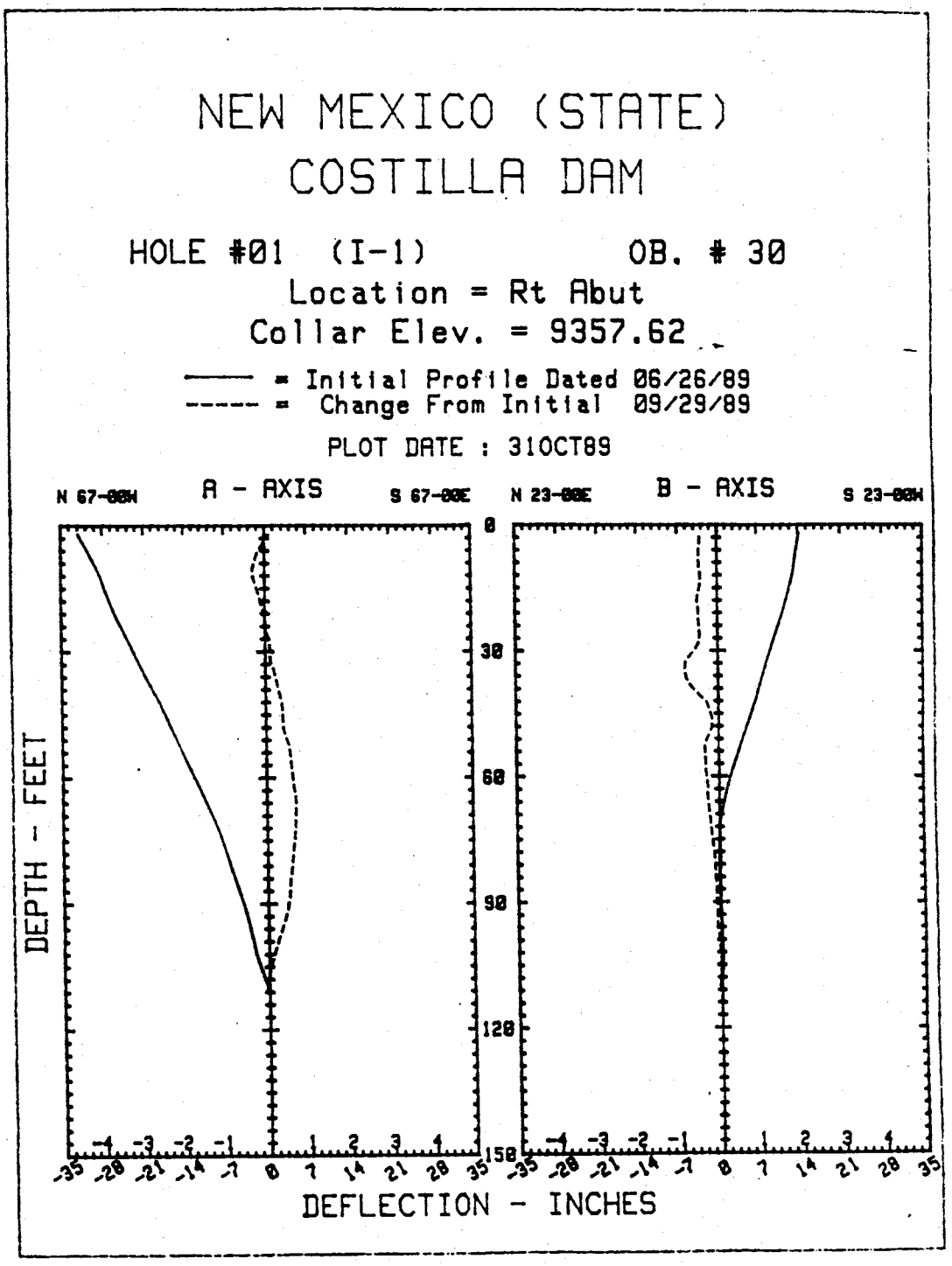
NEW MEXICO (STATE)
COSTILLA DAM
HOLE #01 (I-1) OB. # 30
Location = Rt Abut
Collar Elev. = 9357.62
——— = Initial Profile Dated 06/26/89
----- = Change From Initial 09/29/89
PLOT DATE : 31OCT89
N 67-00W
A - AXIS
S 67-00E
N 23-00E
B - AXIS
S 23-00W
DEPTH - FEET
0
30
60
90
120
150
-35 -28 -21 -14 -7 0 7 14 21 28 35
DEFLECTION - INCHES

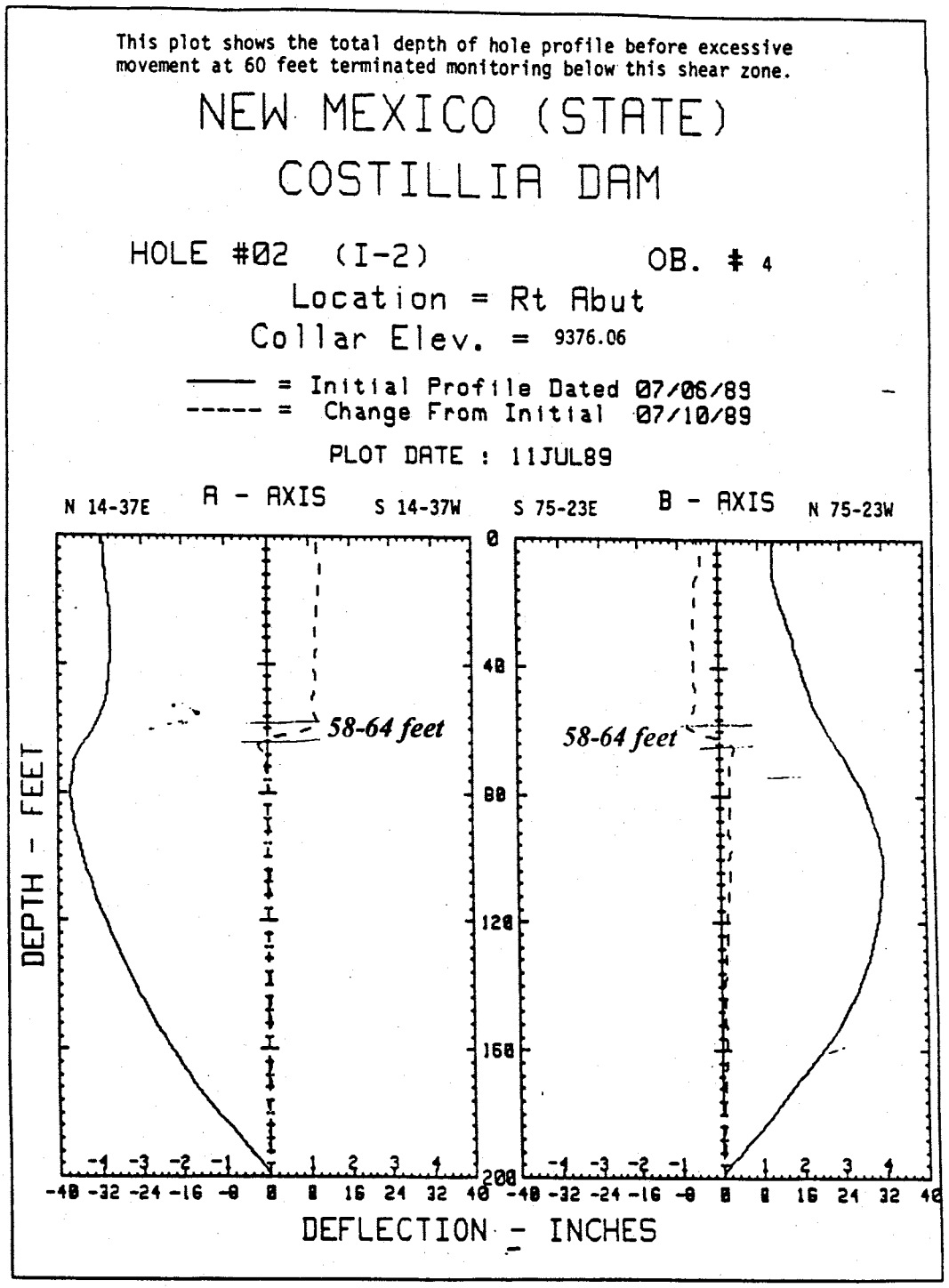
This plot shows the total depth of hole profile before excessive movement at 60 feet terminated monitoring below this shear zone.
NEW MEXICO (STATE)
COSTILLIA DAM
HOLE #02 (I-2)
OB. # 4
Location = Rt Abut
Collar Elev. = 9376.06
= Initial Profile Dated 07/06/89
= Change From Initial 07/10/89
PLOT DATE : 11JUL89
A - AXIS
N 14-37E
S 14-37W
B - AXIS
S 75-23E
N 75-23W
58-64 feet
58-64 feet
DEPTH - FEET
0
40
80
120
160
200
-40 -32 -24 -16 -8 0 8 16 24 32 40
-1 -3 -2 -1 1 2 3 4
DEFLECTION - INCHES

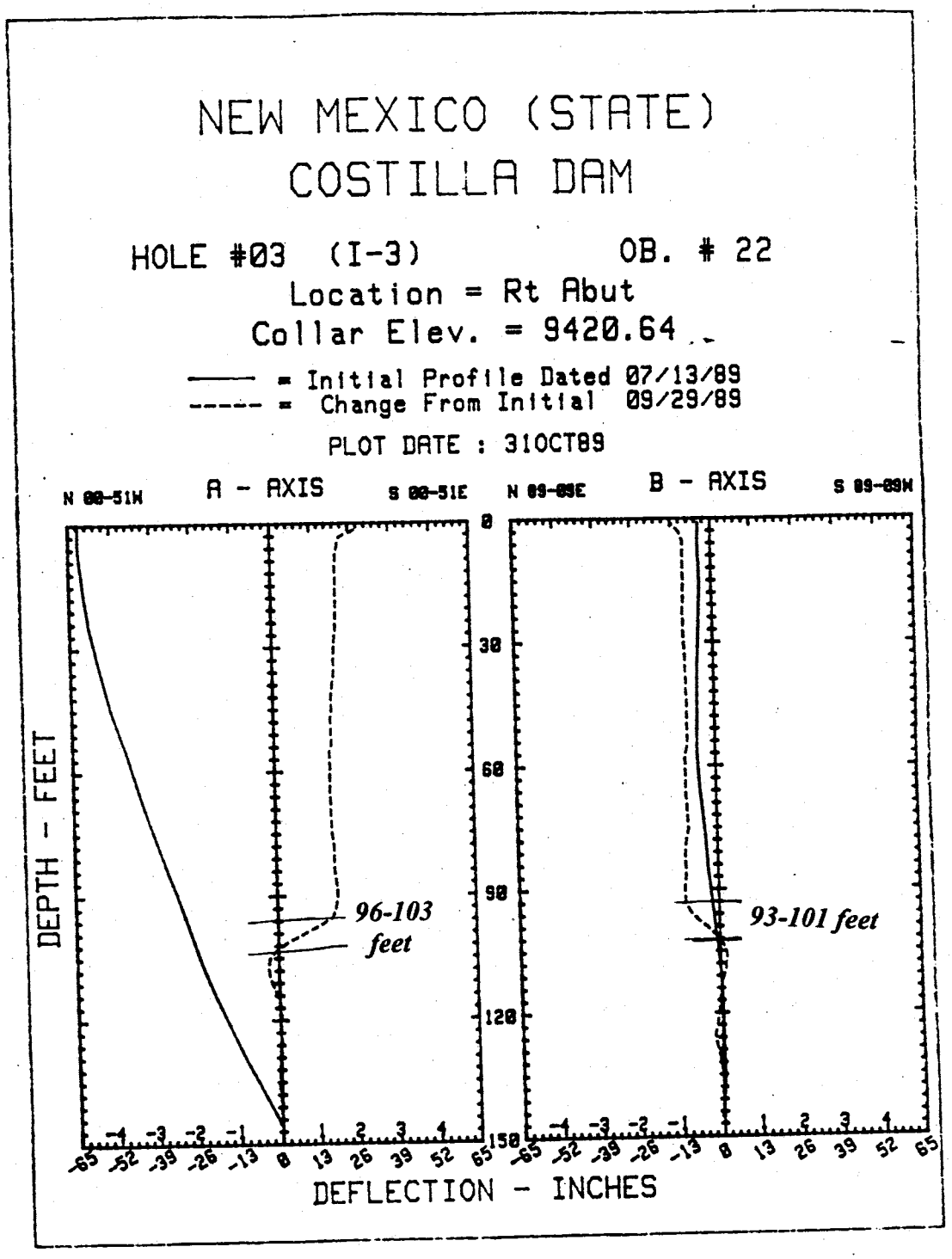
NEW MEXICO (STATE)
COSTILLA DAM
HOLE #03 (I-3) OB. # 22
Location = Rt Abut
Collar Elev. = 9420.64
——— = Initial Profile Dated 07/13/89
----- = Change From Initial 09/29/89
PLOT DATE : 31OCT89
N 00-51W
A - AXIS
S 00-51E
N 09-09E
B - AXIS
S 09-09W
DEPTH - FEET
0
30
60
90
120
150
96-103 feet
93-101 feet
-65 -52 -39 -26 -13 0 13 26 39 52 65
DEFLECTION - INCHES

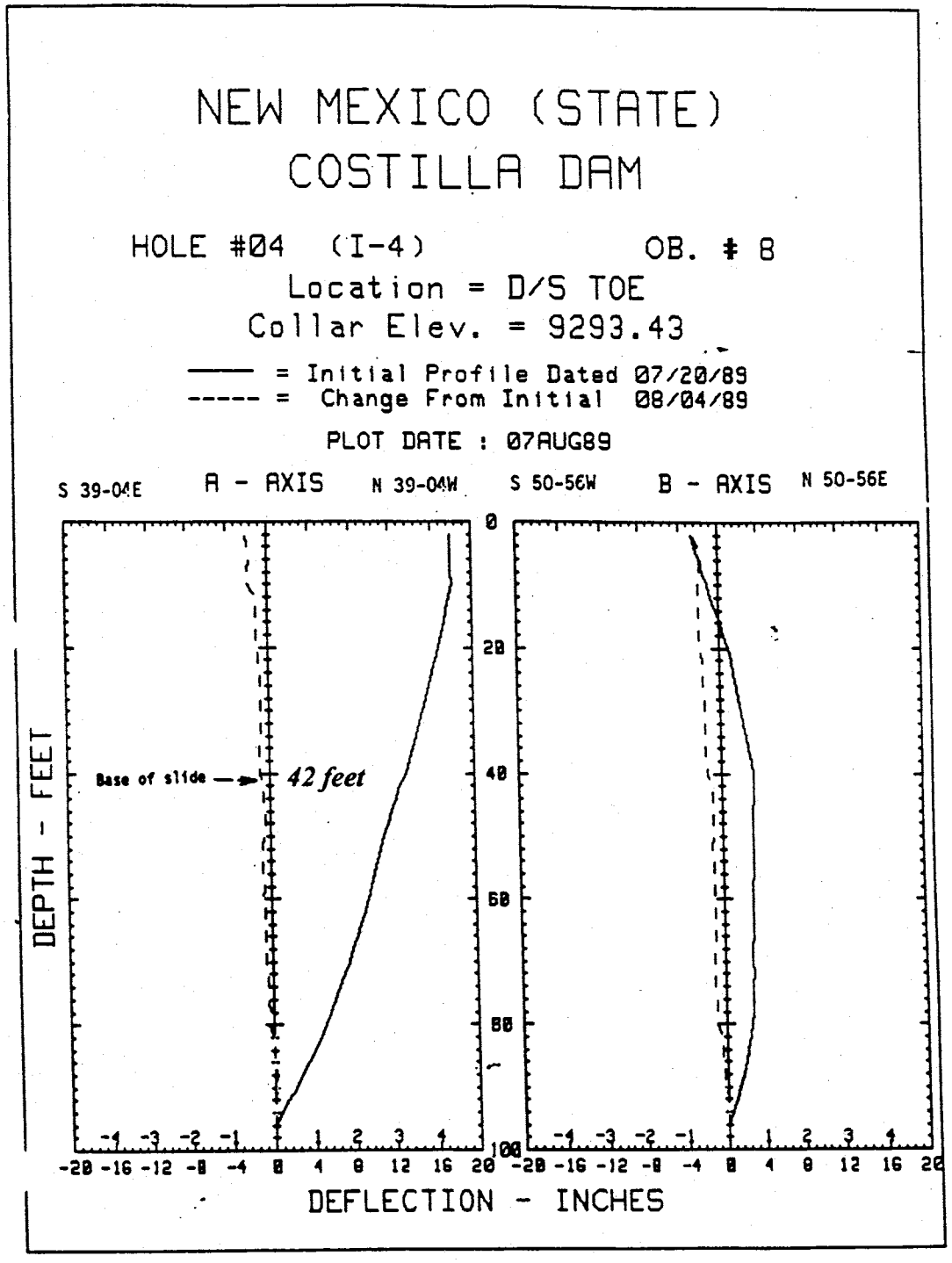
NEW MEXICO (STATE)
COSTILLA DAM
HOLE #04 (I-4)
OB. # 8
Location = D/S TOE
Collar Elev. = 9293.43
——— = Initial Profile Dated 07/20/89
----- = Change From Initial 08/04/89
PLOT DATE : 07AUG89
S 39-04E
A - AXIS
N 39-04W
S 50-56W
B - AXIS
N 50-56E
Base of slide
42 feet
DEPTH - FEET
DEFLECTION - INCHES

APPENDIX VII. STREAM GAUGE DATA

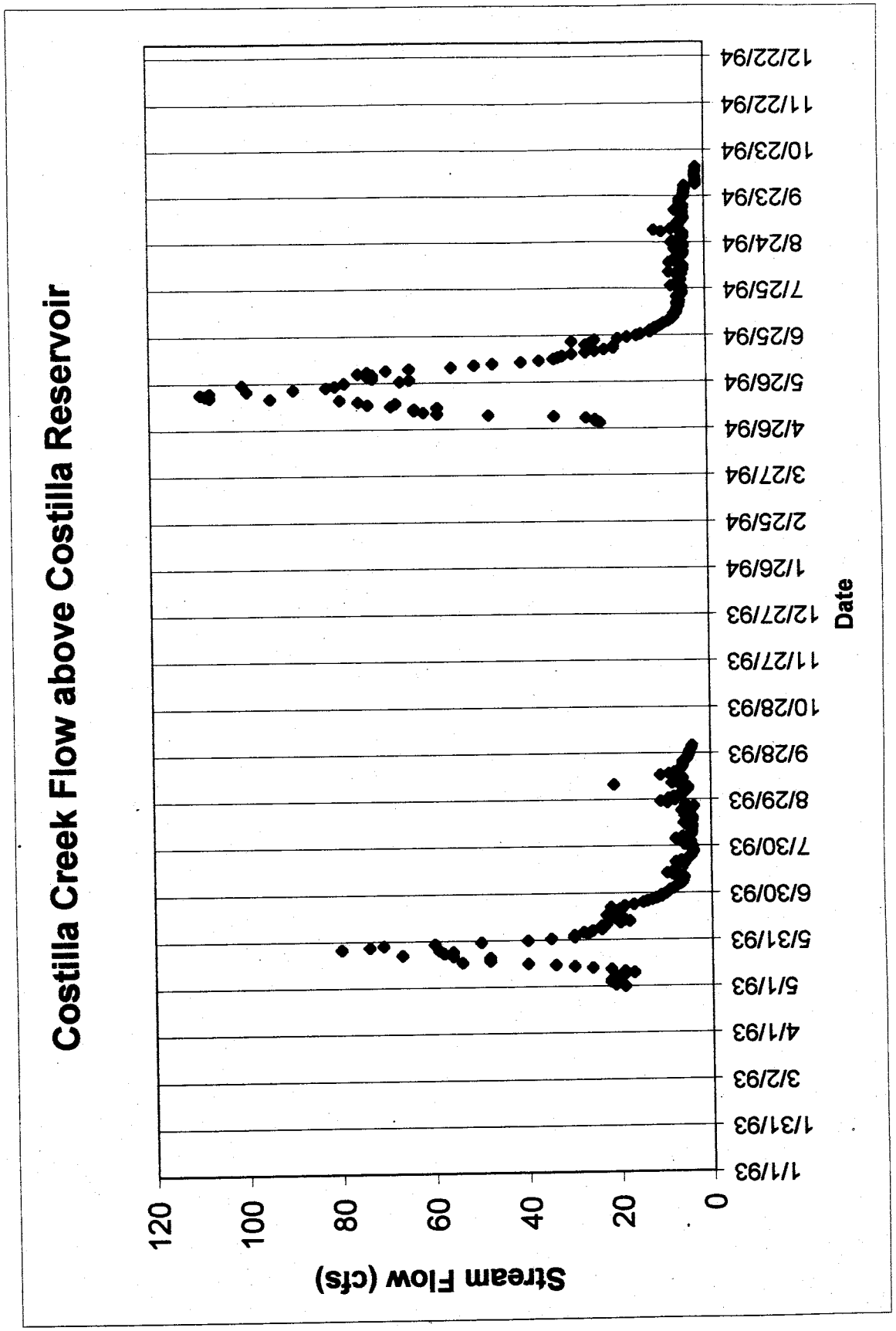
Costilla Creek Flow above Costilla Reservoir
Stream Flow (cfs)
0
20
40
60
80
100
120
Date
1/1/93
1/31/93
3/2/93
4/1/93
5/1/93
5/31/93
6/30/93
7/30/93
8/29/93
9/28/93
10/28/93
11/27/93
12/27/93
1/26/94
2/25/94
3/27/94
4/26/94
5/26/94
6/25/94
7/25/94
8/24/94
9/23/94
10/23/94
11/22/94
12/22/94

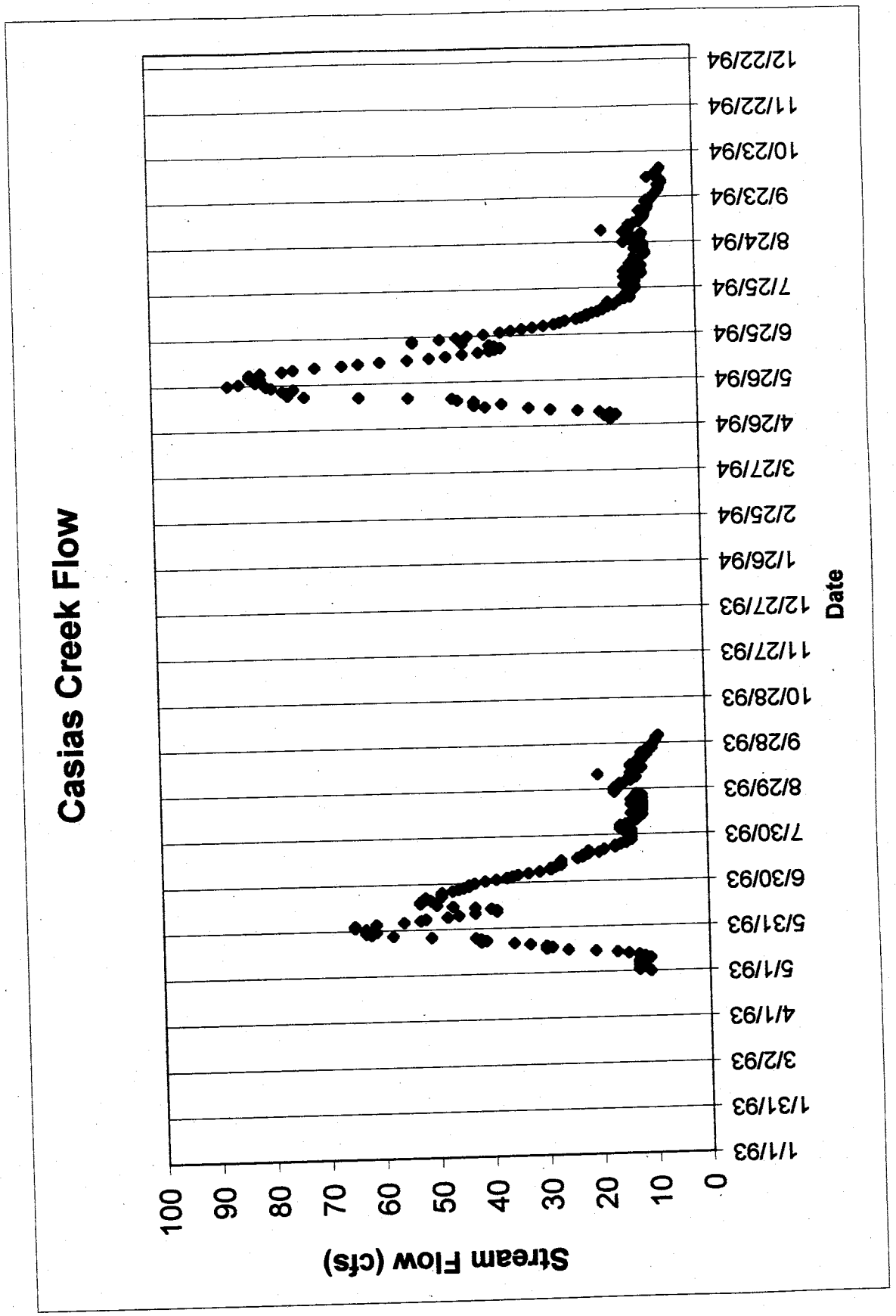
Casias Creek Flow
Stream Flow (cfs)
100
90
80
70
60
50
40
30
20
10
0
Date
1/1/93
1/31/93
3/2/93
4/1/93
5/1/93
5/31/93
6/30/93
7/30/93
8/29/93
9/28/93
10/28/93
11/27/93
12/27/93
1/26/94
2/25/94
3/27/94
4/26/94
5/26/94
6/25/94
7/25/94
8/24/94
9/23/94
10/23/94
11/22/94
12/22/94

Santistevan Creek Flow
Stream Flow (cfs)
0
2
4
6
8
10
12
14
Date
1/1/93
1/31/93
3/2/93
4/1/93
5/1/93
5/31/93
6/30/93
7/30/93
8/29/93
9/28/93
10/28/93
11/27/93
12/27/93
1/26/94
2/25/94
3/27/94
4/26/94
5/26/94
6/25/94
7/25/94
8/24/94
9/23/94
10/23/94
11/22/94
12/22/94

APPENDIX VIII. RESERVOIR DATA

This appendix contains a graph of the data from the reservoir used in this project for the study of the Costilla Dam landslide. The data is from the 1993 and 1994 field seasons, with the elevation indicated in feet. The vertical scale of the reservoir data is different than the scale for the piezometer data, so magnitude of fluctuation can not be compared directly between the two data sets.

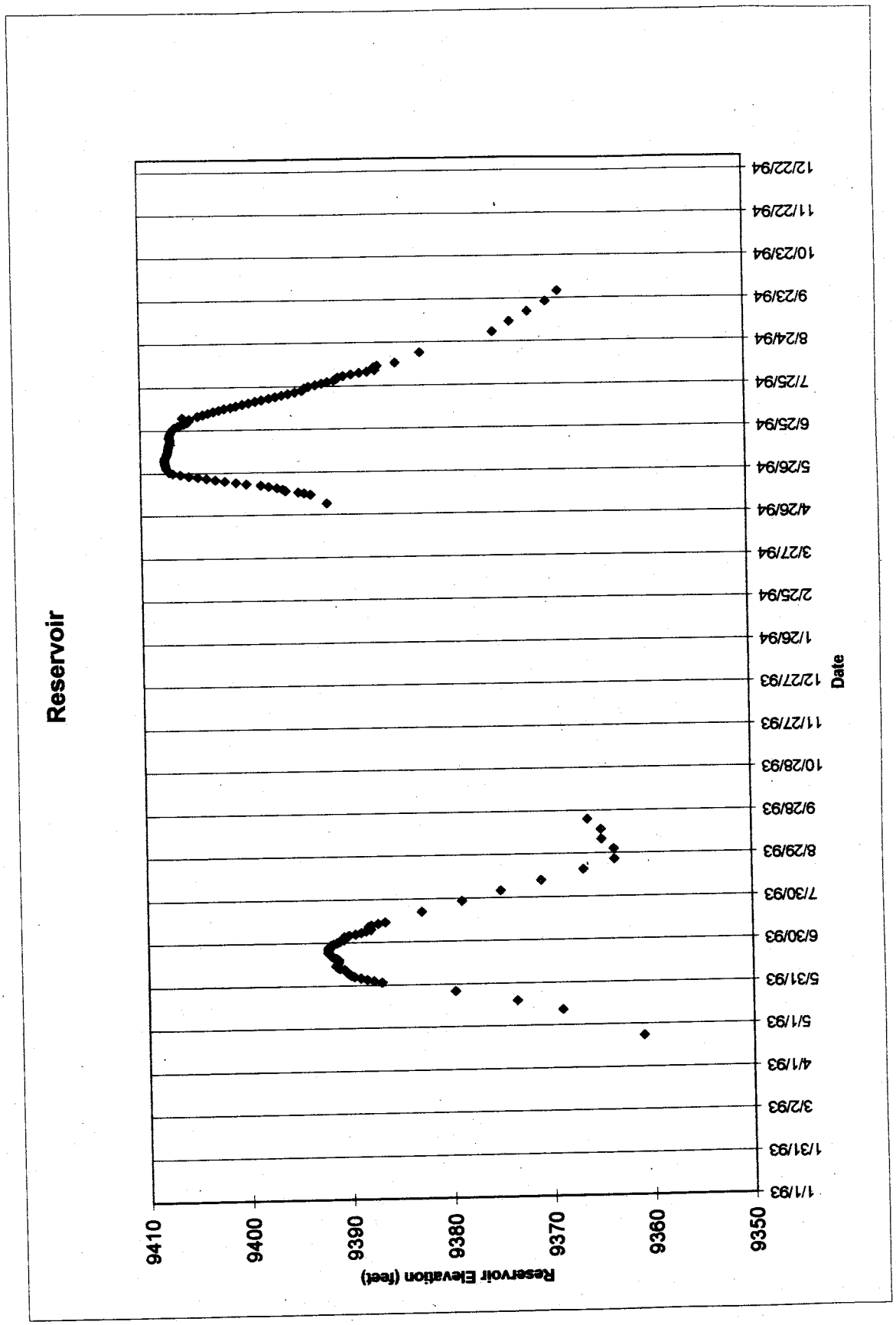
Reservoir
Reservoir Elevation (feet)
9410
9400
9390
9380
9370
9360
9350
Date
1/1/93
1/31/93
3/2/93
4/1/93
5/1/93
5/31/93
6/30/93
7/30/93
8/29/93
9/28/93
10/28/93
11/27/93
12/27/93
1/26/94
2/25/94
3/27/94
4/26/94
5/26/94
6/25/94
7/25/94
8/24/94
9/23/94
10/23/94
11/22/94
12/22/94

APPENDIX IX. PIEZOMETER DATA

This appendix contains graphs of the raw data from the piezometers used in this project for the study of the Costilla Dam landslide. The data is from the 1993 and 1994 field seasons, with the upper piezometer head on the left Y-axis, and the lower piezometer head on the right Y-axis. Each piezometer is plotted on a vertical scale of ten feet, so that the size of fluctuations can be easily compared between upper and lower completions and with other piezometer plots.

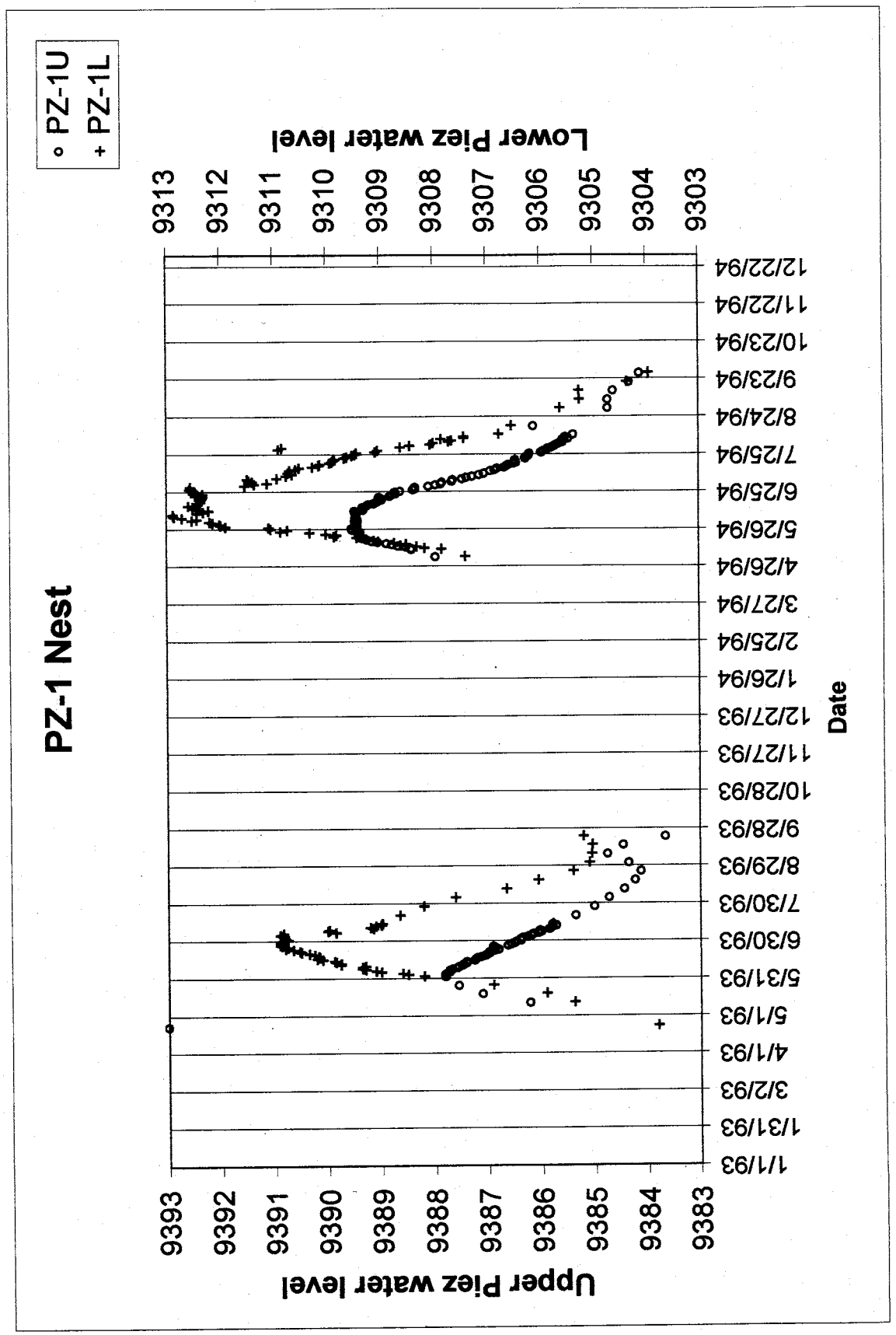
PZ-1 Nest
° PZ-1U
+ PZ-1L
Lower Piez water level
9313
9312
9311
9310
9309
9308
9307
9306
9305
9304
9303
Upper Piez water level
9393
9392
9391
9390
9389
9388
9387
9386
9385
9384
9383
Date
12/22/94
11/22/94
10/23/94
9/23/94
8/24/94
7/25/94
6/25/94
5/26/94
4/26/94
3/27/94
2/25/94
1/26/94
12/27/93
11/27/93
10/28/93
9/28/93
8/29/93
7/30/93
6/30/93
5/31/93
5/1/93
4/1/93
3/2/93
1/31/93
1/1/93

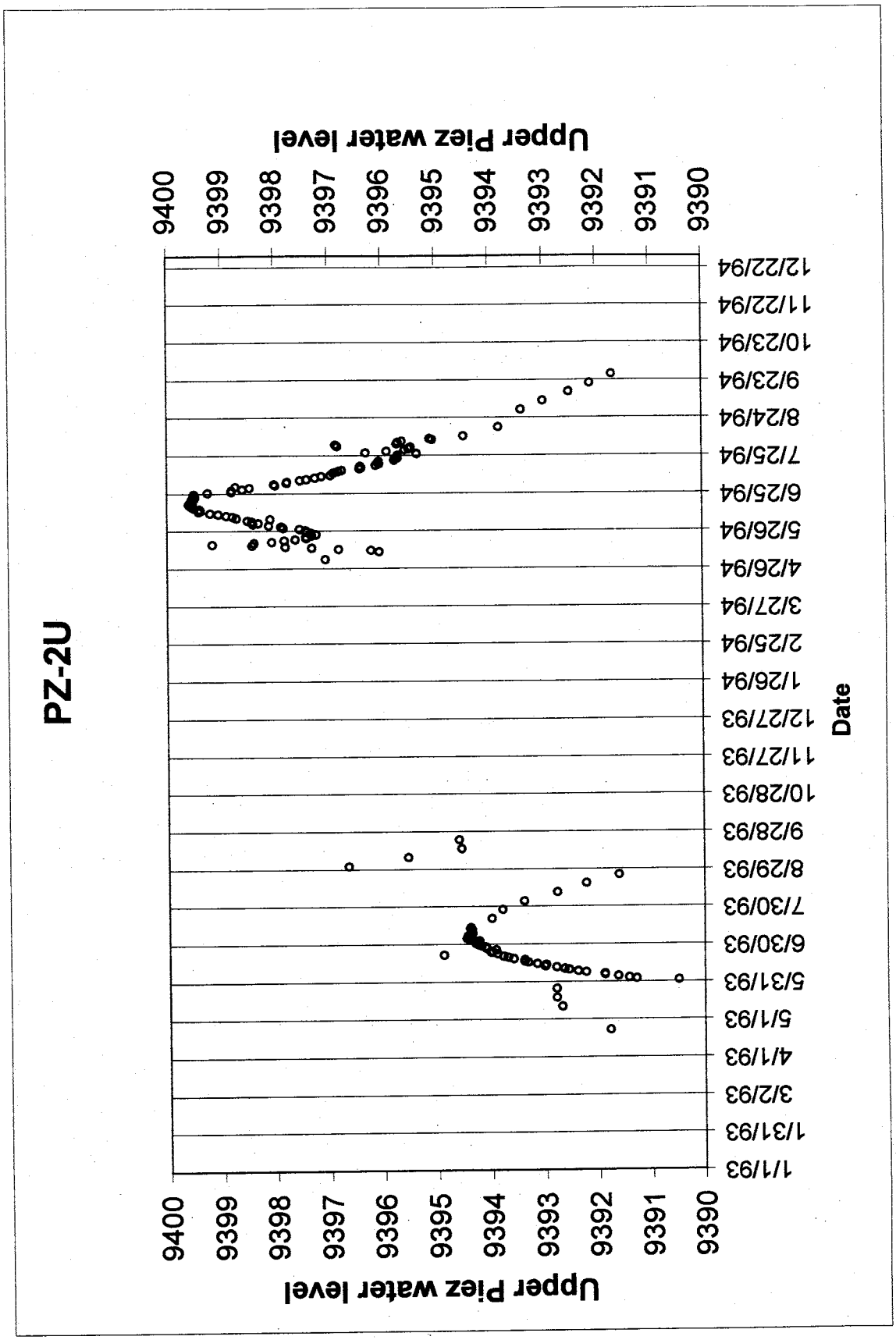
PZ-2U
Upper Piez water level
9400
9399
9398
9397
9396
9395
9394
9393
9392
9391
9390
Date
1/1/93
1/31/93
3/2/93
4/1/93
5/1/93
5/31/93
6/30/93
7/30/93
8/29/93
9/28/93
10/28/93
11/27/93
12/27/93
1/26/94
2/25/94
3/27/94
4/26/94
5/26/94
6/25/94
7/25/94
8/24/94
9/23/94
10/23/94
11/22/94
12/22/94

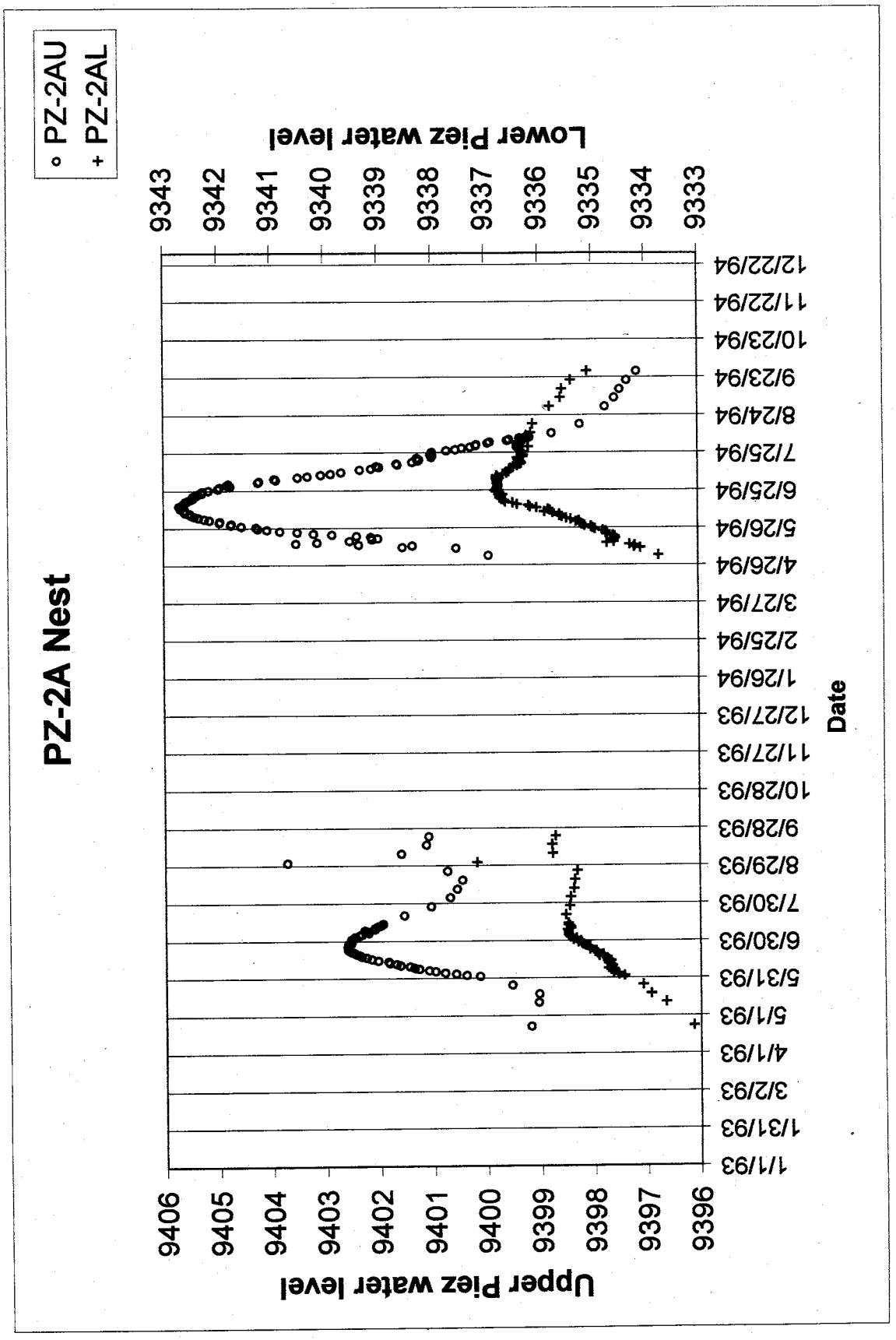
PZ-2A Nest
° PZ-2AU
+ PZ-2AL
Upper Piez water level
9406
9405
9404
9403
9402
9401
9400
9399
9398
9397
9396
Lower Piez water level
9343
9342
9341
9340
9339
9338
9337
9336
9335
9334
9333
Date
1/1/93
1/31/93
3/2/93
4/1/93
5/1/93
5/31/93
6/30/93
7/30/93
8/29/93
9/28/93
10/28/93
11/27/93
12/27/93
1/26/94
2/25/94
3/27/94
4/26/94
5/26/94
6/25/94
7/25/94
8/24/94
9/23/94
10/23/94
11/22/94
12/22/94

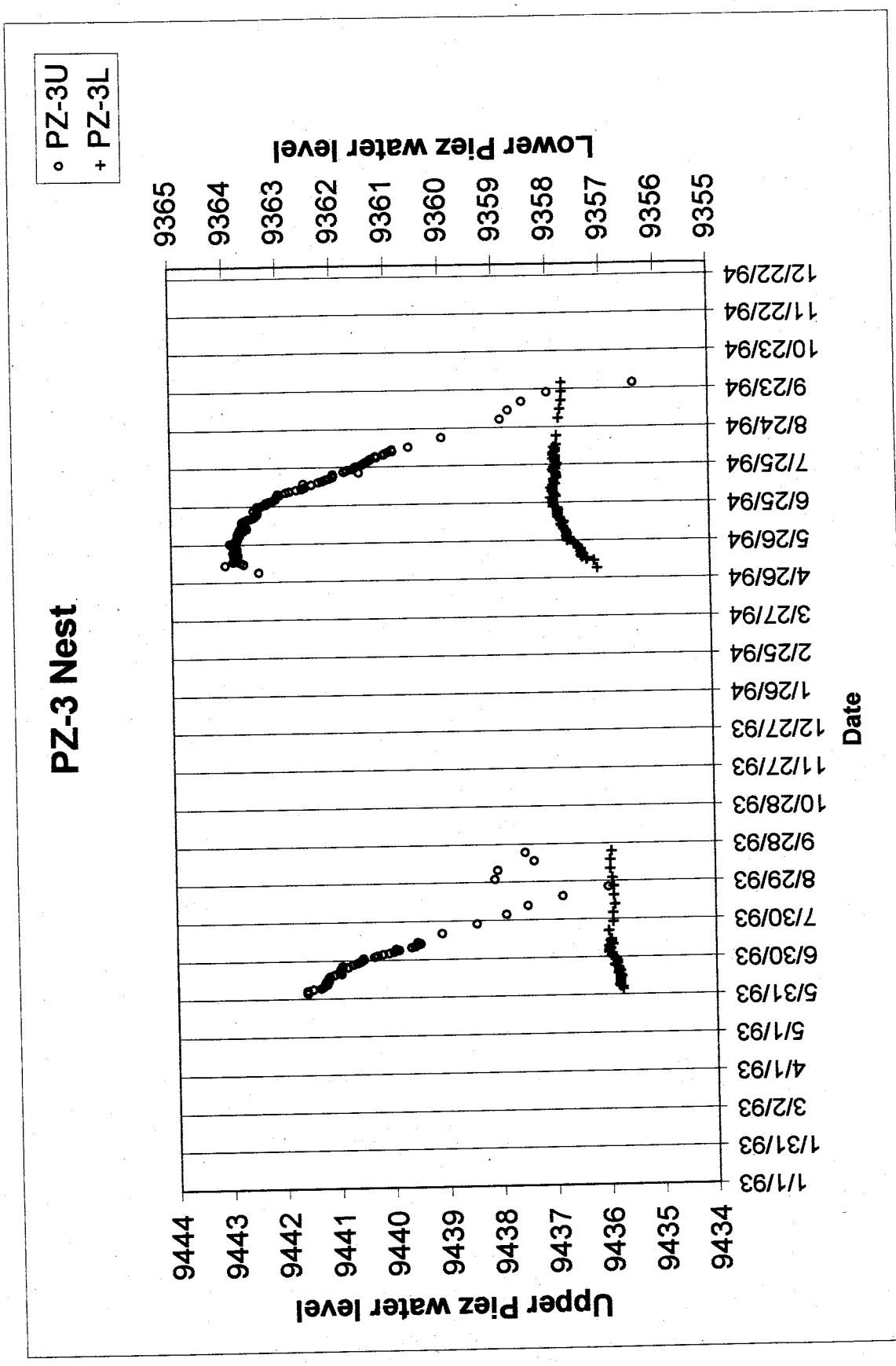
PZ-3 Nest
° PZ-3U
+ PZ-3L
Lower Piez water level
9365
9364
9363
9362
9361
9360
9359
9358
9357
9356
9355
Upper Piez water level
9444
9443
9442
9441
9440
9439
9438
9437
9436
9435
9434
Date
1/1/93
1/31/93
3/2/93
4/1/93
5/1/93
5/31/93
6/30/93
7/30/93
8/29/93
9/28/93
10/28/93
11/27/93
12/27/93
1/26/94
2/25/94
3/27/94
4/26/94
5/26/94
6/25/94
7/25/94
8/24/94
9/23/94
10/23/94
11/22/94
12/22/94

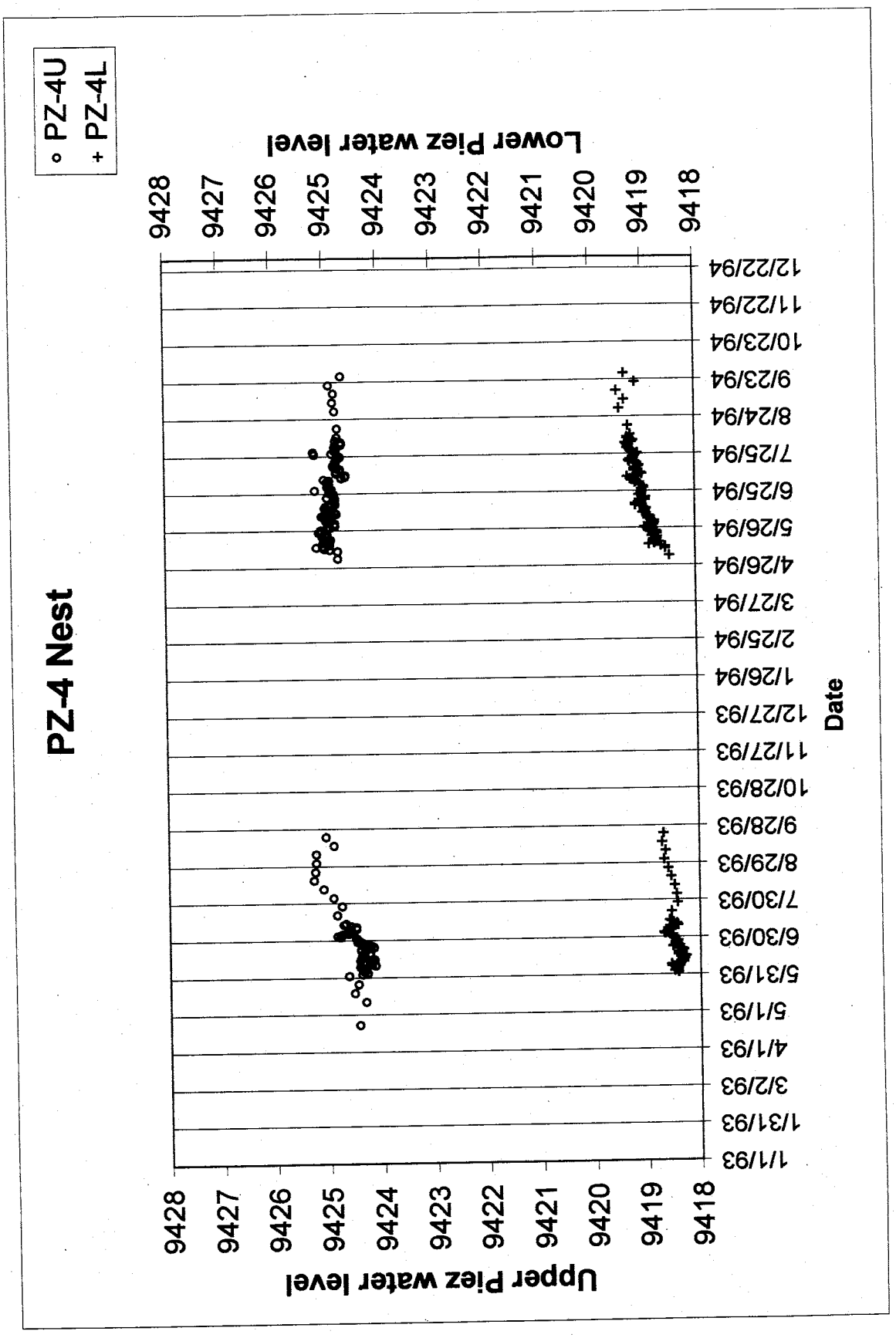
PZ-4 Nest
° PZ-4U
+ PZ-4L
Upper Piez water level
Lower Piez water level
9428
9427
9426
9425
9424
9423
9422
9421
9420
9419
9418
1/1/93
1/31/93
3/2/93
4/1/93
5/1/93
5/31/93
6/30/93
7/30/93
8/29/93
9/28/93
10/28/93
11/27/93
12/27/93
1/26/94
2/25/94
3/27/94
4/26/94
5/26/94
6/25/94
7/25/94
8/24/94
9/23/94
10/23/94
11/22/94
12/22/94
Date

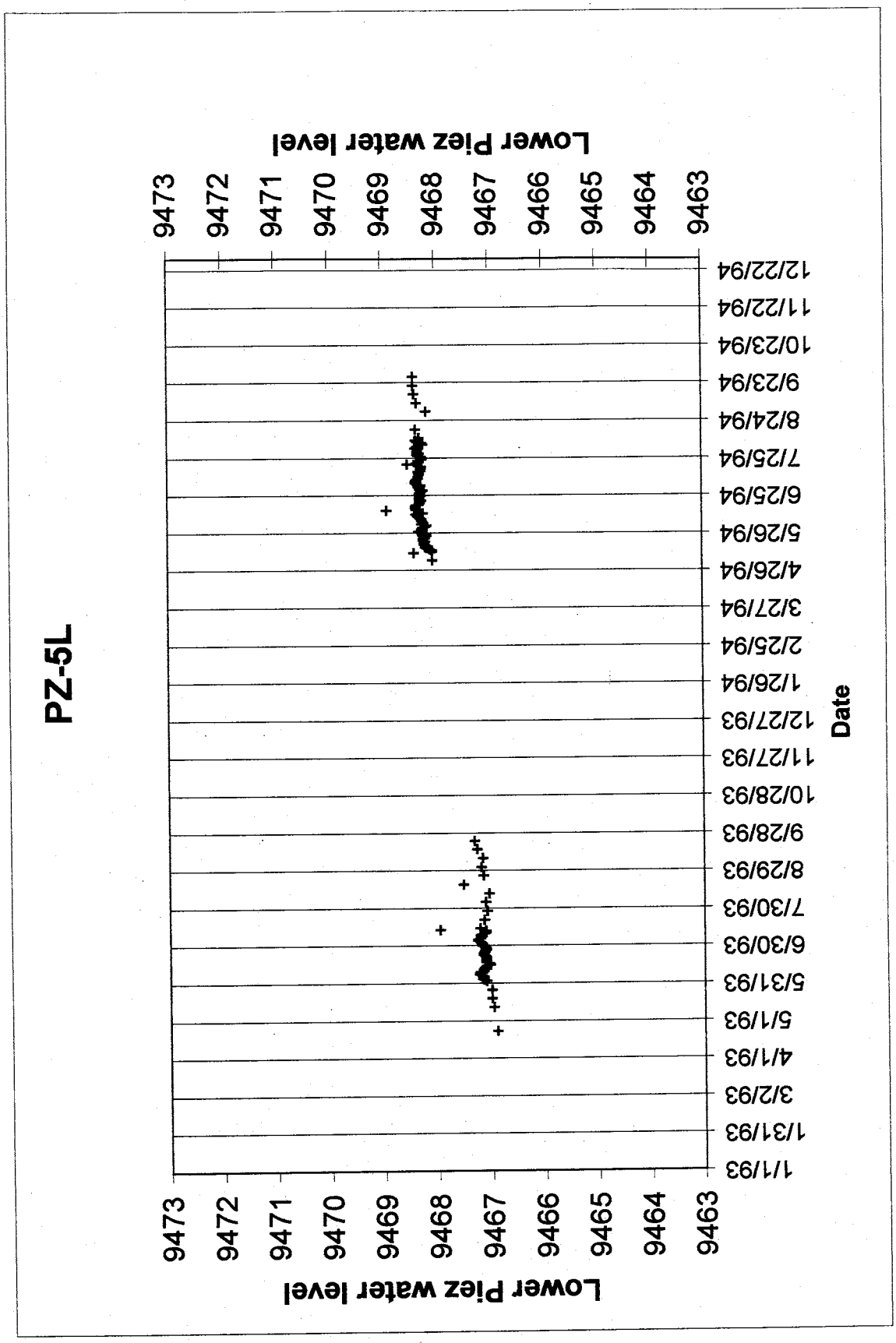
PZ-5L
Lower Piez water level
9473
9472
9471
9470
9469
9468
9467
9466
9465
9464
9463
Date
1/1/93
1/31/93
3/2/93
4/1/93
5/1/93
5/31/93
6/30/93
7/30/93
8/29/93
9/28/93
10/28/93
11/27/93
12/27/93
1/26/94
2/25/94
3/27/94
4/26/94
5/26/94
6/25/94
7/25/94
8/24/94
9/23/94
10/23/94
11/22/94
12/22/94
Lower Piez water level

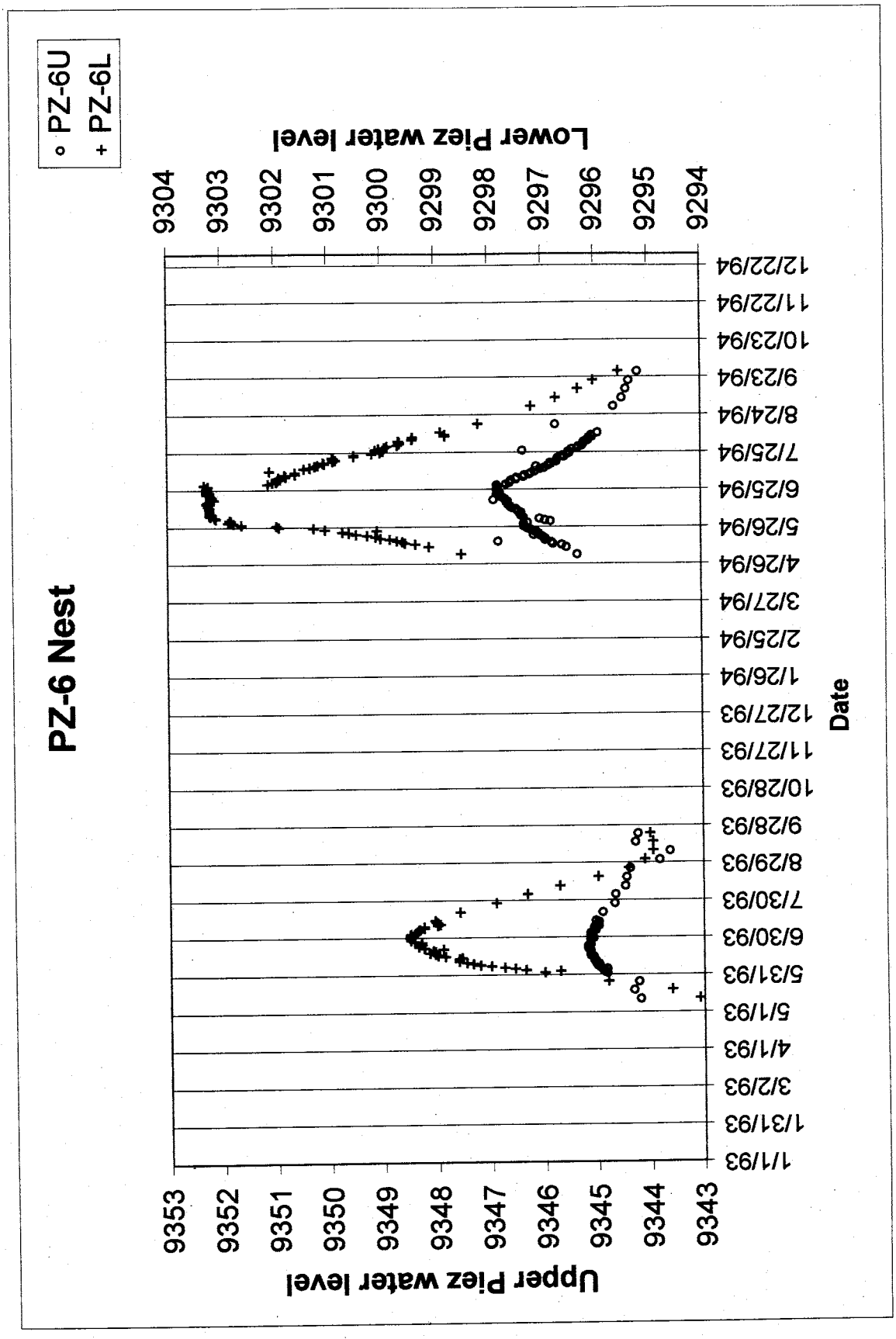
PZ-6 Nest
° PZ-6U
+ PZ-6L
Upper Piez water level
9353
9352
9351
9350
9349
9348
9347
9346
9345
9344
9343
Lower Piez water level
9304
9303
9302
9301
9300
9299
9298
9297
9296
9295
9294
Date
1/1/93
1/31/93
3/2/93
4/1/93
5/1/93
5/31/93
6/30/93
7/30/93
8/29/93
9/28/93
10/28/93
11/27/93
12/27/93
1/26/94
2/25/94
3/27/94
4/26/94
5/26/94
6/25/94
7/25/94
8/24/94
9/23/94
10/23/94
11/22/94
12/22/94

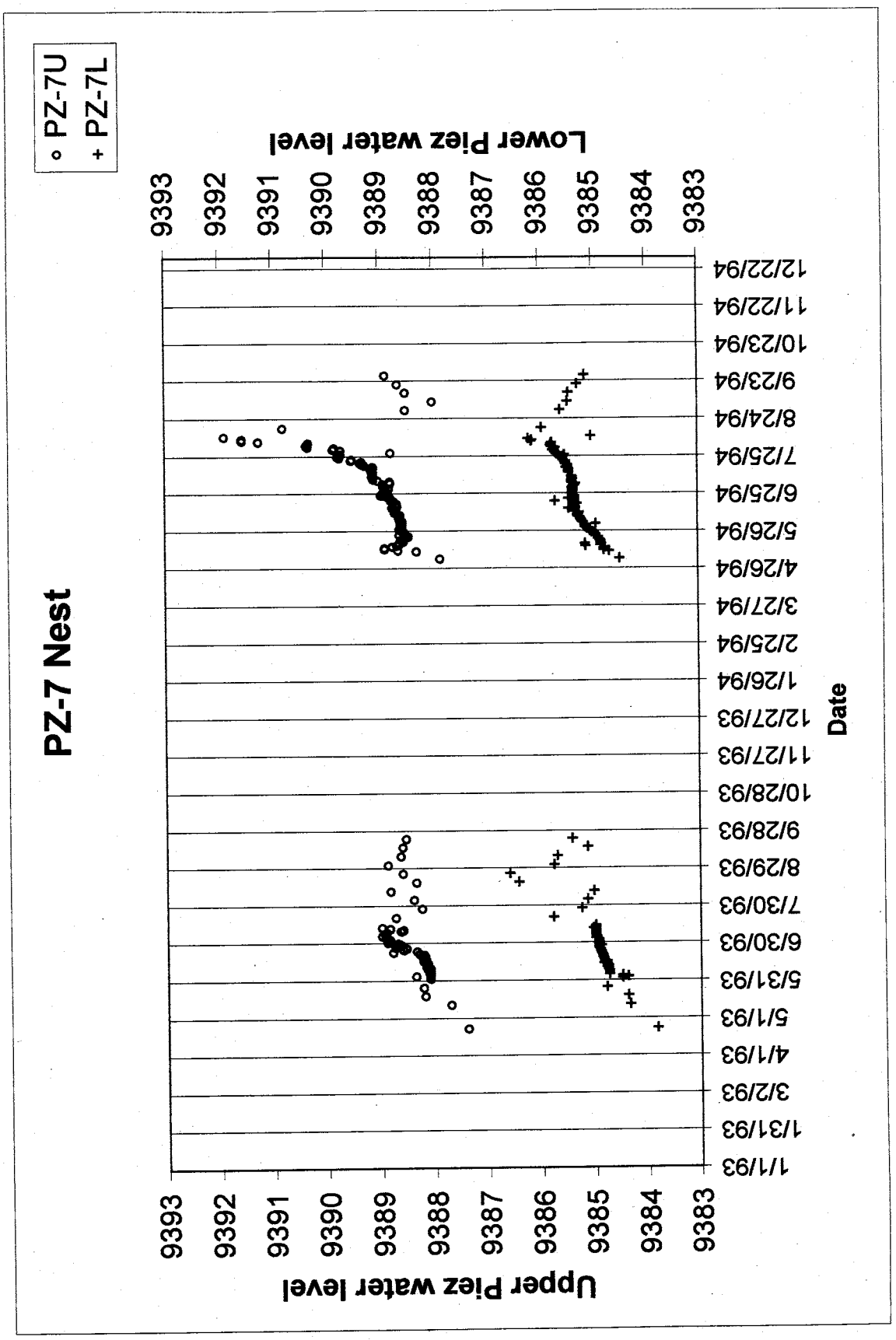
PZ-7 Nest
° PZ-7U
+ PZ-7L
Lower Piez water level
9393
9392
9391
9390
9389
9388
9387
9386
9385
9384
9383
Upper Piez water level
Date
1/1/93
1/31/93
3/2/93
4/1/93
5/1/93
5/31/93
6/30/93
7/30/93
8/29/93
9/28/93
10/28/93
11/27/93
12/27/93
1/26/94
2/25/94
3/27/94
4/26/94
5/26/94
6/25/94
7/25/94
8/24/94
9/23/94
10/23/94
11/22/94
12/22/94

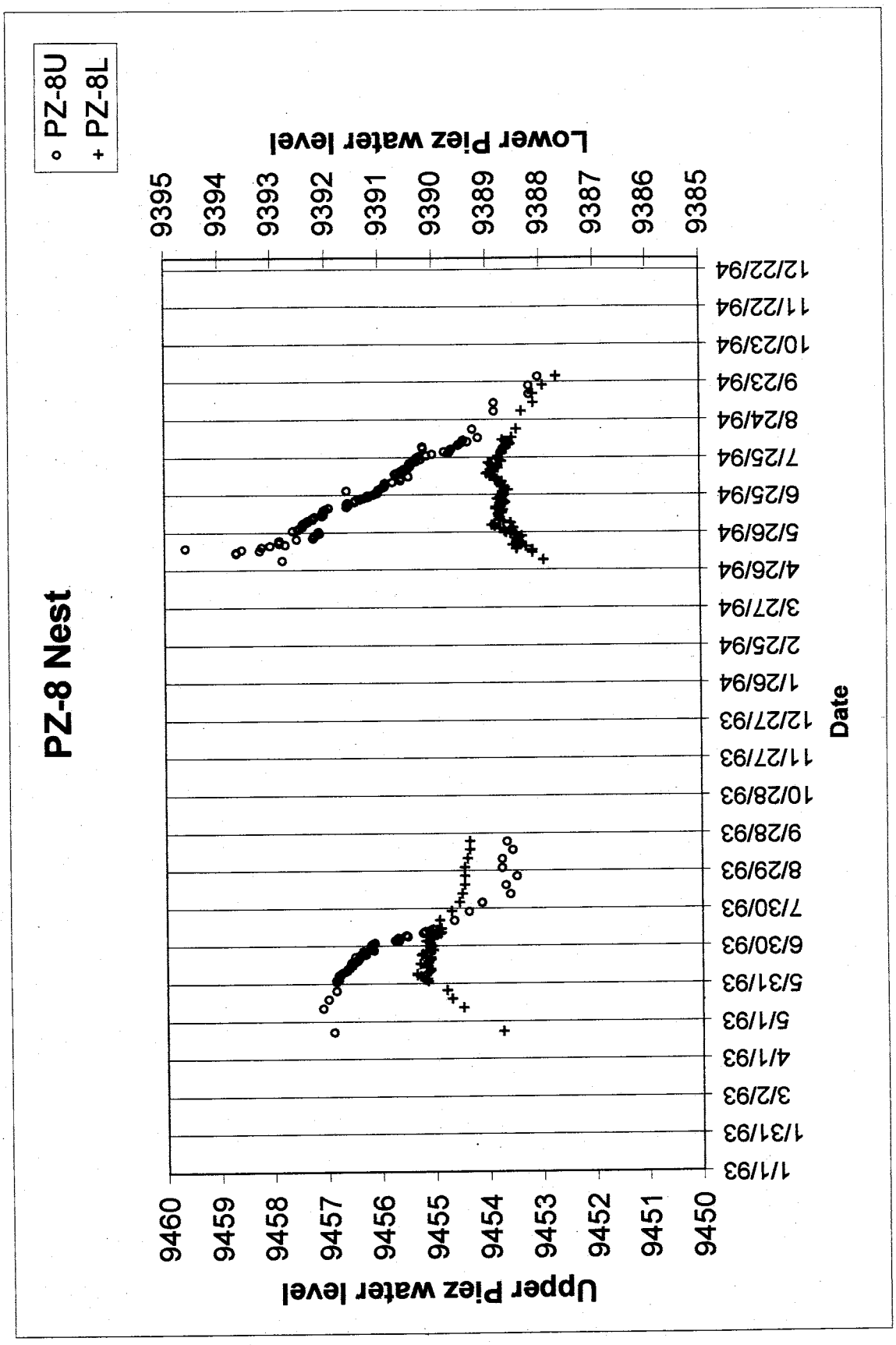
PZ-8 Nest
° PZ-8U
+ PZ-8L
Upper Piez water level
Lower Piez water level
Date
9460
9459
9458
9457
9456
9455
9454
9453
9452
9451
9450
9395
9394
9393
9392
9391
9390
9389
9388
9387
9386
9385
1/1/93
1/31/93
3/2/93
4/1/93
5/1/93
5/31/93
6/30/93
7/30/93
8/29/93
9/28/93
10/28/93
11/27/93
12/27/93
1/26/94
2/25/94
3/27/94
4/26/94
5/26/94
6/25/94
7/25/94
8/24/94
9/23/94
10/23/94
11/22/94
12/22/94

APPENDIX X. SIMULATION OF DIPPING BEDS USING MODFLOW

MODFLOW automatically assumes that each model layer is horizontal, and does not have a built in means of specifying a dipping layer simulation. The only way to produce a dipping layer simulation that retains rectilinear cells is to use trigonometry to alter some of the input data. The altered input data basically tricks MODFLOW into modeling a dipping bed simulation. The necessary alterations of the input data needed to run a dipping bed simulation using MODFLOW are described in this appendix.

The theory involved in using MODFLOW for dipping bed simulations is contained in a Technical Memorandum created by Michael A. Jones entitled "Formulating Dipping Bed Problems Using MODFLOW" dated April 26, 1996. Many of the ideas that I have used in my formulation were borrowed or stemmed from theory explained in this memorandum. The memorandum was concerned with modeling dipping stratigraphic units and model layers that intersect a horizontal ground surface, while my formulation involves a ground surface that dips at the same angle as the model layers. I will only explain the latter formulation and will leave it to the reader to reference the original memorandum.

X.1 ORIENTATION OF GRID

For this formulation, the grid must have a specific orientation. MODFLOW uses the terminology DELR and DELC to represent the size of a model cell along a row and column respectively. In the Cartesian coordinate system these variables would be DELX and DELY respectively. The down dip direction must fall along the rows. So, each column will have the same elevation, while elevation will vary linearly along each row (Figure 47). It is also important to note that this formulation only works for model layers that have a constant dip angle. The formulation could be modified to handle beds of variable dip, but then the model cells would not be rectilinear and this grid distortion would make the finite-difference equations incorrect, which could lead to errors.

X.2 GRID CHARACTERISTICS

With any sloping surface, the plane will differ in appearance if viewed orthogonal to the plane or in map view. For this formulation, the grid will be constructed as if looking at the sloping plane in map view. This formulation only works when DELR is the same along every row and DELC is the same along every column. But, using the ideas presented here, variable DELR AND DELC values could be used without losing the rectilinear grid shape. So, all one has to do is take a map of the hillside to be modeled and construct a rectilinear model grid on the map.

After constructing the grid on the map it is important to notice a few characteristics of this grid. DELC is always the same, independent of whether observed in orthogonal or map view. However, DELR is not the same in orthogonal

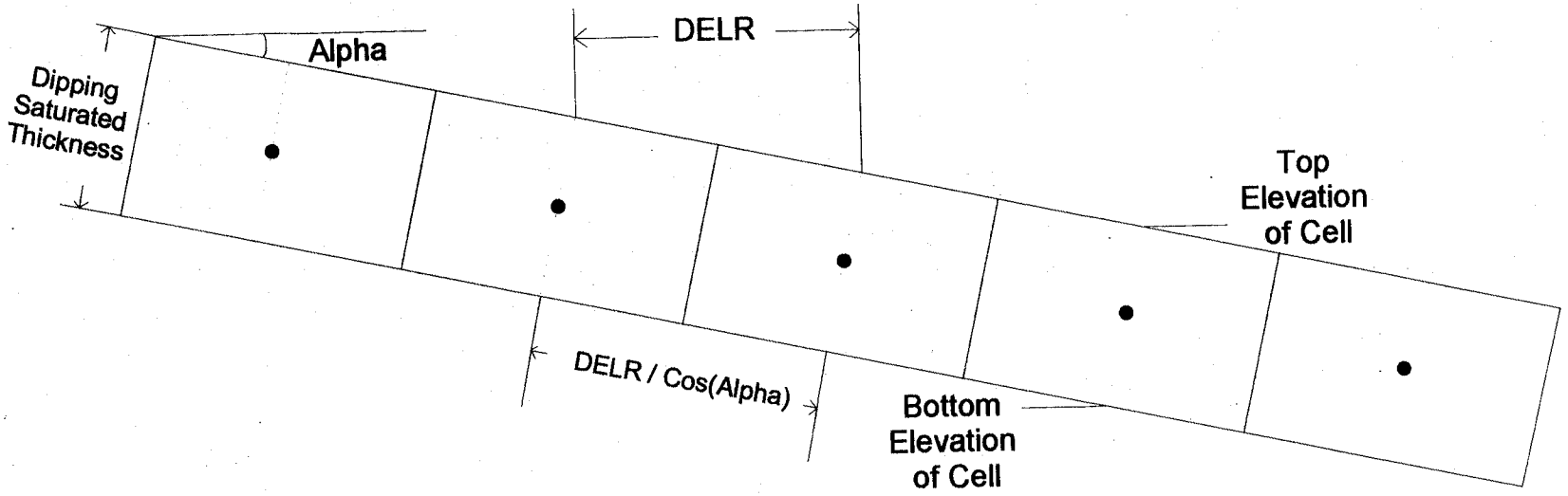

Figure 47 Dipping Model Layer. This figure is a cross section of a dipping MODFLOW model layer. The view is along a column, showing the model layer dipping along a row. A number of the variables shown are involved in altering the actual properties of variables in order to trick MODFLOW into simulating a dipping bed simulation, as described in this appendix.

and map view. For a dipping model layer, DELR will always be smaller in map view than in orthogonal view. All calculations in this formulation will use the DELR of the cells as observed in map view. The actual down-dip length of a cell viewed orthogonal to the layer would be DELR/Cos(ALPHA) (Figure 47).

X.3 FORMULATION OF INPUT DATA

Some model parameters are the same for a flat and dipping bed simulation and do not need to be adjusted. These parameters are DELC, recharge rate, evapotranspiration rate, specific yield, and unconfined hydraulic conductivity. DELC is the distance between nodes (also cell width) measured along columns, which is constant whether viewed orthogonally or in map view. The Recharge and Evaportranspiration packages in MODFLOW compute flow terms based on the map view area of each cell in the grid. So, input for these calculations is correct with the use of the map view DELR as defined above. Specific yield is also proportional to map view area and does not need to be modified. The hydraulic conductivity for an unconfined model layer was calculated to be the same regardless of layer dip. The proof of this follows:

X.3.1 Calculating Down-Dip Hydraulic Conductivity (Model Layer Types 1 and 3)

(For a description of MODFLOW layer types see the end of this appendix.)

First, the grid must be oriented in space. For these model layer types either the bottom elevation, or top and bottom elevations of the layer must be specified. For the dipping grid simulation the bottom of a cell is taken as the elevation at the midpoint of

the base of a cell. The top elevation is simply the elevation at the midpoint of the top of a cell (Figure 47). For stacked layers, the bottom elevation of a cell is the same as the top elevation for the cell directly below it. DELH is the difference in head between adjacent nodes.

X.3.1.1 MODFLOW Calculations

Saturated thickness for unconfined layer = Head-Bottom

Transmissivity for an unconfined layer = Model Hydraulic Conductivity * (Head-Bottom)

Unconfined flow = Model Hydraulic Conductivity * (Head-Bottom) * DELC*(DELH/DELR)

X.3.1.2 True Calculations

Saturated thickness for unconfined dipping layer = (Head-Bottom)/Cos(ALPHA)

Transmissivity calculated for an unconfined dipping layer = Actual Hydraulic Conductivity *[(Head-Bottom)/Cos(ALPHA)]

Unconfined flow = Actual Hydraulic Conductivity * [(Head-Bottom)/Cos(ALPHA)]*DELC*[{DELH*Cos(ALPHA)}/DELR]

The Cos(ALPHA) terms cancel out and you are left with:

Unconfined flow = Actual Hydraulic Conductivity * (Head-Bottom)*DELC*(DELH/DELR)

Therefore, MODFLOW will accurately calculate flow in a dipping unconfined layer if the actual hydraulic conductivity is used. So,

Model Hydraulic Conductivity = Actual Hydraulic Conductivity

Some model parameters are different for a flat and dipping bed simulation and need to be adjusted. These parameters are DELR, transmissivity, storage coefficient, vertical conductance, and anisotropy. As discussed previously, DELR is the map view distance between nodes, and is not the actual down-dip distance between nodes. Since the map view DELR is used, it creates problems with all variables that MODFLOW calculates based on it, such as the transmissivity, storage coefficient, and vertical conductance. The anisotropy needs to be adjusted because of the distance between nodes with respect to the row and column directions.

X.3.2 Calculating Down-Dip Transmissivity (Model Layer Types 0 and 2)

(For a description of MODFLOW layer types see the end of this appendix.)

If there is no unconfined layer, and it has not already been done, the grid must be oriented in space. For these model layer types the top and bottom elevations of the layer do not matter to MODFLOW and do not need to be specified.

X.3.2.1 MODFLOW Calculations

Flow = Model Transmissivity * DELC *[DELH/DELR]

X.3.2.2 True Calculations

Flow = Actual Transmissivity * DELC * [DELH/[DELR/Cos(ALPHA)]]

Actual Transmissivity = Actual Hydraulic Conductivity * Dipping Saturated Thickness

Or

Flow = Actual Transmissivity * DELC * [DELH/DELR] * Cos(ALPHA)

Therefore, MODFLOW will compute the correct down-dip confined flow if:

Model Transmissivity = Actual Transmissivity * Cos(ALPHA)

X.3.3 Vertical Conductance (All Model Layer Types)

Vertical conductance is a value that determines how water will move vertically, or perpendicular to dip, from one model layer to the next. In MODFLOW this value is defined as VCONT. This formulation was created using the equation for vertical hydraulic conductivity defined below:

Vertical Hydraulic Conductivity = 2/[(Sloping thickness of layer n/Actual Hyd Cond of layer n)+(Sloping thickness of layer n+1 /Actual Hyd Cond of layer n+1)]

One way to compute the vertical conductance of sloping layers is:

Actual Vertical Conductance = Actual Vertical Hydraulic Conductivity / (Distance between vertically offset nodes)

X.3.3.1 MODFLOW Calculations

Cross-Layer Flow = Model Vertical Conductance*DELR*DELC*DELH

X.3.3.2 True Calculations

Cross-Layer Flow = Actual Vertical Conductance*[DELR/Cos(ALPHA)]*DELC*DELH

Therefore, MODFLOW will compute the correct vertical conductance for the dipping problem if:

Model Vertical Conductance = Actual Vertical Hydraulic Conductivity/[Distance between vertically offset nodes*Cos(ALPHA)]

X.3.4 Confined Storage Coefficient (Model Layer Types 0, 2, and 3)

For a dipping simulation:

Storage Coefficient = Actual Specific Storage * Dipping Saturated Thickness

MODFLOW later multiplies the Storage Coefficient by DELR*DELC which is the map view cell area, but not the correct surface area for the cell, which is DELC*[DELR/Cos(ALPHA)]

MODFLOW will calculate the correct amount of water released from storage if the Storage Coefficient is input as:

Model Storage Coefficient = [Actual Specific Storage / Cos(ALPHA)] * Dipping Saturated Thickness

X.3.5 Anisotropy

This formulation assumes that the model layers are isotropic along rows and columns. In a horizontal MODFLOW layer, isotropy would be represented by the TRPY variable being assigned as 1.00. However, in a dipping-bed simulation this is not the case. MODFLOW calculates the transmissivity or hydraulic conductivity along columns by multiplying the value input for the rows by the value given for the anisotropy. Both unconfined and confined formulations will be demonstrated, but both produce the same outcome. First, for the confined case:

X.3.5.1 Confined Layer Anisotropy MODFLOW Calculations

Model cross-dip flow = Model Transmissivity*DELR*[DELH/DELC]

From the section on calculating down-dip transmissivity, we remember that

Down-dip Model Transmissivity = Actual Transmissivity*Cos(ALPHA)

So,

Model cross-dip flow = Actual Transmissivity*Cos(ALPHA)*DELR*[DELH/DELC]

X.3.5.2 Confined Layer Anisotropy True Calculations

Cross-dip flow = Actual Transmissivity*[DELR/Cos(ALPHA)]*(DELH/DELC)

Or

Cross-dip flow = Actual Transmissivity/Cos(ALPHA)*DELR*(DELH/DELC)

Cross-dip Transmissivity = Actual Transmissivity/Cos(ALPHA)

Anisotropy = True Cross-dip Transmissivity/ Model Down-Dip Transmissivity

Or

Anisotropy = (Actual Transmissivity)/[Actual

Transmissivity*Cos(ALPHA)*Cos(ALPHA)

Model Anisotropy = $1/[\cos^2(\text{ALPHA})]$

X.3.5.3 Unconfined Layer Anisotropy

MODFLOW computes unconfined cross-dip flow as Model Hydraulic Conductivity*(Head-Bottom)*DELR*DELH/DELC

True cross-dip unconfined flow is Actual Hydraulic Conductivity *[(Head-Bottom)/Cos(ALPHA)]*[DELR/Cos(ALPHA)]*DELH/DELC

So, the true cross-dip hydraulic conductivity = Actual Hydraulic Conductivity/$\cos^2(\text{ALPHA})$

And remember that model down-dip hydraulic conductivity = Actual Hydraulic Conductivity

Model Anisotropy = [Actual Hydraulic Conductivity/$\cos^2(\text{ALPHA})$]/Actual Hydraulic Conductivity

Model Anisotropy = $1/[\cos^2(\text{ALPHA})]$

So, for all types of model layers and every layer in the model, the anisotropy variable (TRPY) is the same (since the dip is the same) as:

Model Anisotropy = $1/[\cos^2(\text{ALPHA})]$

X.4 MODFLOW MODEL LAYER TYPES

0 - Confined – Transmissivity and storage coefficient of the layer are constant for the entire simulation.

1 - Unconfined – Transmissivity of the layer varies. It is calculated from the saturated thickness and hydraulic conductivity. The storage coefficient is constant. This type code is only valid for layer 1.

2 - Confined/Unconfined – Transmissivity of the layer is constant. The storage coefficient may alternate between confined and unconfined values. Vertical flow from above is limited if the layer desaturates.

3 - Confined/Unconfined – Transmissivity of the layer varies. It is calculated from the saturated thickness and hydraulic conductivity. The storage coefficient may alternate between confined and unconfined values. Vertical flow from above is limited if the aquifer desaturates.

REFERENCES

Abramson, L. W., Lee, T. S., Sharma, S., and Boyce, G. M.; 1996; Slope Stability and Stabilization Methods; New York; John Wiley and Sons; 629 p.

Bovay Engineers, Inc.; August 1978; Phase I Inspection Report; National Inspection of Dams Program; Costilla Dam, Taos County, New Mexico.

Carslaw, H. S., and Jaeger, J. C.; 1959; Conduction of Heat in Solids; Oxford, University Press; 510 p.

Compton, R. R.; 1985; Geology in the Field; New York; John Wiley and Sons; 398 p.

D'Appolonia, E., Catanach, R. B., Haneberg, W. C., James, R. L., O'Neill, A. L.; November 1992; Report of the Independent Review Panel of the Costilla Dam Slide; For the Interstate Stream Commission, State of New Mexico.

Domenico, P. A., and Schwartz, F. W., 1990, Physical and Chemical Hydrogeolgy; New York; John Wiley and Sons, 824 p.

Haneberg, W. C.; 1991a; Observation and Analysis of Pore Pressure Fluctuations in a Thin Colluvium Landslide Complex Near Cincinnati, Ohio; Engineering Geology, Volume 31, p. 159-184.

Haneberg, W. C.; 1991b; Pore Pressure Diffusion and the Hydrologic Response of Nearly Saturated, Thin Landslide Deposits to Rainfall; Journal of Geology, Volume 99, p. 886-892.

Haneberg, W. C.; September 17, 1992; phone interview with Richard Lueck (New Mexico State Highway Department).

Haneberg, W. C.; September 18, 1992; phone interview with Gerald Burk (United States Bureau of Reclamation).

Haneberg, W. C.; September 22, 1992; phone interview with Joe Jackson (United States Bureau of Reclamation).

Haneberg, W. C.; November 6, 1992; Letter to Richard Catanach.

Haneberg, W. C.; June 29, 1993; Costilla Slide Bi-weekly Report, June 5 though June 28, 1993; Prepared for Gordon McKeen (University of New Mexico).

Haneberg, W. C.; July 27, 1993; Costilla Slide Report, June 29 though July 21, 1993; Prepared for Gordon McKeen (University of New Mexico).

Haneberg, B.; September 15, 1993; Revised Costilla slide stability analyses; To Elio D'Appolonia.

Haneberg, W. C.; September 9, 1994; end-of-season visual inspection of the Costilla Dam landslide and stability berm; Prepared for Gordon McKeen (University of New Mexico).

Haneberg, W. C.; 1995; Groundwater Flow and the Stability of Heterogeneous Infinite Slopes Underlain by Impervious Substrata, in Haneberg, W. C., and Anderson, S. A., eds.; Clay and Shale Slope Instability; Geological Society of America Reviews in Engineering Geology; Boulder, Colorado; Geological Society of America, p. 63-77.

Haneberg, W. C. and Gökce, A. Ö.; 1994; Rapid Water-Level Fluctuations in a Thin Colluvium Landslide West of Cincinnati, Ohio; U. S. Geological Survey Bulletin 2058-C; Washington; United States Government Printing Office; 16 p.

Harbaugh, A. W. and McDonald, M. G.; 1996; User's Documentation for MODFLOW-96, an update to the U.S. Geological Survey Modular Finite-Difference Ground-Water Flow Model; U. S. Geological Survey Open-File Report 96-485; Reston; Virginia.

Hendron Jr., A. J., Morgenstern, N. R., and Swinger W. F.; April 22, 1994; Costilla Dam; Findings of the Factfinding Board.

Hodge, R. A. L., and Freeze, R. A.; 1978; Groundwater Flow Systems and Slope Stability; Canadian Geotechnical Journal, Volume 14, p. 446-476.

Iverson, R. M., and Major, J. J.; 1987; Rainfall, Ground-water Flow, and Seasonal Movement at Minor Creek Landslide, Northwestern California: Physical Interpretation of Empirical Results; Geological Society of America Bulletin, Volume 99, p. 579-594.

Jackson, C. R., and Cundy, T. W.; 1992; A Model of Transient, Topographically Driven, Saturated Subsurface Flow; Water Resources Research, Volume 28, p. 1417-1427.

Janbu, N.; 1973; Slope Stability Computations; *in* Hirschfield, R. C., and Poulos, S. J., eds.; Embankment Dam Engineering (Casagrande Volume); New York; John Wiley and Sons; p. 47-86.

Jones, M. A.; 4/26/1996; Formulating Dipping Bed Problems Using MODFLOW; Technical Memorandum to file USDOJ/AAMODT, 10 p.

Keller, C. K., van der Kamp, G., and Cherry, J. A.; 1989; A Multiscale Study of the Permeability of a Thick Clayey Till; Water Resources Research, Volume 25, p. 2299-2317.

Leake, S. A. and Lilly, M. R.; 1997; Documentation of a Computer Program (FBH1) for Assignment of Transient Specified-Flow and Specified-Head Boundaries in Applications of the Modular Finite-Difference Ground-Water Flow Model (MODFLOW); U. S. Geological Survey Open-File Report 97-571; Tuscon; Arizona.

Lipman, P. W., and Reed, J. C. Jr.; 1984; Day 2: Supplemental Road Log 2C, From Amalia to Costilla Reservoir; *in* 1984 Rio Grande Rift: Northern New Mexico; Annual Field Conference, Edition 35; New Mexico Geological Society.

Lipman, P. W., and Reed, J. C. Jr.; 1989; Geologic Map of the Latir Volcanic Field and Adjacent Areas, Northern New Mexico; United States Geological Survey; Miscellaneous Investigations Map I-1907.

Lozinsky, R. P.; 1994; Cenozoic stratigraphy, sandstone petrology, and depositional history of the Albuquerque Basin, central New Mexico; *in* Keller, G. R., and Cather, S. M., eds.; Basins of the Rio Grande Rift: Structure, Stratigraphy, and Tectonic Setting: Boulder, Colorado, Geological Society of America Special Paper 291.

McKeen, R. G.; January 31, 1994; letter with summary of 1993 data; Prepared for Eddie Trujillo (New Mexico Interstate Stream Commission).

McKeen, R. G.; August 2, 1994; Report of Monitoring of Costilla Dam June 2, 1994 through June 28, 1994; Prepared for Eddie Trujillo (New Mexico Interstate Stream Commission).

McKeen, R. G.; August 25, 1994; Report of Monitoring of Costilla Dam June 29, 1994 through July 15, 1994; Prepared for Eddie Trujillo (New Mexico Interstate Stream Commission).

McKinlay, P. F.; 1956; Geology of Costilla and Latir Peak Quadrangles, Taos County, New Mexico; Bulletin 42; New Mexico Bureau of Mines and Mineral Resources.

New Mexico Interstate Stream Commission, Santa Fe, New Mexico; March 31, 1994; Position Paper on Costilla Dam Modification Dispute Between the New Mexico Interstate Stream Commission and the Bureau of Reclamation.

New Mexico State Engineer Office; May 26, 1989; Re: File No. 599; letter to Philip B. Mutz (New Mexico Interstate Stream Commission)

New Mexico State Engineer Office; June 20, 1989; Memorandum: Costilla Dam Inspection of Construction and Meeting - File #599; letter to Donald T. Lopez (State Engineer Office); from David O. Quintana (State Engineer Office).

New Mexico State Engineer Office; July 28, 1989; Memorandum: Meeting in Denver with Bureau of Reclamation, Costilla Dam Modification; to File; from Joseph P. Bartley (New Mexico Interstate Stream Commission) and Donald T. Lopez (State Engineer Office).

New Mexico State Engineer Office; January 12, 1990; Draft: Statement on Costilla Dam Modification Project Right Abutment Slide.

New Mexico State Engineer Office; September 10, 1991; Memorandum: Cursory Stability Analysis of Costilla Dam Right Abutment Slide in Spring of 1989 – File 1659; to Donald T. Lopez (State Engineer Office); from David O. Quintana (State Engineer Office).

Reid, M. E.; 1994; A Pore-Pressure Diffusion Model for Estimating Landslide-Inducing Rainfall; Journal of Geology, Volume 102, p. 709-717.

Sidle, R. C.; 1984; Shallow Groundwater Fluctuations in Unstable Hillslopes of Coastal Alaska; Zeitschrift Fur Gletscherkunde und Glazialgeologie, Volume 20, p. 79-95.

Sidle, R. C., and Tsuboyama, Y.; 1992; A Comparison of Piezometric Response in Unchanneled Hillslope Hollows: Coastal Alaska and Japan; J. Japan Soc. Hydrology and Water Resources, Volume 5, p. 3-11.

Smith, L., and Wheatcraft, S. W.; 1993; Groundwater Flow; *in* Maidment, D. R., ed.; Handbook of Hydrology; New York; McGraw-Hill, Inc.

Stephenson, G. R., and Freeze, R. A.; 1974; Mathematical Simulation of Subsurface Flow Contributions to Snowmelt Runoff, Reynolds Creek Watershed, Idaho; Water Resources Research, Volume 10, p. 284-294.

United States Bureau of Reclamation; September 1985; Feasibility Technical Memorandum; Costilla Dam Rehabilitation, Costilla Project, New Mexico; Technical Memorandum No. CDM-230-1.

United States Bureau of Reclamation; July 16, 1986; Contract Between the United States of America and the New Mexico Interstate Stream Commission for the Preparation of Specifications and Supervision of Construction for Modification of Costilla Dam; Contract No. 6-AG-50-5900.

United States Bureau of Reclamation; December 1986; Design Data for Specifications Design, (with Geologic Appendix), Costilla Dam; Costilla Dam Modification Project, New Mexico.

United States Bureau of Reclamation; September 1987; Evaluation and Selection of Spillway Design Option; Costilla Project, New Mexico; Technical Memorandum No. CD-222-1; Prepared by Warren A. Smith.

United States Bureau of Reclamation; October 1987a; Structural Design of Costilla Dam Spillway; Costilla Project, New Mexico; Technical Memorandum No. CD-222-3; Prepared by Warren A. Smith.

United States Bureau of Reclamation; October 1987b; Hydraulic Design of Costilla Dam Spillway; Costilla Project, New Mexico; Technical Memorandum No. CD-222-4; Prepared by Warren A. Smith.

United States Bureau of Reclamation; February 1988a; Static Slope Stability Analysis; Costilla Dam Modification, New Mexico; Technical Memorandum No. CDM-230-1; Prepared by Joy Martin.

United States Bureau of Reclamation; February 1988b; Zoning Design, Material Specifications Requirements, and Construction Source Review for the Zone 1 and Zone 3 Earthfill; Costilla Dam Modification, Southwest Region, New Mexico; Technical Memorandum No. CDM-230-2; Prepared by Joy M. Martin.

United States Bureau of Reclamation; February 1988c; Toe Drain Design for Costilla Dam Modification; New Mexico Interstate Stream Commission, Costilla Project; Technical Memorandum No. CDM-230-4; Prepared by David A. Martinez.

United States Bureau of Reclamation; February 1988d; Analysis of Slope Protection Requirements; Costilla Dam Modification, Southwest Region, New Mexico; Technical Memorandum No. CDM-230-5; Prepared by David A. Martinez.

United States Bureau of Reclamation; February 1988e; Instrumentation Plan for Costilla Dam Modification; Costilla Dam Modification, San Luis Valley, State of New Mexico; Technical Memorandum No. CL-3352-25; Prepared by Robert J. Roelofsz.

United States Bureau of Reclamation; April 1988; Costilla Dam Modification, Taos County, New Mexico; Volume 2 of 2; Document No. 1-553.01-1.

United States Bureau of Reclamation; June 1988; Filter and Drain Design and Gradation Requirements for Costilla Dam Modification; New Mexico Interstate Stream Commission, Costilla Project; Technical Memorandum No. CDM-230-3; Prepared by Greg Rappl.

United States Bureau of Reclamation; June 1988; Foundation Analysis of Costilla Spillway; Costilla Project, New Mexico; Technical Memorandum No. CD-222-5; Prepared by M. J. Romansky.

United States Bureau of Reclamation; November 12, 1988; Memorandum: Weekly Report of Construction Activities November 7, 1988 through November 12, 1988; to Assistant Commissioner; from Project Construction Engineer.

United States Bureau of Reclamation; November 19, 1988; Memorandum: Weekly Report of Construction Activities November 13, 1988 through November 19, 1988; to Assistant Commissioner; from Project Construction Engineer.

United States Bureau of Reclamation; November 26, 1988; Memorandum: Weekly Report of Construction Activities November 20, 1988 through November 26, 1988; to Assistant Commissioner; from Project Construction Engineer.

United States Bureau of Reclamation; April 9, 1989; Memorandum: Weekly Report of Construction Activities April 2, 1989 through April 9, 1989; to Assistant Commissioner; from Project Construction Engineer.

United States Bureau of Reclamation; April 15, 1989; Memorandum: Weekly Report of Construction Activities April 9, 1989 through April 15, 1989; to Assistant Commissioner; from Project Construction Engineer.

United States Bureau of Reclamation; August 16, 1989; Answers to Phil Mutz' first 5 questions; facsimile.

United States Bureau of Reclamation; April 22, 1989; Memorandum: Weekly Report of Construction Activities April 16, 1989 through April 22, 1989; to Assistant Commissioner; from Project Construction Engineer.

United States Bureau of Reclamation; April 29, 1989; Memorandum: Weekly Report of Construction Activities April 23, 1989 through April 29, 1989; to Assistant Commissioner; from Project Construction Engineer.

United States Bureau of Reclamation; May 4, 1989; Memorandum: Weekly Report of Construction Activities April 30, 1989 through May 4, 1989; to Assistant Commissioner; from Project Construction Engineer.

United States Bureau of Reclamation; May 11, 1989; Memorandum: Weekly Report of Construction Activities May 5, 1989 through May 11, 1989; to Assistant Commissioner; from Project Construction Engineer.

United States Bureau of Reclamation; May 18, 1989; Memorandum: Weekly Report of Construction Activities May 12, 1989 through May 18, 1989; to Assistant Commissioner; from Project Construction Engineer.

United States Bureau of Reclamation; May 24, 1989; Revised Stockpiling Plan; letter to Mr. McMurren (Twin Mountain Rock Company); from Project Construction Engineer.

United States Bureau of Reclamation; May 25, 1989; Memorandum: Weekly Report of Construction Activities May 19, 1989 through May 25, 1989; to Assistant Commissioner; from Project Construction Engineer.

United States Bureau of Reclamation; June 1, 1989; Memorandum: Weekly Report of Construction Activities May 26, 1989 through June 1, 1989; to Assistant Commissioner; from Project Construction Engineer.

United States Bureau of Reclamation; June 8, 1989; Memorandum: Weekly Report of Construction Activities June 2, 1989 through June 8, 1989; to Assistant Commissioner; from Project Construction Engineer.

United States Bureau of Reclamation; June 15, 1989; Memorandum: Weekly Report of Construction Activities June 9, 1989 through June 15, 1989; to Assistant Commissioner; from Project Construction Engineer.

United States Bureau of Reclamation; June 16, 1989; Stockpile Movement, Suspension of Excavation in the Spillway Stilling Basin, Filling of Cracks from Earth Movements; to Project Construction Engineer; from Chief, Construction Division.

United States Bureau of Reclamation; June 22, 1989; Memorandum: Weekly Reports of Construction Activities – June 16, 1989 through June 22, 1989; to Assistant Commissioner; from Project Construction Engineer.

United States Bureau of Reclamation; June 29, 1989; Memorandum: Review of Costilla Slide, Costilla Dam, New Mexico (Geology); from Louis R. Frei, to Design Team, Costilla Dam Modification.

United States Bureau of Reclamation; July 10, 1989; Travel Report: Inclinometer Installation at Costilla Dam – Costilla Project, New Mexico (Dam Instrumentation); letter to Chief, Geotechnical Engineering and Geology Division; from Dan Groins, Supervisory Civil Engineering Technician.

United States Bureau of Reclamation; November 1989; Costilla Slide Stabilization, Costilla Dam, Costilla Project, New Mexico; Technical Memorandum No. CS-3620-1; Report to New Mexico Interstate Stream Commission.

United States Bureau of Reclamation; January 1992; Report on Costilla Dam Modification; Energy and Water Development Appropriation Act – 1992, Senate Report 102-80.

United States Bureau of Reclamation; June 15, 1992; Instrumentation Data from Costilla Slide Monitoring System, Costilla Slide Stabilization, Costilla Dam Modification Completion; Document No. 1-553.01-2.

United States Bureau of Reclamation; March 1994; Position Paper on Landslide, Costilla Dam Modification.

United States Bureau of Reclamation; April 1995; Final Construction Geology Report; Costilla Dam and Spillway Modification; Costilla Dam Modification Project, New Mexico.

Subject: RE: MS Thesis title
From: "Axness, Carl L" <claxnes@sandia.gov>
Date: Tue, 1 Jul 2008 14:22:49 -0600
To: "sdelap@nmt.edu" <sdelap@nmt.edu>

Yes, I did an independent study, probably the longest and the one that involved the most work of any of your independent studies. Here is the reference according to my CV:

Axness, C. L. and L. W. Gelhar, Stochastic Analysis of Macrodispersion in Three-Dimensionally Heterogeneous Aquifers, NMIMT Hydrology Research Program, Report No. H-8, Aug., 1981.

Yes, Lynn was my advisor.

Hope that helps. CA

Thesis db updated
1 July 2008
Megan

Carl L. Axness, Ph.D.
Sandia National Laboratories
Performance Assessment Integration, Dept. 6781
P. O. Box 5800
Mail Stop 0776
Albuquerque, NM 87185-0776
tel: 505-844-0084
fax: 505-284-4002

-----Original Message-----
From: Susan Delap [mailto:sdelap@nmt.edu]
Sent: Tuesday, July 01, 2008 1:56 PM
To: Axness, Carl L
Subject: MS Thesis title

Hi Carl,

I am updating the EES department's thesis database, and I can't find a title for your MS thesis. Did you do an independent study instead? Could you send me the title? Also, was your advisor Lynn Gelhar?

Thanks,
Susan

--
Susan E. Delap
Computer Publishing & Graphics Specialist, EES Webmaster Department of Earth & Environmental Science New Mexico Tech
801 Leroy Place
Socorro, New Mexico 87801
Phone: (575) 835-5307
Fax: (575) 835-6436
Office: MSEC 258
Email: sdelap@nmt.edu
Web: http://www.ees.nmt.edu/delap/

April 20, 2001

John Wilson,

I want to thank you for your excellent review of my paper and helping make sure that I was finished by the deadline. Keep working the students hard. They might grumble and groan, but they will also learn more than they could have ever imagined, I know I did.

Thanks Again,

Andrew B. Dunn
1914 Olympia Way #12
Longview, WA 98632
(360) 501-5177
shellyandydunn@hotmail.com